THE UNIVERSITY
of EDINBURGH

Analysis of the role of BimA phosphorylation on *B. pseudomallei* actin-based motility

Seb Cotton

Masters by Research

The University of Edinburgh

2015

Postgraduate Research Thesis Declaration

I declare that this thesis has been composed solely by myself and that it has not been submitted, in whole or in part, in any previous application for a degree. Except where states otherwise by reference or acknowledgment, the work presented is entirely my own.

Abstract

Burkholderia pseudomallei is an intracellular pathogen that causes a severe disease known as melioidosis affecting both animals and humans in South East Asia and Northern Australia. *B. pseudomallei* displays actin-based motility in the cytoplasm of infected cells, although its mechanism is largely unknown. Located at the pole of the bacterium is BimA which is vital for motility, survival and virulence. BimA interacts with actin and initiates the formation of actin tails independently of the Arp 2/3 complex. *Listeria monocytogenes* actin-based motility has been shown to be affected by the host cell enzyme Casein Kinase II. This enzyme phosphorylates the bacterial factor ActA which is required for *L. monocytogenes* intracellular motility. My project aims to investigate the effect of phosphorylation of BimA on actin-based motility in *B. pseudomallei*. Online prediction tools were used to perform a bioinformatics analysis of BimA and identify potential phosphorylation sites. Actual phosphorylation sites were identified by mass spectrometry analysis of ectopically expressed BimA protein in HeLa cells and from *in vitro* kinase assays on recombinant GST-BimA protein. BimA phosphorylation mutant proteins were generated and expressed in a *bimA* mutant. Analysis of phosphorylation sites that are important to the function of BimA could lead to the development of novel anti-infectives.

Lay Summary

Burkholderia pseudomallei is a bacterium that is able to invade and replicate inside the host cell. It causes a severe disease known as melioidosis affecting both animals and humans in South East Asia and Northern Australia. *B. pseudomallei* is able to use host cell actin to form a tail behind it and power movement inside the cell. This process is called actin-based motility and the mechanism is largely unknown. Located at the pole of the bacterium is a bacterial factor known as BimA which is vital for motility and survival. BimA interacts with actin and initiates the formation of actin tails. *Listeria monocytogenes* is another bacteria that utilises actin-based motility to promote movement in the host cell. It has been shown to be affected by the host cell enzyme Casein Kinase II. This enzyme phosphorylates the actin-based motility factor ActA in *Listeria*. My project aims to investigate the effect of phosphorylation of BimA on actin-based motility in *B. pseudomallei*. Analysis of phosphorylation sites that are important to the function of BimA could lead to the development of novel anti-infectives.

Contents

Chapter 1: Introduction

Certain intracellular bacterial pathogens have developed unique mechanisms to invade host cells by utilising the host cell actin (reviewed in Stevens *et al*. 2006). Once inside the cell the bacteria needs to escape the endosome first before it can rapidly polymerise actin leading to the formation of actin-rich tails and movement within the cytoplasm. This process is known as actin-based motility and leads to the formation of membrane protrusions, allowing entry into adjacent cells and cell to cell spread (Monach and Theriot 2001) (Kespichayawattana *et al*. 2000). Certain species of *Listeria, Rickettsia, Burkholderia, Shigella* and *Mycobacterium* are able to exploit host cell actin polymerisation pathways to avoid the adaptive immune system and remain undetected, thereby promoting their own survival. There are many different actin polymerisation pathways in the host cell and each bacterium has evolved different factors to polymerise actin. The detailed molecular mechanisms underlying these processes are still not fully understood and are active areas of ongoing research. The polymerisation of actin by the host cell is often regulated by phosphorylation by cellular kinases. This project will study whether actin-based motility of *B. pseudomallei* is regulated by phosphorylation.

Burkholderia pseudomallei

Burkholderia pseudomallei is a Gram negative bacterium that causes a severe disease known as melioidosis affecting both animals and humans in South East Asia and Northern Australia (White 2003) (reviewed in Stevens and Stevens 2009). Sporadic cases have also been seen in the Middle East, China, India and South America. *B. pseudomallei* is an environmental soil saprotype that is most likely to survive by obtaining nutrition from rotting organic matter or opportunistically from invasion of protozoa (reviewed in Lazar-Adler *et al*. 2009). *B. pseudomallei* is commonly found in wet and stagnant waters such as rice paddies with most cases occurring in people who are in regular contact with the soil (reviewed in Wiersinga *et al*. 2012). The number of cases increases during the rainy season because flooding increases the spread of the bacteria from its natural habitat (reviewed in Brett *et al.* 2000).

It is very rare for *B. pseudomallei* to be transmitted from person to person and so the routes of infection are by inhalation, ingestion or cutaneous inoculation of contaminated soil or water. The incubation period normally lasts between 1-21 days with typical symptoms including pneumonia and the formation of abscesses in internal organs such as the lungs or liver (reviewed in Wiersinga *et al.* 2012). Melioidosis can display different forms of disease, the type of infection varying depending on the route of inoculation. *B. pseudomallei* can spread to internal organs such as the liver, spleen or

brain, or to the blood, resulting in septicaemia (reviewed in White, 2003). The mechanism of the secondary spread is not known but as the bacteria can invade and survive in macrophages they could be a potential transport vehicle via the lymphatic system (reviewed in Lazar-Adler *et al*. 2009). Acute localised infections occur from inoculation of abrasions in the skin resulting in fever, muscle soreness and skin abscesses which could lead to septicaemia. Pulmonary infections occur through inhalation causing mild bronchitis leading to severe pneumonia. Additionally, patients will also often suffer from high fever, headache and muscle soreness. This is followed by the appearance of abscesses in the lungs and death within a few days if left untreated (reviewed in Cheng *et al*. 2005). Often symptoms are associated with pre-disposing factors such as diabetes and alcoholism.

The *Burkholderia* genus consists of 40 species and the closest genetic relatives to *B. pseudomallei* are *Burkholderia mallei* and *Burkholderia thailandensis*. *B. mallei* causes the disease glanders which primarily affects horses but can infect humans with high mortality. *B. thailandensis* is an avirulent soil saprophyte found in certain soil types in Thailand. *B. thailandensis* is similar to *B. pseudomallei* in that it can survive outside of the host in the soil whereas *B. mallei* cannot. *B. mallei* lacks the functional flagella seen in its genetic relatives and has not yet been isolated from a non-animal environment (Kim *et al*. 2005). *B. thailandensis* has been used as a model for *B. pseudomallei* in a number of studies as it contains a number of homologues such as known virulence factors and the Type 3 secretion system (Haraga *et al.* 2008) (Sarkar-Tyson *et al*. 2009). The advantage of using *B. thailandensis* as a model for *B. pseudomallei* is being able to perform research at containment level two as opposed to containment level three.

B. pseudomallei is considered a schedule 5 bioterrorism agent by the UK government as it is transmitted by aerosol and has a very low infectious dose. It is resistant to many antibiotics including penicillin, quinolones and aminoglycosides and recommended treatment is a combination therapy of intravenous Ceftazidime or Meropenem for 14 days followed by oral Trimethoprim-sulfamethoxazole or Doxycycline for 3-6 months as there is no vaccine currently available (Moore *et al.* 1999) (Lipsitz *et al*. 2012). The intracellular life cycle of the bacterium makes it difficult for effective antibiotic treatment because the drug is needed to target the bacteria inside the host cell.

B. pseudomallei **life cycle**

B. pseudomallei is a motile pathogen that is able to invade both phagocytic and non-phagocytic cells. There are many stages to this infection process involving: Adhesion, Type 3 Secretion System-

mediated cell entry or phagocytosis, escape from the vacuole, actin-based motility, and formation of multinucleated giant cells (Figure 1).

Figure 1: Intracellular life of *B. pseudomallei*

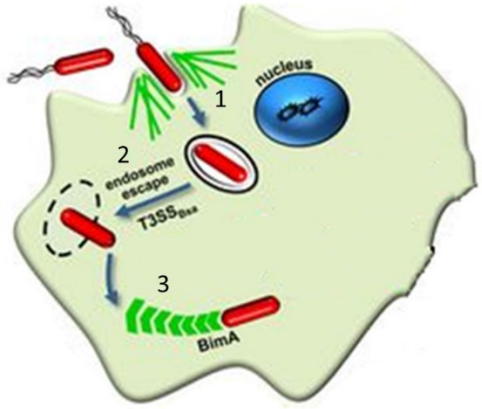

The intracellular life of *B. pseudomallei*: 1) Invasion of the host cell involves adhesins BoaA, BoaB and pilA for attachment before the T3SS is used to enter the cell. 2) Escape from the endosome uses the T3SS to release effectors to break down the endosome membrane. 3) Actin-based motility stage involves bacterial factor BimA to initiate formation of actin tails in the cytosol. (Adapted from French *et al.* 2011)

Adhesion is the initial step in bacterial pathogenesis and the exact method of attachment is still unclear although it is thought to involve Type IV pili (Essex-Lopresti *et al.* 2005) (Reviewed in Galyov *et al.* 2010). These filaments and the proteins they contain are suggested to play a role in virulence. The PilA gene that encodes the pilin subunit protein was shown to be important for adhesion to the host cell (Essex-Lopresti *et al.* 2005) (Boddey *et al*. 2006). Adhesins BoaA and BoaB are also involved in this process (Balder *et al*. 2010) (reviewed in Allwood *et al*. 2011). The thin layer of polysaccharide around the bacteria known as the capsule has also been shown to be important for adhesion to epithelial cells (Ahmed *et al.* 1999).

After attachment to the host cell *B. pseudomallei* can enter the cell either via phagocytosis or invasion. For invasion, a Type 3 Secretion System apparatus (T3SS) encoded by the *bsa* (*Burkholderia* secretion apparatus) locus is used to target host cell pathways (Stevens *et al.* 2002). The T3SS consists of around 20 proteins that are assembled into a needle-like structure which injects bacterial proteins into the host cell. This structure allows the bacteria to secrete effector molecules into the host that can hijack cellular pathways. Some key proteins in the *bsa* locus are the structural proteins BipD (translocator), BsaQ (structural component), and BopE (effector) (reviewed in Sun and Gan 2010) (reviewed in Allwood *et al.* 2011). The BopE effector is a guanine nucleotide exchange factor that works by rearranging the host actin cytoskeleton for entry. A *bopE* mutant displayed reduced invasion of

epithelial cells (Stevens *et al*. 2003). A T3SS apparatus *bipD* mutant also exhibited an impairment in invasion, suggesting that more than one T3SS effector is involved in invasion (Stevens *et al*. 2003).

Following uptake, the bacteria has to escape endocytic vacuoles (Stevens *et al.* 2002). This process is also thought to involve the T3SS, which releases effectors that break down vacuolar membranes of the phagosome and help promote escape into the cytosol (reviewed in Galyov *et al*. 2010). Mutants within the T3SS demonstrate a defect in vacuolar escape, which results in a variety of effects, including reduced actin-tail formation, intracellular survival, cytotoxicity and intracellular spread (Stevens *et al*. 2002) (Stevens *et al*. 2003).

Invasion of both epithelial and macrophage cells by *B. pseudomallei* induces autophagy, a cellular process that allows the degradation and recycling of cellular components. It is a catabolic pathway that uses lysosomes to break down cellular components and forms an important part of the innate immune response. *B. pseudomallei* is able to successfully evade autophagy and the T3SS plays a role in this evasion. BopA, a T3SS effector protein, has been shown to be important for evading autophagy and efficient escape from the phagosome (Gong *et al.* 2011). BopA is thought to be involved in modulating the host cell response as a *bopA* mutant showed increased colocalization with microtubule-associated protein light chain 3 (LC3) and reduced intracellular survival (Cullinane *et al.* 2008). LC3 is an autophagy marker protein that is recruited to phagosomes to stimulate killing of *B. pseudomallei*.

Once inside the cell cytoplasm the bacterium is able to form actin comet tails and promote its own survival by a process known as actin-based motility. *B. pseudomallei* uses the protein BimA (*Burkholderia* intracellular motility factor A) to initiate the formation of actin tails in the cytosol (Stevens *et al*. 2005). BimA is a putative Type V secreted protein which is important for intracellular survival (Sitthidet *et al*. 2011), virulence (Lazar-Adler *et al*. 2015) and actin-based motility (Stevens *et al*. 2005 and unpublished data from the Stevens laboratory). A *bimA* mutant was shown to lack actin-based motility but was able to invade the cell and escape from the vacuole (Stevens *et al*. 2005). The mechanism by which it recruits and activates factors to assemble actin is still being researched, however it is known that BimA directly binds with actin and can stimulate its polymerisation *in vitro* (Stevens 2005). BimA has been recently suggested to mimic Ena/Vasp proteins in the elongation of actin tails (Benanti *et al*. 2015). Like other bacterial factors involved in actin-based motility it is located at the pole of a single daughter cell. It is likely a trimeric protein which improves its stability against proteases (Benanti *et al*. 2015).

B. pseudomallei is able to use a Type 6 Secretion System (T6SS) to deliver effectors that enhance its ability to replicate. A T6SS effector protein mutant (*hcp)* showed slightly reduced actin-based motility

compare to the wildtype (Burtnick *et al*. 2010). Actin-based motility results in the formation of membrane protrusions into adjacent cells and leads to multinucleated giant cell formation. The T6SS is also involved in this process where the protein VgrG-5 has been shown to be important for membrane fusion (Schwarz *et al*. 2014) (Toesca *et al*. 2014). This multinucleated giant cell formation is unique to *Burkholderia* and has not been seen in other intracellular bacteria.

Host cell actin nucleation and polymerisation

Actin is one of the most abundant proteins in the cell and a major component of the cytoskeleton. It provides the roadways for proteins resulting in many processes such as: cell motility, cell adhesion, phagocytosis and cell division. The cytoskeleton is a highly dynamic environment with rapid assembly and disassembly of actin filaments in the cell. Actin has two forms; G-actin which is ATP-bound and F-actin which is ADP-bound. The G-actin is assembled to form a filament of F-actin which has a fast growing barbed end and a slow growing pointed end (reviewed in Firat-Karalar *et al*. 2011) (Figure 2). Polymerisation of actin filaments requires ATP hydrolysis and this process is regulated by actin-binding proteins. The stimulation of actin polymerization drives many essential cellular processes, including cell migration.

In eukaryotic cells the initial nucleation of actin requires actin-nucleating proteins. These fall into three groups: Actin-related protein 2/3 complex (Arp 2/3) and Nucleation promoting factors (NPFs), formins and tandem-monomer-binding nucleators (reviewed in Firat-Karalar *et al*. 2011). The different mechanisms of nucleation are shown in Figure 2.

The Arp 2/3 complex initiates and nucleates the growth of actin filaments. It is a conserved ubiquitous complex of seven polypeptides comprising actin-related proteins Arp2 and Arp3. Wiskott-Aldrich syndrome protein (WASP) and other NPFs regulate the activity of Arp 2/3 (reviewed in Campellone *et al*. 2010). The components of the Arp 2/3 complex directly bind to actin after activation by an NPF. Host cell nucleation-promoting factors bind and activate the Arp2/3 complex through the C and A regions of their VCA domain (reviewed in Goley and Welch 2006). NPFs are needed to activate the Arp2/3 complex which then nucleates the formation of new filaments that extend from the sides of existing filaments at a 70 degree angle to form a Y-branched network (reviewed in Goley and Welch 2006). WASP and N-WASP are multidomain proteins that help regulate the actin cytoskeleton. They contain small GTPase-binding domains which interact with Cdc42, a Rho GTPase. They also contain a C-terminal verpolin central acidic domain (VCA) which interacts with Arp2/3 (reviewed in Pollitt and Insall 2009).

Tandem-monomer-binding nucleators contain tandem G actin-binding motifs, which bring together monomers to form a polymerisation nucleus (reviewed in Chesarone *et al*. 2009). Spir, Cordon bleu and Leiomodin are all examples and contain actin monomer-binding WASP- homology 2 (WH2) domains (reviewed in Chesarone *et al*. 2009) (reviewed in Paunola *et al.* 2012). These nucleators stimulate polymerisation of an unbranched filament.

Formins are multidomain proteins that function as dimers to assemble straight unbranched actin filaments (reviewed in Chesarone *et al*. 2009). Formins nucleate actin and act as elongation factors for growing actin filaments. They use their doughnut-shaped domains to crown the barbed end and progressively move with the growing filament end (reviewed in Chesarone *et al.* 2009). Another elongation factor that has been characterised is Enabled/vasodilator-stimulated phosphoprotein (Ena/ VASP). Like formins, Ena/VASP proteins bind to actin and move with the growing filament, but form tetramers rather than dimers. They are able to group and elongate two filaments at once (Winkleman *et al*. 2014).

Figure 2: Nucleation of actin

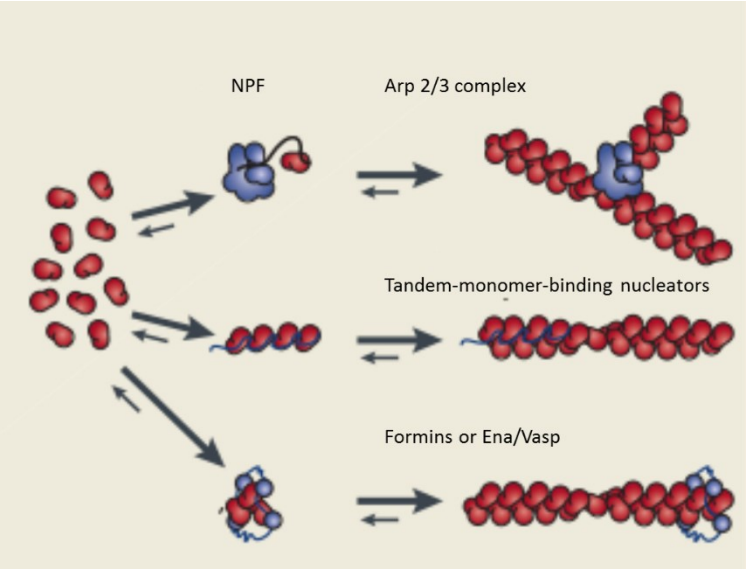

Diagram showing the three main classes of protein that have been identified to nucleate actin by a distinct mechanism. NPFs work with the Arp 2/3 complex to form branched actin filaments from monomers. Tandem-monomer-binding nucleators function as a scaffold for polymerisation to generate an unbranched filament. Formins attach to the end of the actin and move along with the growing filament. (Adapted from Goley *et al*. 2006).

After nucleation the filaments grow freely at their barbed ends until there is a lower level of monomers or capping proteins terminate elongation. Elongation factors are able to promote the growth of filaments whereas capping proteins limit the growth by binding to the barbed end of an actin filament and blocking the addition or removal of actin subunits (reviewed in Edwards *et al*. 2014).

Severing existing filaments into multiple smaller ones can generate new ends. Actin-binding proteins such as Actin Depolymerising factor (ADF)/cofilin promote this debranching and depolymerisation to generate a new pool of monomers. Rho-family GTPases activate p21-Activated Kinase (PAK) and LIM-1 kinase, which in turn phosphorylate ADF/cofilin. This slows down the turnover of the filaments by inhibition of ADF/cofilin (Pollard *et al*. 2003). Actin monomers are then nucleated again by the Arp 2/3 complex to complete the cycle of actin assembly in the eukaryotic cell.

The whole process of actin nucleation and polymerisation is a dynamic and changing environment that needs to be regulated by the cell. Phosphorylation of actin-binding proteins by host cell kinases is a key modification that helps to achieve this. For example, Cortactin is an actin-binding protein enriched in lamellipodia of motile cells, that has been shown to be phosphorylated by Protein Kinase D (PKD) and Pak1 kinases (Eiseler *et al*. 2010) (Grassart *et al*. 2010). Phosphorylation of Cortactin by these kinases regulated the interaction of N-WASP proteins with Arp 2/3 and it's activation. Additionally WASP proteins have been shown to be phosphorylated by many host cell kinases. Phosphorylation of Serine residues in WASP by Casein Kinase 2 (CK2) increased the affinity for Arp 2/3 complex (Cory *et al*. 2003). Tyrosine residues of WASP proteins have also been shown to be phosphorylated by activated Cdc42-associated kinase-1 (Ack1) and Proto-oncogene tyrosine-protein (Src) family kinases which enhanced actin polymerisation *in vitro* (Yokoyama *et al*. 2005) (Cory *et al.* 2002). Furthermore, Formin proteins can be activated by phosphorylation to form actin-based structures called stress fibres. The Formin homology domain protein 1 (FHOD1) has been shown to be phosphorylated by Rho-dependent protein kinase (ROCK) to activate the formation of stress fibres (Takeya *et al.* 2008).

Actin-based motility of pathogens

Many intracellular pathogens are able to use actin-based motility to move within and between cells and display speeds between 3 to 87 µm per minute depending on the host cell type (reviewed in Stevens *et al*. 2006). They are able to interfere with the host cell actin structure by reorganizing it for movement inside the cell which leads to the formation of an actin tail at one pole of the bacterium. These tails are made up of growing actin filaments that propel the bacterium through the cytosol at high speed. The actin does not move with the bacterium but is fixed in the cytosol and depolymerizes at a constant rate. Therefore the length of the actin tail is proportional to the rate at which the bacterium is moving (reviewed in Stevens *et al*. 2006).

Most pathogens that utilise actin-based motility rely on the cellular Arp 2/3 complex. The organisation and distribution of actin filaments is determined by nucleation and elongation factors such as Arp2/3

complex and NPFs that assemble actin networks. Bacteria are able to exploit this mechanism for their own benefit where they mimic host cell WASP or recruit WASP to the bacterial pole (reviewed in Stevens *et al*. 2006). Activation of Arp 2/3 leads to a conformational change initiating the formation of new actin filaments and generates a branched actin network which forms the actin tail (Amann and Pollard 2001, Gouin *et al*. 2004). Bacteria can form comet tails that consist of either branched or unbranched actin filaments. Many of the bacterial factors that are necessary for intracellular motility are expressed at the pole of the bacterium from which the actin-rich tail forms. Two known mechanisms of actin-based motility deployed by intracellular pathogens using the Arp 2/3 complex are shown in Figure 3.

Figure 3: Arp 2/3-dependent actin-based motility of intracellular pathogens

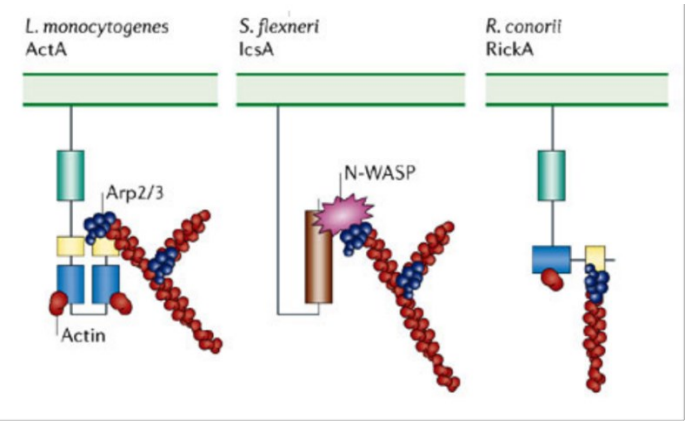

Mechanisms by which intracellular pathogens recruit and activate Arp2/3-dependent actin polymerization at the bacterial pole of the cell. Bacterial factors in *Listeria* and *Rickettsia*, ActA and RickA, are able to mimic Nucleation-promoting factors and bind directly to Arp 2/3 complex. In contrast *Shigella* employs a bacterial factor, IcsA that requires recruitment of N-WASP to bind to Arp 2/3 complex. (From Stevens *et al.* 2006)

Shigella flexneri

Shigella is a Gram negative bacterium that infects the intestinal epithelium, causing a diarrhoeal disease called shigellosis. It is a member of the group of pathogens that use actin-based motility to spread between cells. The bacterial factor IcsA is an autotransporter protein and a major virulence factor in the bacterium (May *et al.* 2012) (Sansonetti *et al*. 1991). IcsA is located at the pole of the outer membrane, where it orchestrates the actin polymerisation necessary for actin-based motility and cell spreading. IcsA interacts indirectly with the Arp 2/3 complex by recruiting N-WASP proteins to bind to the Arp 2/3 complex (reviewed in Welch *et al*. 2013).This links signalling pathways and aids in the *de novo* polymerisation of actin to start the formation of the actin tail (Suzuki *et al.* 1998).

IcsA belongs to a family of virulence-associated auto-secreted proteins of Gram negative bacteria. Autotransporters are proteins that have been translocated by the Type V secretion pathway in Gram

negative bacteria. Autotransporters can display many different functions and act as invasins, adhesins, proteases, or actin-nucleating factors (reviewed in Lazar-Adler *et al.* 2011). Autotransporter proteins are found in many Gram negative bacteria and have many functional domains. They include an N-terminal signal peptide, an internal passenger domain, and a C-terminal membrane anchor domain (reviewed in Cotter *et al*. 2005).

Host cell kinases play important roles in the stages of cell invasion by *Shigella*. They are known to have a role in bacterial cell entry and more recently in actin-based motility. Burton tyrosine kinase (Btk) depletion in *Shigella*-infected cells led to a decrease in N-WASP phosphorylation which affected the N-WASP recruitment to the bacterial surface and decreased actin-based motility (Dragoi *et al*. 2013). Host cell Abl kinases are also required for actin tail formation and motility. These kinases have been shown to phosphorylate N-WASP and help regulate actin tail formation and are important to the intracellular motility of *Shigella* (Burton *et al.* 2005).

Mycobacterium marinum

The Gram-positive bacterium *M. marinum* causes a systemic tuberculosis-like disease in fish and amphibians. It also causes pulmonary and cutaneous lesions in humans. It replicates inside macrophages, escapes into the cytosol and is able to actively polymerise actin (Stamm *et al.* 2003). Actin tails normally appear 15 hrs after infection and motility is dependent upon host WASP family proteins (Stamm *et al*. 2005). Inhibition of both WASP and N-WASP lead to incomplete actin polymerisation (Stamm *et a*l.2005). Actin-based motility occurs independently of known N-WASP activators such as Nck, and Cdc42 (Stamm *et al*. 2005). However little is known about the mechanism behind actin-based motility for *Mycobacterium* as a bacterial factor has yet to be identified.

Rickettsia

Rickettsia species are intracellular Gram negative bacteria that are responsible for a number of serious human diseases, including typhus and a variety of spotted fevers. Actin-based motility however is only seen in *R. conorii* and *R. rickettsia* which cause spotted fevers.

Rickettsia contains two bacterial factors that enable it to display different actin-based motility for different stages of infection. Initial motility is slow and uses the RickA protein whereas late motility involves Surface cell antigen 2 (Sca2) which is much faster due to the protein mimicking host formins

(Reed *et al.* 2014). RickA assembles branched actin networks and Sca2 assembles unbranched networks (Haglund *et al*. 2010) (Figure 4). For some strains of *Rickettsia* they only have Sca2 or RickA.

Sca2 is a bacterial actin-assembly factor that functionally mimics eukaryotic formin proteins, polymerising actin in an Arp 2/3-independent manner. Sca2 nucleates unbranched actin filaments which then polymerise and elongate into a tail (Haglund *et al.* 2010). The tails are seen to be long and straight rather than branched when deploying RickA (reviewed in Alberts and Way 2011). RickA mimics Nucleation-promoting factors and binds directly to Arp 2/3 complex to initiate the formation of an actin tail.

Figure 4: Sca2 and RickA mediated tails

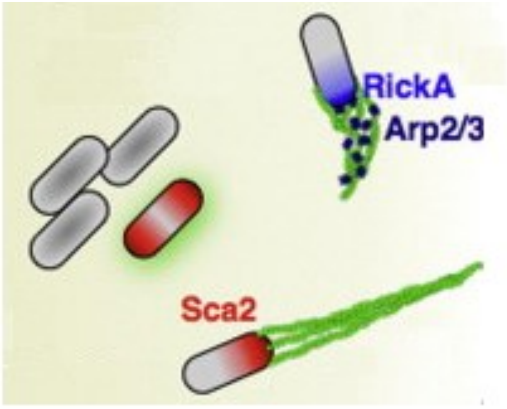

Diagram showing the two bacterial factors deployed by *Rickettsia* to form an actin tail. RickA mimics NPFs to bind directly to the Arp 2/3 complex and form branched networks. Sca2 mimics formin proteins to elongate straight actin filaments. (Adapted from Reed *et al*. 2014).

Listeria

Listeria is a rare foodborne pathogen that infects the intestinal mucosa and causes the disease Listeriosis. The bacterial factor ActA is able to mimic NPFs to recruit the important proteins of the actin machinery (Welch *et al*. 1998). It displays structural similarity with the VCA domain of other WASP proteins where the Arp 2/3 complex can bind (Zalevsky *et al*. 2001). The central region of ActA has four proline-rich repeats that contain FPPPP or FPPIP motifs. These mimic host cell cytoskeletal proteins zyxin, vinculin and palladin. The proline-rich sequences in these proteins, as well as ActA, bind to proteins of the Ena-VASP family which can then stimulate profilin (Witke 2004). These are small actin-binding proteins found in all cells that control the direction of actin networks and their rate of polymerisation (Auerbach *et al*. 2003).

ActA has been shown to be targeted by host cell Casein kinase 2 (CK2) which phosphorylates the WASP-binding region of Arp 2/3 on ActA (Chong *et al.* 2009). Studies on *Listeria monocytogenes* have shown that inhibition of CK2 reduced actin-based motility, raising the possibility that phosphorylation

plays a key role in this function (Chong *et al*. 2009). CK2 is an enzyme that phosphorylates Serines and Threonines. There are more than 300 cellular substrates that are ubiquitous and described for CK2 including: signalling proteins, transcription factors and cytoskeletal structural proteins. CK2 is a tetrameric enzyme displaying 2 redundant catalytic sub-units, CSNK2A1 and CSNK2A2, and two regulatory subunits, CSNK2B. Individual removal of these subunits showed no effect but both together showed it is required for *L. monocytogenes* cell to cell spread (Chong *et al*. 2011). The role of CK2 in *Listeria* actin-based motility was confirmed by an independent RNAi screen for kinases involved in *Listeria* actin-based motility (Chong *et al*. 2011).

Interestingly, in the same study Casein Kinase 1 (CK1) was shown to be dispensable for actin-based motility, but CK1 depletion showed a decrease in membrane protrusions into adjacent cells (Chong *et al*. 2011). Phosphorylation of the Arp 2/3 binding domain in ActA is regulated by CK2. It was shown to be vital for actin tail formation because the Arp2/3 complex did not co-localize with the bacteria and form tails in CK2-depleted cells (Chong *et al*. 2009). It is possible that a region of the BimA protein in *B. pseudomallei,* which is required for *B. pseudomallei* actin-based motility, may also be targeted by CK2 or other host cell kinases which could have a key role in controlling actin-based motility.

<u>*Vaccinia* Virus</u>

A close relative of the agent of smallpox (Variola virus) is the *Vaccinia* virus. It has been shown to use host cell actin for cell to cell spread of the virus. The virus is able to mimic receptor tyrosine kinase signalling pathways that control actin polymerisation at the plasma membrane. Phosphorylation of the viral protein A36R at tyrosine 112 and 132 are key to this motility as this results in direct interaction with the adaptor protein Nck and recruitment of N-WASP to the site of actin assembly stimulating Arp 2/3 (Frischknecht *et al.* 1999).

CK2 has been shown to also be important to *Vaccinia* actin-based motility where depletion of the enzyme impaired actin tail formation (*Alvarez et al*. 2012). It is possible that CK2 may stimulate adaptor protein recruitment potentionally through A36 phosphorylation.

<u>Enteropathogenic *Escherichia coli*</u>

Enteropathogenic *Escherichia coli* (EPEC) is a Gram negative bacterium that causes diarrhoea in humans as a result of infection in the small intestine. Attachment is followed by the formation of actin pedestals beneath the bacteria. EPEC use Type 3 secretion machinery to translocate the receptor

protein Tir (translocate intimin receptor), allowing it to link the bacterium to the actin cytoskeleton of the host cell (Kenny *et al*. 1997a). A Type 3 secreted effector protein Tccp (Tir cytoskeleton coupling protein) is required for Tir to mediate actin accumulation. Tccp binds to N-WASP which stimulates Arp2/3 resulting in polymerisation of actin.

Studies have shown that for actin assembly in EPEC, Tir requires phosphorylation of a tyrosine residue in the cytosolic C-terminal domain by phospholipase C-γ1 (Kenny *et al*. 1997b). Interestingly for a closely related species Enterohaemorrhagic *Escherichia coli* EHEC, the phosphorylation of the Tir protein is not required for actin assembly (Kenny *et al*. 1999).

Chlamydia trachomatis

Chlamydia is a Gram-negative intracellular bacterium which causes eye and genital disease. It is the most prevalent sexually transmitted bacterial pathogen in the western world. *Chlamydia* initiate their developmental life cycle once they have actively gained entry into host cells. The bacterium uses the T3SS to inject the translocated actin recruiting phosphoprotein (Tarp) into the cytosol. Actin is then recruited by Tarp to the attachment site and polymerised to allow entry. This is an example of a bacterial actin-binding protein that mediates invasion rather than actin-based motility. Studies have shown that phosphorylation of tyrosine residues in Tarp by Src and Ab1 family kinases had no effect on bacterial entry into host cells (Mehlitz *et al.* 2008) (Jewett *et al.* 2008).

***B. pseudomallei* actin-based motility**

B. pseudomallei is different from other bacteria as it does not express an actin mediator that mimics Nuclear Promotion Factors to initiate Arp 2/3 activity. The Arp 2/3 complex has been shown to be on the pole of *B. pseudomallei* during actin-based motility but N-WASP proteins were not important for actin polymerisation (Breitbach *et al*. 2003). Work from the Stevens lab indicates that *B. pseudomallei* BimA polymerises actin *in vitro* independently of the Arp 2/3 complex (Stevens *et al*. 2005). A recent BimC paper shows that *B. pseudomallei* actin-based motility is not inhibited by Arp2/3 inhibitors (Lu *et al*. 2014). This therefore means that the bacterium is likely to display a unique mechanism of actin-based motility that is different from other intracellular pathogens. Recent studies have shown that BimA mimics host Ena/VASP proteins in nucleating and elongating actin filaments (Benanti *et al*. 2015). They showed that BimA mediated the elongation of 2/3 actin filaments and was able to remove capping proteins.

The mechanism of the polar targeting of the bacterial factor BimA is unknown. However, a recent screen has revealed a gene *bimC* (*Burkholderia* intracellular motility factor C), directly upstream of the *bimA* gene, that is required for actin tail formation by *B. thailandensis* (Lu *et al.* 2015). Deletion of *bimC* resulted in an even spread of BimA over the bacterial surface suggesting its potential role in polar targeting (Lu *et al*. 2015). A *bimC* mutant failed to show actin tails and motility but further studies are needed to investigate the effect on survival and virulence. In *B. thailandensis bimC* acts as an iron-binding protein and has been shown to interact with the transmembrane domain of *bimA* in an iron-dependent manner (Lu *et al*. 2015). *bimC* encodes a glycotransferase which could affect actin-based motility by glycosylation of proteins.

The *Burkholderia* species display different mechanisms of actin-based motility. In *B. thailandensis* the motility is Arp 2/3 dependent and nucleates branched filaments (Sitthidet *et al*. 2010) (Benanti *et al*. 2015). In contrast, in *B. pseudomallei* and *B. mallei* motility, BimA independently nucleates unbranched filaments (Benanti *et al*. 2015). The tail structure also differs between the species, as *B. thailandensis* actin tails are curved and dense whereas *B. pseudomallei* tails are longer and straighter, shown in Figure 5.

Figure 5: Different mechanisms of actin-based motility in *Burkholderia*

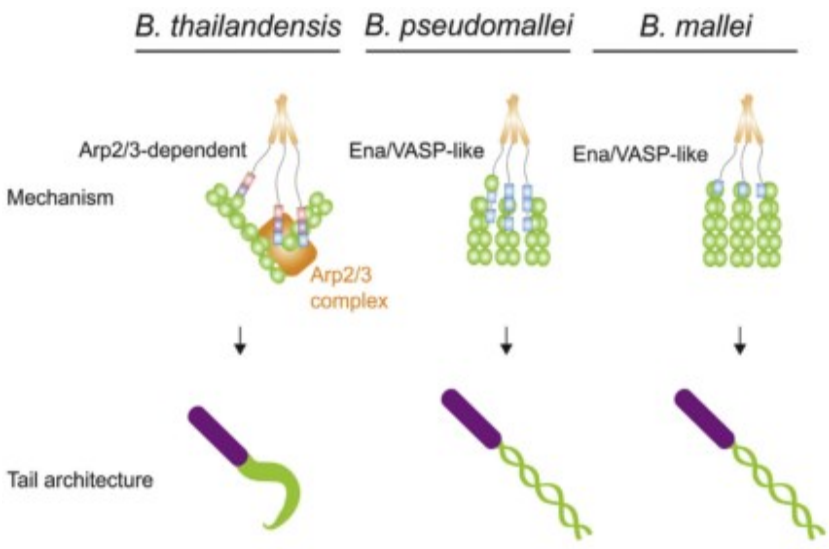

Diagram displaying the different mechanisms and tail structure amongst the *Burkholderia* species. *B. thailandensis* activates host Arp 2/3 complex to assemble branched actin networks. *B. pseudomallei* and *B. mallei* mimic Ena/VASP proteins to form unbranched networks in an Arp 2/3-independent manner. (From Benanti *et al*. 2015).

Distinct differences have been seen in the BimA protein among the closely related *Burkholderia* species as shown in Figure 6. *B. thailandensis* is different to *B. pseudomallei* in that $BimA_{th}$ contains a central acidic (CA) domain which is a key component to binding the Arp 2/3 complex (Sitthidet *et al.*

2010). This CA domain is commonly found in WASP binding proteins and is found in other bacterial factors such as *Listeria* ActA, and *Rickettsia* RickA. They also differ in the number of WH2 domains and proline-rich motifs (Stevens *et al*. 2005). $BimA_{ps}$ contains three WH2 domains whereas $BimA_{th}$ and $BimA_{ma}$ only contain one WH2 domain (Stevens *et al*. 2005). The PDAST repeat region is also only present in $BimA_{ps}$. $BimA_{ma}$ is also much shorter and more proline rich. Interestingly a *bimA* mutant of *B. pseudomallei* actin-based motility can be restored by $BimA_{th}$ and $BimA_{ma}$ (Stevens *et al*. 2005). It has been shown that BimA is highly conserved amongst natural populations of *Burkholderia* species (Sitthidet *et al*. 2008).

Figure 6: The functional domains of BimA in the closely related Burkholderia species

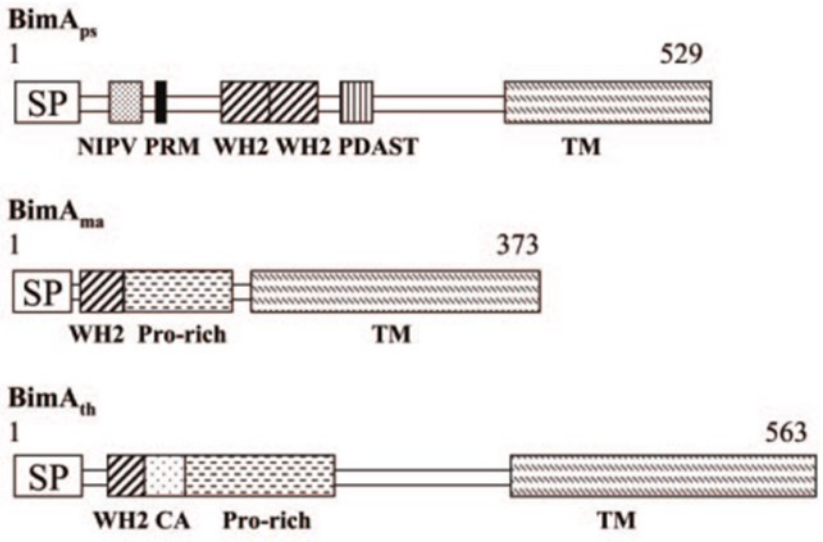

Figure shows functional domains of BimA in *B. thailandensis*, *B. mallei* and *B. pseudomallei*. Unique to $BimA_{ps}$ is the additional WH2 domains and PDAST repeat region. Unique to $BimA_{th}$ is the CA domain. (From Stevens et al. 2005)

Burkholderia **intracellular motility factor A**

Analysis of the *B. pseudomallei* BimA protein has led to a better understanding of its function. Figure 7 shows a schematic of the predicted functional domains in BimA. The first 1-53 amino acids are a predicted signal sequence. The C terminus acts as a membrane anchor similar to other Type V secreted proteins. There is a proline rich motif which is not needed for actin binding and polymerisation (Sitthidet *et al*. 2011). The protein contains three actin-binding WASP homology (WH2) domains and removal of either of these inhibited actin-based motility. These domains were shown to be vital to actin binding and polymerisation (Sitthidet *et al*. 2011). There are varying numbers of PDAST repeats, ranging between 2-7 motifs, which have been shown to affect actin polymerisation (Sitthidet *et al*.

2011). As the number of PDAST repeats increased so did the rate of actin polymerisation, however the repeats did not influence actin binding.

Figure 7 showing predicted functional domains of BimA protein:

Figure shows the amino acid sequence of BimA with the functional domains highlighted. **X** – Putative signal sequence, **X** – C-terminus, **X** – Proline-rich motif, **X** – direct PDAST repeats, **X** and **X** WH2-like motifs.

MPSSTNPTSLPIDMHAKASSSHAPDAPKPSSIATTLCRALASLSLGLSMDAEANPPEPPGGTNIPVPPPMPGGGA
NIPVPPPMPGGGAN**IPPPPPPP**GGIGGATPSPPPLTPVNGNPGA**STPTKTGLLKTLNRLSAELQNNPRVTEDVVD**
NVDAVIRNAVNLAPDAN**GDFSGRSAMPIEMAANAALRSLKKNPGDAGHAAPAYLPAERIGQLREKVRRTIEAL**
ESNRPPKPQPRSTPPQSTPPKPTQHPTAPNPNV**PDASTPDASTPDASTPDASTPDAST**PSR**PAPAPRAGTGAPA**
ASAATRAPAFANRVRKPNPAMPAASSHAIASDFASSNAFAIGDDSTAVGAQAIAFSEQSIAIGSRAIAAGARSIA
VGTDATAAAPDSVALGSGSIAEREGTVSVGRDGHERQITHVASGTEPTDAVNVTQLRAAMSNANAYTNQRIG
DLQQSITDTARDAYSGVAAATALTMIPDVDRDKRVSIGVGGAVYKGHRAVALGGTARINENLKVRAGVAMSA
GGNAVGIGMSWQW

A similar observation has been seen in Enterohaemorrhagic *Escherichia coli (EHEC)* a common food-borne pathogen. It colonises the gut epithelium at the border of the microvilli forming actin pedestals beneath adherent bacteria. EHEC translocates the receptor protein Tir, allowing it to link the bacterium to the actin cytoskeleton of the host cell. A Type 3 Secreted effector protein Tccp (Tir cytoskeleton coupling protein) is required for Tir to mediate actin accumulation. Tccp binds to N-WASP which stimulates Arp 2/3 resulting in polymerisation of actin. The number of proline rich motifs in Tccp was shown to influence actin pedestal formation (Garmendia *et al*. 2006). Proline rich motifs are found in most pathogens that utilise NPFs in their weaponry to influence recruitment of actin monomers. The number of proline motifs in *Listeria* ActA has also been shown to influence the rate of motility (Smith *et al*. 1996).

Aim and Objectives

To investigate the effect of phosphorylation of BimA on actin-based motility of *B. pseudomallei*

This project aims to reveal new insights into the mechanism behind actin-based motility of *B. pseudomalle*i. Actin polymerisation has been shown to be vitally important to intracellular survival of *B. pseudomallei* and the identification of phosphorylation sites in the BimA protein could lead to the development of novel anti-infectives. The PDAST repeats are a potential target for phosphorylation and their varying number suggests they could play an important role in the function of the protein. Specific phosphorylation sites in the BimA protein and predicted protein targets of CK2 have been identified raising the possibility of exploiting this information to improve therapy strategies. Vaccines could potentially be developed to provide protection against this pathogen that causes severe disease. *Listeria* ActA has already shown good promise as a vaccine candidate (Darji *et al*. 2003) and the aim is for BimA to be a possible candidate from the results of this study.

Objectives:

- Perform a bioinformatics analysis to identify potential phosphorylation sites of BimA and the identity of cellular kinases involved in this modification.
- Identify sites of phosphorylation by mass spectrometry of BimA immuno-precipitated from cells.
- Generation of a *B. thailandensis bimA* deletion mutant which would allow live cell imaging at lower containment level.
- Generate Phospho-mimicking and phospho-null BimA mutant proteins by substituting Serines residues in the PDAST repeat region for alanine (for a null mutant) and aspartic acid (for a charged constitutively-phosphorylated mutant). These will be used to show the effect of phosphorylation on actin-based motility by expressing these mutant proteins in a *Burkholderia bimA* mutant.

Chapter 2: Materials and Methods

Bioinformatics analysis of *B. pseudomallei* BimA

Three online phosphorylation prediction databases were used to identify predicted phosphorylation sites in the *B. pseudomallei* BimA amino acid sequence (strain 10276, accession number EU439427):

Netphos (http://www.cbs.dtu.dk/services/NetPhos/)

ELM (http://elm.eu.org/)

GPS 3.0 (http://gps.biocuckoo.org/)

GPS 3.0 was then used to search for host cell kinases predicted to phosphorylate each residue. The score value is calculated by the GPS algorithm to evaluate the potential of phosphorylation at each residue. The higher the value, the higher the likelihood the residue is phosphorylated. The highest scoring kinases predicted for each phosphorylation site were recorded.

Transfection of HeLa cells with CD32-BimA

A HeLa cell suspension was diluted in Dulbecco's Modified Eagle Medium (DMEM) supplemented with 10 % (v/v) heat inactivated foetal calf serum (FCS) to achieve a concentration of 5.5×10^5 cells / ml. 1.1×10^6 cells were seeded to each test well on a 6-well plate. The 6-well plates were incubated at 37 ˚C with 5% CO_2 overnight.

pCD32-BimA was purified using the Qiagen miniprep spin kit from an overnight culture of *E. coli* containing pCD32-BimA (previously generated by Stevens laboratory, Stevens *et al.* 2005). 2µg pCD32-BimA was added to Optimem (Gibco) before combining with Lipofectamine (Invitrogen) for 20 mins at room temperature. The combined 2µg pCD32-BimA and Lipofectamine was then added to the test wells and incubated for the appropriate time at 37 ˚C with 5% CO_2. Optimem was added to control wells.

Costaining of cells

Following 24 or 48 hours incubation of cells transfected with pCD32-BimA, media was removed and cells were fixed overnight with 4% Paraformaldehyde/Phosphate Buffered Saline (PBS). Cells were washed twice with PBS and then permeabilised with 0.5% Triton X-100 in PBS for 15 minutes

at room temperature. Cells were washed twice with PBS. 0.5% Bovine serum albumin (BSA)/PBS was then added for 30 minutes at room temperature. Coverslips were transferred onto parafilm on wet tissue paper. 1 µg/ml anti-CD32 antibody (Genetex) in BSA/PBS was added to the coverslips at 37 °C for 1 hour. Coverslips were washed thoroughly in PBS. 1 µg/ml anti-mouse antibody 568 in BSA/PBS was added to the coverslips and incubated at 37 °C for 1 hour. Coverslips were washed as before. 5 U/ml Phalloidin 488 was added for 20 minutes at room temperature. Coverslips were washed as before. Coverslips were then stained with 9.53 µM DAPI and then washed in water before being mounted on glass slides with 15 µl of Prolong Gold (Molecular Probes).

In some experiments, intracellular bacteria were detected by incubating with either primary antibody used was anti-LPS Rab 204 at 1 in 200 dilution. 2nd antibody used was 1 µg/ml anti-rab 568 (Invitrogen) or primary antibody used was 1 µg/ml mouse anti-*Pseudomonas mallei* LPS. Secondary antibody used was 1 µg/ml anti-mouse 568 (Cell signalling).

Confocal microscopy

Coverslips were imaged using Zeiss LSM 710 confocal microscope and a 40X lens objective. Fluorophores were excited with lasers at 365 nm, 488 nm and 568 nm. Emissions were detected using mirror/ band-pass filters at 420-470 nm, 500-550 nm and 570-640 nm. Images were then processed using Zen and Image J software.

Immunoprecipitation

Media from a pCD32-BimA transfected 6-well plate was removed and cells were washed twice with PBS. Cells were lysed with Non-denaturing lysis buffer (NaCl 150 mM, Tris (Ultrol) 10 mM, NP40 2 %, EDTA 5 mM) containing inhibitors: 1 mM PMSF, 2 mM Na orthovanovate, 10 µg/ml Leupeptin, 10 µg/ml Aprotonin, 1 µg/ml Pepstatin, 4 mM NaF, 2 mM Napyrophosphate and centrifuged at 16000 X g for 5 minutes. The supernatant was transferred into an eppendorf and incubated with 2 µg anti-CD32 antibody (Genetex) overnight at 4°C on a rocking platform. 80 µl of protein A-agarose beads (Sigma) (pre-washed in PBS) was added and incubated at room temperature for 1 hour. The immunoprecipitated protein was washed three times with ice-cold Tris pH 8.

SDS-polyacrylamide gel electrophoresis (SDS-PAGE)

Protein separations by SDS-polyacrylamide gel electrophoresis (SDS-PAGE) were as described by Laemmli (1970). Samples were prepared by adding an equal volume of 2X Reducing Sample Treatment Buffer (RSTB) with 1/50 volumes of β-Mercaptoethanol. Samples were incubated at 95°C for 10 minutes immediately prior to electrophoresis. Gels (Bio-Rad Any Kd) were run using Bio-Rad Protein 2 apparatus and gels were submerged in running buffer (25 mM Tris-HCL, 192 mM glycine, 0.1 % SDS) for electrophoresis.

Gels washed twice for 5 minutes with water were then stained with Simplyblue Safestain for 1 hour at room temperature. Gels were then de-stained in water. Alternatively gels were silver-stained. Gels were fixed twice for 15 minutes in 30 % (v/v) ethanol and 10 % (v/v) acetic acid solution followed by two washes for 5 minutes in 10 % (v/v) ethanol, then two washes for 5 minutes in water. Gel was sensitized with Sensitizer solution (0.2 % Sensitizer in water, Pierce Technologies) for 1 minute, then washed twice for 1 minute with water. Gel was then stained with Stain solution (2 % Enhancer in Silver stain, Pierce Technologies) for 30 minutes before two washes for 1 minute with water. Gel was then developed with Developer solution (2 % Enhancer in Developer, Pierce Technologies) until bands appeared before a final wash with 5 % (v/v) acetic acid.

Western blotting

Transfer of protein to nitrocellulose membranes (GE Healthcare Life Science) was performed using Bio-Rad Trans-Blot Turbo transfer apparatus at 2.5 A and 25 V for 3 minutes, submersed in transfer buffer (25 mM Tris-HCL, 192 mM glycine, 20 % methanol). Following transfer, membranes were first blocked using PBS containing 5 % (w/v) non-fat milk protein for 1 hour at room temperature. Following two 5 minutes washes in PBS containing 0.1 % (v/v) Tween-20 (PBS-T), membranes were then incubated in 1˚ antibody diluted in PBS-T. Primary antibodies used were mouse anti-FB5, anti-AF8 and anti-FG11 at 0.5 µg/ml and 1 µg/ml goat anti-actin (Genetex). Following two 5 minutes washes in PBS-T membranes were incubated for 1 hour at room temperature with 2˚ antibody diluted in PBS-T. Secondary antibodies used were anti-mouse ^{680} (Cell signalling) and anti-goat ^{800} (IR Dye) at 1 µg/ml. Membranes were then washed five times for 5 minutes in PBS-T before a final wash of PBS for 5 minutes. Antigens were detected using the Li-Cor (Biosciences) image system according to the manufacturer's instructions.

In-Gel Trypsin Digest of Proteins Separated by SDS-PAGE

Gel bands were excised with a clean scalpel and diced into 1 mm cubes before being transferred to a 1.5 ml Protein Low binding eppendorf. Bands were washed with 25 mM Ammonium Bicarbonate for 30 minutes at room temperature. Bands were then washed with 50 % (v/v) 25 mM Ammonium bicarbonate in Acetonitrile for 30 minutes and again with Acetonitrile for 10 minutes. Samples were dried in a SpeedVac for 10 minutes before incubation with the reducing reagent 10 mM DTT (25 mM Ammonium Bicarbonate solution) for 1 hour at 56 ˚C. Gel pieces were washed with 5 mM Ammonium Bicarbonate solution and then incubated with the alkylating reagent 55 mM Iodoacetamide for 30 minutes in dark at room temperature. Following two washes with 50 % (v/v) 25 mM Ammonium bicarbonate in Acetonitrile for 10 minutes and one wash with Acetonitrile for 10 minutes the gel pieces were dried in SpeedVac for 10 minutes. Trypsin was added and the gel was digested overnight. Extraction buffer 50 % (v/v) Acetonitrile and 0.1 % Formic acid was added and incubated for 30 minutes before drying and analysis by Proton Magnetic Resonance (PMR) Spectrometer.

Mass Spectrometry analysis

Analysis was carried out on the in-gel Trypsin digest of CD32-BimA by the proteomics team at the Roslin institute. Another sample of immunoprecipitated CD32-BimA was generated and eluted in an elution buffer containing 100 mM Tris-HCl (pH7.6) and 4% (w/v) SDS before mass spectrometry analysis by Dundee Cell Products. Expected peptides were generated by trypsin digest of CD32-BimA *in silico* generated using ExPASY peptide cutter (Gasteiger *et al*. 2005).

Extraction of *B. thailandensis* genomic DNA

A *B. thailandensis* (E30 strain) 10 ml stationary phase culture was collected by centrifugation at 16000 X g for 5 minutes. Cells were resuspended in 567 µl TE buffer (10 mM Tris-HCl (pH8.0) and 1 mM EDTA (pH8.0). 30 µl of 10 % SDS and 3 µl of 20 mg/ml Proteinase K was added and incubated at 37 °C for 2 hours. 100 µl of 5 M NaCl was added before 80 µl of CTAB/NaCl solution (8.2 g NaCl, 20 g hexadecyltri-methyl ammonium bromide (CTAB) in 200 ml water; filter-sterilised). 750 µl of phenol:chloroform:isoamyl alcohol was added to the CTAB/NaCl solution, mixed thoroughly and centrifuged at 16000 X g for 40 minutes. The aqueous supernatant was removed to a fresh microfuge tube and the wash step was repeated and centrifuged for 30 minutes. A third extraction was repeated and centrifuged for 15 minutes. The aqueous supernatant was removed and 450 µl

of room temperature isopropanol was added before being centrifuged at 16000 X g for 10 minutes. Supernatant was removed and 400 μl 70 % (v/v) ethanol was added to rinse the pellet before being centrifuged at 16000 X g for 5 minutes. Supernatant was removed and pellet was allowed to air dry. This was resuspended in 50 μl water before adding RNase to a final concentration of 10 μg/ml and incubated for 20 minutes at room temperature. The DNA was then quantified using the Nanodrop spectrometer (ND-1000 Labtech International).

Polymerase chain reaction

Polymerase chain reactions (PCR) were performed in 20 μl volumes, using 1 μg template DNA, 0.5 μM oligonucleotide primers and 500 μM deoxynucleotides. To each reaction GC Rich Phusion buffer (Invitrogen) was added to final concentration of 1.5 mM $MgCl_2$ and 1 % DMSO. 0.4 units of Phusion polymerase (Invitrogen) was then added and 50 cycles of amplification performed. Templates were denatured at 98 ˚C for 3 minutes, primers annealed at 65 ˚C and extension performed at 72 ˚C.

Agarose gel electrophoresis

Agarose was used at 1 % (w/v) for resolution of DNA fragments, in TAE buffer pH 7.7 (40 mM Tris-acetate, 1 mM EDTA) containing 1 % (v/v) Syber safe DNA stain (Invitrogen). Prior to loading, samples were mixed with 1/6 volumes of 6 X loading dye (Invitrogen) Electrophoresis was performed at a constant voltage of 90 V in TAE buffer. DNA was visualised under ultraviolet light using a Geldoc (Alpha Innotech).

PCR product gel purification

DNA bands were cut out of the gel and purified following the protocol in the Geneclean kit. The DNA was then quantified using the Nanodrop spectrophotometer (ND-1000 Labtech International).

PCR-Ligation-PCR (PLP) mutagenesis

To construct fusions between the upstream and downstream flanking sequences of *B. thailandensis bimA*, the method of PLP mutagenesis described by Ali and Steinkasserer (1995) was used. Firstly, the two sequences to be fused together were separately amplified by PCR using Phusion polymerase. Approximately the same molar quantities were then phosphorylated at 37 ˚C for 2 hours. Phosphorylation reactions were performed in a 30 µl reaction volume containing 1 mM ATP, 50 U T4 Polynucleotide kinase (Promega) and T4 Polynucleotide kinase buffer (Promega) consisting of 50 mM Tris-HCl, 10 mM MgCl2, 5 mM DTT, 100 µM spermidine. Ligation was performed by combining 25 µl of the phosphorylation mix with 3U of T4 ligase (Promega) and T4 ligase buffer (Promega) at 4˚C overnight. Finally 1 µl of ligation reaction was used in a PCR reaction using external primers to amplify the fusion product.

Subcloning into pGEMT

Firstly, the sequence to be fused into pGEMT (Promega) was amplified by PCR using Phusion polymerase. The product was A-tailed at 72 ˚C for 30 minutes. A-tailing reactions were performed in a 10 µl reaction volume containing 1 mM $MgCl_2$, 2.5 U Taq DNA polymerase (Invitrogen), 1 mM dATP and PCR buffer (Invitrogen). Ligation was performed by combining the 10 µl mix with 3 U T4 ligase (Promega), 50 ng pGEMT EASY (Promega) and T4 ligase buffer (Promega) at 4 ˚C overnight.

Transformation of *E. coli*

50 µl XL1-Blue Competent cells (Agilent Technologies) or 50 µl PIR1 One Shot cells and typically 0.1 to 1 µg plasmid DNA were mixed and incubated on ice for 30 minutes. The cells were then incubated at 42 ˚C for 30 seconds, placed on ice for 2 minutes and then 0.5 ml Super Optimal broth with Catabolite repression (SOC) medium was added. Transformed cells were incubated at 37 ˚C for 1 hour and dilutions then plated onto selective medium.

Plasmid purification

Colonies from transformation were grown to mid-logarithmic phase (A_{600}~ 0.5) in Luria Broth (LB). Cells were centrifuged at 3000 X g for 10 minutes and plasmid DNA was purified following the protocol in the QIAgen miniprep kit.

Restriction digest of plasmids

Purified plasmids were cut using restriction enzymes at 37 ˚C for 4 hours. Restriction digests were performed in a 10 µl reaction volume containing either 12 U EcoR1 (Promega), 20 U Xho1 (Promega) or 15 U Xba1 (Invitrogen) and CutsmartBuffer (Biolabs). Products were analysed by agarose gel electrophoresis.

Cloning into pDM4

Firstly, the insert and pDM4 were digested with Xho1 and Xba1 to generate sticky ends. Approximately the same molar quantities were then ligated at 4 ˚C overnight. Ligation was performed by combining the 20 µl mix with 9 U T4 ligase (Promega), 1 mM ATP and T4 ligase buffer (Promega).

Colony PCR

For rapid screening of bacteria for specific DNA sequences, colony PCR was performed (Clackson *et al*. 1991). A reaction mix consisting of primers, deoxynucleotides, Phusion polymerase (Invitrogen) in a GC rich Phusion buffer (Invitrogen) was prepared and 20 µl dispensed into 0.2 ml PCR tubes. To each tube, a small amount of bacteria was then added using a sterile pipette. Reactions were heated to 98 ˚C for 3 minutes then 50 cycles of PCR performed. New primers were designed so that they would amplify the flanking regions of *bimA* and be specific for both *B. pseudomallei and B. thailandensis*. The new primers required a lower annealing temperature at 46 °C.

Growth of *B. thailandensis* strains

Glycerol stocks of *B. thailandensis* strains E30, BpG488, Bp9, Bp69, BpG1190 and Bp4 were spread onto LB plates with or without selection (50 µg/ml Chloramphenicol or 50 µg/ml Kanamycin) and incubated at 37 ˚C for 24 hours.

Conjugation of S17- λ pir pDM4-*bimA* with *B. thailandensis*

Single colonies of *B. thailandensis* E30 and S17- λ pir pDM4-*bimA* were grown to stationary phase in LB and selective LB media and then diluted in LB broth to A_{600} ~ 0.5. S17- λ pir pDM4-*bimA* has been previously generated by Charles Vander Broek. Conjugation reactions containing 10 mM $MgSO_4$ and 0.5 ml bacterial culture were performed through a filter membrane into sterile universals. The filter was placed on a LA plate and incubated at 37 °C overnight. The filter was vortexed in LB broth before serial dilutions were spread on selective plates and incubated at 37 °C for 2 days. Colony PCR was performed on single colonies and then agarose gel electrophoresis.

Sucrose selection

Positive single colonies showing the correct size band from PCR screen were grown to stationary phase in LB broth. Serial dilutions were then spread on 15 % (w/v) sucrose plates lacking NaCl and incubated at 30 °C for 2 days. Colony PCR was performed on single colonies and analysed by agarose gel electrophoresis.

Sucrose plates

4 g Tryptone (Oxoid), 2 g Yeast Extract (Oxoid) and 6 g Bacto Agar (Difco), in 200 ml distilled water (pH 7.25) with 15% (w/v) Sucrose (Sigma).

Infection of HeLa cells with possible *B. thailandensis bimA* mutants

Sterile coverslips were placed in a 24-well plate and 2 X 10^5 cells/ml HeLa cell suspension was seeded overnight at 37 ˚C with 5 % CO_2. Positive single colonies showing the correct size band from PCR screen were grown to stationary phase in LB broth. Bacterial culture was diluted 1/100 in DMEM and added to the wells. The plates were centrifuged for 5 minutes at 300 x g and then incubated at 37 ˚C for 30 minutes. Media was removed and then an overlay of 1 ml DMEM with kanamycin 250 µg/ ml was added. The plate was incubated overnight at 37 ˚C with 5 % CO_2 and then fixed with 4 % paraformaldehyde. Coverslips were then stained to detect bacteria and actin tails before being imaged on the confocal microscope.

Generation of a null and constitutively phosphorylated mutant pME-BimA

Glycerol stocks of *E. coli* containing pME and pME-BimA (previously generated from Stevens laboratory) were streaked onto LB agar containing 15 µg/ml tetracycline. Single colonies were then grown to stationary phase in selective LB broth. Cells were pelleted at 3000 X g at 4 ˚C for 10 minutes before the plasmid was purified using the Qiagen Maxiprep spin kit. Purified pME-BimA was then mutated by Dundee Cell Proteomics. Phosphorylation mutant plasmids pME-BimA S/A and pME-BimA S/D were generated by mutating the Serines in the PDAST repeat region of BimA to Alanines for a phospho-null and Aspartic acid for a phospho-mimic.

Transformation of pME-BimA into *B. pseudomallei*

Transformation of BimA mutant plasmids *B. pseudomallei* were performed by Jo Stevens. *B. pseudomallei* harbouring pME-BimA S/D and pME-BimA S/A was grown to stationary phase in LB broth containing 0.25 mM IPTG and 15 µg/ml tetracycline and expression of BimA was checked by western blot from bacterial lysates.

Infection of HeLa cells with *B. pseudomallei ΔbimA* mutant strains

Single colonies of *B. pseudomallei* 10276 and *ΔbimA* mutants carrying pME, pME-bimA, pME-bimA S/A and pME-bimA S/D were grown to stationary phase in LB broth containing 0.25 mM IPTG and 15 µg/ml tetracycline. Strains were then sub-cultured into LB broth containing 0.25 mM IPTG and 15 µg/ml tetracycline and incubated with shaking at 200 rpm at 37 °C for 4 hours.

Bacterial cultures were diluted to A_{600} ~ 0.5 followed by diluting 1/100 in DMEM containing 0.25 mM IPTG to produce the infection inoculum. Media was removed from wells that had been seeded with HeLa cells in suspension at 2 x 10^5 cells/ml on coverslips. 1 ml of the inoculum was added to each well. The infection was synchronised by centrifugation at 300 x g for 5 minutes. The plate was then incubated at 37 °C for 30 minutes. Infection media was removed and then replaced with DMEM containing 10 % FCS, 0.25 mM IPTG and 250 µg/ml Kanamycin. Plates were incubated at 37 ˚C for 20 hours.

Media was removed from all wells and replaced with 1 ml 4 % PFA in PBS to fix the cells. Coverslips were stained for bacteria and actin or bacteria and BimA before being imaged on the confocal microscope.

ImageJ analysis

Images taken from confocal microscopy were further analysed in Image J to calculate the actin tail length. The protocol from the Image J manual was followed to calculate the Feret's diameter. This value is the longest distance between any two points along the selection boundary and is also known as the maximum calliper.

Intracellular survival of *B. pseudomallei ΔbimA* mutant strains

An infection of HeLa cells by *B. pseudomallei* 10276 and *ΔbimA* mutants was performed. Bacterial cultures were diluted to A_{600}~ 0.5 followed by diluting 1/100 in DMEM. At 20 hours post-infection, media was removed and cells were washed twice with PBS. Cells were then lysed with 200 µl of 0.1 % (v/v) triton X in PBS followed by serial dilution in LB broth and plating onto LA plates. Plates were incubated for 2 days at 37 ˚C. The infection inoculum was serially diluted in LB broth and followed by plating onto LA plates incubated at 37 °C for 2 days.

Purification and concentration of GST-BimA

Single colonies of *E. coli* containing pGex-BimA were grown to stationary phase in LB broth containing 100 µg/ml ampicillin. This was sub-cultured into LB broth containing 100 µg/ml ampicillin and 10 µg/ml chloramphenicol at 37 °C for 3 hours. IPTG was added to achieve a final concentration of 0.25 mM and then incubated for a further 3 hours. Cells were centrifuged at 3000 X g at 4 ˚C for 10 minutes before being lysed with 5 % (v/v) Bugbuster (Novagen) and then incubated at room temperature for 20 minutes. The insoluble debris from the Bugbuster (Novagen) extractions was centrifuged at 3000 X g at 4 ˚C for 10 minutes. 200 µl of GSH agarose (pre-washed in 500 µl PBS) was added to the supernatant and incubated on a rocking platform at room temperature for 30 minutes. The GSH was then washed 4 times with PBS. 150 µl of elution buffer (10 mM reduced glutathione in 50 mM Tris, pH8.0) was added to GSH and incubated at room temperature for 10 minutes on a rocking platform. The sample was then centrifuged 16000 X g to pellet the beads and the eluate was transferred to a chilled eppendorf. This step was repeated 3 times to achieve a combined eluate of ~600 µl. Beads were washed by vortexing in PBS and centrifuged at 16000 X g before transferring the wash to the eppendorf containing the eluted protein. The eluate was then passed through a Novagen 2ml spin filter column and centrifuged at 16000 X g to remove any remaining beads and stored at 4 ˚C. The protein sample was diluted to 1.5 ml with 50mM Tris, pH7.5 and loaded into a U-tube concentrator 2H-2 centrifuged 16000 X g

for 30 minutes. The sample was diluted to 1.5 ml and centrifuged again. This step was repeated 5 times leaving ~200 µl protein solution.

In vitro Phosphorylation of GST-BimA by host cell kinases

Phosphorylation reactions of GST-BimA were performed in a 40 µl reaction volume containing 200 µM ATP, 1000U Casein Kinase 2 (NEB) or Glycogen synthase kinase 3 (NEB), 2 mM Na orthovanovate, 4 mM Na F, 2 mM Na pyrophosphate and NEB buffer (NEB) at 30 °C for 2 hours. Samples were loaded into a Phostag gel and run by SDS-PAGE electrophoresis. The gel was then SimplyBlue stained and the correct band was cut out and sent for mass spectrometry analysis at Dundee Cell Products. Trypsin gel digest and mass spectrometry analysis was then carried out by Dundee cell Products on *in vitro* kinase reaction of GST-BimA.

Recipes for 100 µM Phostag Gel:

2 ml stacking gel

30% acrylamide	300µl
1M Tris pH 6.8(to 375µM)	750µl
10% SDS	20µl
Water	930 µl
TEMED	10 µl
10% Ammonium persulfate	50 µl

4ml resolving gel (10%)

30% acrylamide	1.333 µl
1M Tris pH 6.8(to 375µM)	1.5ml
10% SDS	40 µl
Water	967 µl
TEMED	12 µl
10% Ammonium persulfate	60 µl
5mM Phostag	80 µl
10mM MnCl2	80 µl

Table of primers used for PCR

Primers	Sequence	Restriction Enzyme site	Experiment
P1	ATATAT**CTCGAG**ACGTCGCATACAGCCT	Xho1	PLP
P2	CATACGGCGAGGATGGATTGAA		PLP
P3	TGAGCGCGCCGCAAGCGCTCACCGCACACA		PLP
P4	ATATAT**GGTTACC**CGAAGAGCGAAGAGCGCGCCGCGC	BSte2	PLP
P2	ATATAT**TCTAGAC**ATACGGCGAGGATGGATTGAA	Xba1	Subcloning pGEMT
P1	ATTCACGCATCCGGTCA		Colony PCR
P2	ATGCTCTCGTTGAACTC		Colony PCR

Chapter 3: Identification of sites of BimA phosphorylation

Bioinformatics analysis of phosphorylation sites of BimA

There are around 500 kinases in the human genome many of which regulate key proteins by phosphorylation. A bioinformatics analysis of a protein of interest allows for phosphorylation sites and associated kinases to be predicted and potentially investigated further. It is possible that a predicted phosphorylated site in BimA could enhance its function and affect the actin-based motility of *B. pseudomallei*.

Online prediction tools (NetPhos, Elm and GPS 3.0) have been used to predict phosphorylation sites of BimA (Blom *et al*. 1999) (Puntervoll *et al.* 2003) (Xue *et al.* 2011). The amino acid sequence was searched through these databases and the combined data showed that in total 37 sites (18 Serines, 17 Threonines and 2 Tyrosines) in the BimA sequence are predicted to be phosphorylated as shown in Figure 8. Figure 9 displays the GPS 3.0 output of these phosphorylation sites and identifies candidate host cell kinases that are predicted to phosphorylate BimA at these sites.

Figure 8: Predicted phosphorylation sites of BimA

Figure shows the combined predicted phosphorylation sites of BimA sequence from online prediction tools. Predicted phosphorylated amino acids are shown by either S, T or Y for Serine, Threonine or Tyrosine. The functional domains are also highlighted: X – Signal sequence 1-53, X – Proline rich motif 90-97, X – WH2 motifs 120-158 and 168-246, X - PDAST repeat region 257-282, X C-terminal domain 285-529.

Figure 9: Host cell kinases predicted to phosphorylate BimA

The BimA amino acid sequence (1-529) was searched through GPS 3.0 on a high threshold and the highest scoring kinases are shown in the table. For each site the functional domain, position in sequence and specific predicted kinases are given. In red is the predicted phosphorylated Serine/Threonine/Tyrosine.

Functional Domain	Position	Sequence	Enzyme
Signal Seq	19	HAKASSSHA	DUN1, IKKb, BARK1
	20	AKASSSHAP	PIM2, SIK2, CK1e, TRPM7
	30	APKPSSIAT	NEK6, RPS6KA4
	35	SIATTLCRA	PLK2, CaMKK1, CaMKK2
	104	IGGATPSPP	ERK5, ERK2, GSK3
	111	PPPLTPVNG	MAPK14, JNK2, MAPK11, NLK, ERK2
	121	PGASTPTKT	CDK2, MAPK12, JNK1, ERK2
	135	LNRLSAELQ	ROCK1, PAK4, PKC-gamma, PKA C-alpha
	145	NPRVTEDVV	MAP2K2
WH2 motifs	171	NGDFSGRSA	IKKb
	188	AALRSLKKN	PKA C-alpha
	225	EALESNRPP	MAPK13
	235	PQPRSTPPQ	CDK6, DYPR1
	236	QPRSTPPQS	MAPK14, GSK3, NLK, JNK2, ERK1
	241	PPQSTPPKP	GSK3, MAPK14, MAPK12, JNK2, ERK2
	246	PPKPTQHPT	HIPK2
PDAST repeats	260	VPDASTPDA	BARK1, AMPKA2, CLK1, MNK1, DUN1, CK2a1
	261	PDASTPDAS	MAPK13, GSK3, CDK6, ERK1, CK1e
	265	TPDASTPDA	BARK1, AMPKA2, CLK1, MNK1, DUN1, CK2a1
	266	PDASTPDAS	MAPK13, GSK3, CDK6, ERK1, CK1e
	270	TPDASTPDA	BARK1, AMPKA2, CLK1, MNK1, DUN1, CK2a1
	271	PDASTPDAS	MAPK14, GSK3, CDK6, ERK1, CK1e
	275	TPDASTPDA	BARK1, AMPKA2, CLK1, MNK1, DUN1, CK2a1
	276	PDASTPDAS	MAPK14, GSK3, CDK6, ERK1, CK1e
	280	TPDASTPSR	MNK1, AMPKA2, TRPM7, BARK1, DUN1, CK2a1
	281	PDASTPSRP	MAPK14, GSK3, ERK2, MAPK13, CK1e
C terminal	293	PRAGTGAPA	CDK8
	391	LGSGSIAER	BRSK1, NPR1
	398	EREGTVSVG	PLK4, DYRK2, MRKCKa, CAMK2
	400	EGTVSVGRD	PLK4,
	411	ERQITHVAS	DAPK1
	415	THVASGTEP	LIMK1
	438	NANAYTNQR	PTK6
	449	DLQQSITDT	GRK4
	453	SITDTARDA	AMPKA1
	458	ARDAYSGVA	SRC2
	480	DKRVSIGVG	ROCK1, ERK3, IPL1, PRKD2

Predicted phosphorylation sites were identified in all functional domains of BimA apart from the proline rich motif. This region has previously been shown to be dispensable for actin binding (Sitthidet *et al.* 2011). A higher number of sites were predicted to be phosphorylated in the PDAST repeat region compared to other regions of BimA. This suggests the PDAST repeat region is more likely to be phosphorylated. Recent studies have showed an additive effect on actin polymerisation as the number of PDAST repeats increases (Sitthidet *et al.* 2011). This could be because of phosphorylation and so the Serine and Threonines in this region are good targets for BimA mutagenesis.

The analysis shows that BimA contains a lot of predicted sites for phosphorylation by cellular kinases, particularly serine/ threonine kinases. CK2 is a highly conserved protein kinase able to phosphorylate more than 300 substrates. Many of these proteins are involved in signal transduction, gene expression and other nuclear functions (Pinna 2002). Studies have shown a role in regulating cytoskeletal proteins as phosphorylation of Serine residues in WASP by CK2 increased the affinity for Arp 2/3 complex (Cory *et al*. 2003).

CK2 is a serine/threonine kinase that is ubiquitously expressed and has been shown to affect *Listeria* actin-based motility by phosphorylating the bacterial factor ActA (Chong *et al*. 2009). ActA is able to mimic host NPFs and recruit the Arp 2/3 complex to the pole of the cell. It displays structural similarity with the VCA domain of other NPFs where the Arp 2/3 complex can bind. It is within this region where CK2 phosphorylates ActA. Studies have shown that within the C region of the VCA domain is a CK2 binding motif (Chong *et al.* 2009). This motif contains two Serines that are phosphorylated by CK2. ActA phosphorylation mutants showed the importance of these two Serines as survival in a mouse model of a S/A and S/D mutant was affected. A reduced bacterial load was seen for the phosphorylation mutants compared to the wildtype. The phospho-mimic mutants were attenuated in their ability to spread from cell to cell and the data suggests that phosphorylation of this region needs to be tightly regulated for efficient actin-based motility (Chong *et al.* 2009). Therefore CK2 is vital to actin-based motility of *Listeria* by regulating the binding of the Arp 2/3 complex to ActA.

CK2 was predicted to phosphorylate Serines in the PDAST region of BimA shown in Figure 9. It is possible CK2 could phosphorylate BimA and affect *B. pseudomallei* actin-based motility in a similar way as in *Listeria*. However for *B. pseudomallei* actin-based motility has been shown to be independent of the Arp 2/3 complex. CK2 could potentially phosphorylate BimA in the PDAST region and regulate the binding of another host protein. CK2 has also been shown to be important for actin tail formation in another intracellular pathogen, vaccinia virus (Alvarez *et al.* 2012). A GST-BimA fusion protein has also been shown to be phosphorylated by CK2 in an in vitro kinase assay using radiolabelled ^{32}P-ATP (unpublished data from Stevens laboratory). CK2 therefore is a good candidate because it has been predicted to phosphorylate BimA, regulates cytoskeletal proteins and it has a role in actin tail formation for other intracellular pathogens. Inhibitors for CK2 such as 4, 5, 6, 7-tetrabromo-2-azabenzimidazole (TBB) could be used to investigate the effect of phosphorylation on actin-based motility of *B. pseudomallei* (Sarno *et al.* 2002).

Other kinases could also phosphorylate BimA and glycogen synthase kinase-3 (GSK-3) was another prominent kinase that came out of the bioinformatics analysis shown in Figures 6 and 7. GSK-3 was predicted to phosphorylate Threonines in the PDAST region by the online prediction tools. It was

originally identified as a regulator of glycogen metabolism, but now is understood to be involved in protein synthesis, cell proliferation, cell differentiation, microtubule dynamics and cell motility (reviewed in Frame *et al*. 2001). GSK-3 displays ubiquitous cytoplasmic expression (reviewed in Frame *et al*. 2001). GSK-3 could function similarly as CK2 does in *Listeria* actin-based motility to regulate the binding of host proteins to BimA through phosphorylation. CK2 and GSK-3 could be investigated further to investigate their effect on actin-based motility. It is also possible that any of the predicted host cell kinases may regulate the binding of actin to BimA or a host protein that stimulates the polymerisation of actin.

Phosphorylation has been predicted in the WH2 domains. These domains are known to be important in actin binding (Sitthidet *et al.* 2011) and studies have shown they are able to mimic host Ena/Vasp proteins to initiate the formation of the actin tail (Benanti *et al.* 2015). Phosphorylation in these domains could play a role in regulating the binding of actin to BimA and tail formation.

Two Tyrosine residues in the C terminal domain have been predicted to be phosphorylated from this analysis. Studies have shown that for actin assembly in EPEC, Tir requires phosphorylation of a tyrosine residue in the cytosolic C-terminal domain (Kenny *et al*. 1997b). This phosphorylation is important for formation of actin pedestals in EPEC and could be similar in *B. pseudomallei*.

Many kinases have been predicted to phosphorylate BimA and it is possible that multiple kinases phosphorylate BimA. These kinases may work together in regulating BimA for an effect to be seen in actin-based motility. Many sites have been predicted to be phosphorylated by multiple kinases and inhibiting one may not have an effect if another kinase compensates and phosphorylates the same site. Further studies could be done to inhibit multiple kinases if no effect is seen for just one. It is also possible BimA could be phosphorylated and this has no effect on actin-based motility. This has been seen in *Chlamydia* where phosphorylation of Tarp had no effect on its recruitment of actin (Mehlitz *et al.* 2008) (Jewett *et al*. 2008).

Ultimately we want to know if BimA is modified by host cellular kinases to affect the actin-based motility of *B. pseudomallei*. Phosphorylation of these sites could be an important modification for BimA to enhance the actin-based motility of *B. pseudomallei* in the host cell which therefore may increase its survival in a host. The phosphorylation sites identified from this analysis are only a prediction and may not actually occur however by combining multiple online prediction tools this improves reliability. The 37 sites that have been predicted should be compared to actual phosphorylation sites identified by standard LC/MS-MS techniques before further studies into their effect on actin-based motility are performed.

Identifying actual BimA phosphorylation sites

To identify which of the predicted sites are actual phosphorylation sites for host cell kinases, pCD32-BimA was transfected into HeLa cells so it can be expressed and then regulated by the cell. Initial experiments involved optimising conditions by investigating different concentrations of pCD32-BimA and time points of cell lysis. BimA has previously been cloned into a eukaryotic expression vector where the cytoplasmic sequences of CD32 have been replaced with BimA residues (Stevens *et al*. 2005). This resulting fusion protein, CD32-BimA, targets the membrane of the eukaryotic cell and mimics the localisation of BimA in *B. pseudomallei* where it is exposed to the cell cytosol (Stevens *et al.* 2005). Following transfection and expression in the cell the BimA protein was then immunoprecipitated and samples were generated for LC/MS-MS.

Transfection of HeLa cells with pCD32-BimA

HeLa cells were transfected with pCD32-BimA at two concentrations 2 µg and 4 µg to find the optimum concentration for expression. Samples were lysed at 48 hours and analysis by western blot showed HeLa cells expressing the protein, seen in Figure 10. A positive control of purified GST-BimA was used for the BimA antibodies which has a molecular weight of 68 kDa. For both concentrations CD32-BimA could be detected at the correct size band of 60 kDa. As both showed good expression, 2 µg was chosen as the optimal concentration for transfection and used for the immunoprecipitation experiments. Three negative controls were used: a non-transfected cell, cells transfected with only Lipofectamine, cells transfected with pCD32. Actin was present in all lysates at the correct size band of 42 kDa and acted as a protein loading control.

Figure 10: Western blot of lysates from transfected HeLa cells at 48 hours

Western blot showing expression of CD32-BimA in HeLa cells lysed at 48 hours after transfection with 2µg and 4 µg of pCD32-BimA using Lipofectamine. Negative controls of transfected, Lipofectamine-treated and cells transfected with pCD32 were used. Positive control of GST-BimA was used for the BimA antibodies. Proteins detected by incubation with anti-BimA and anti-actin followed by anti-mouse 680 and anti-goat 800 and imaged by Li-COR. Arrows point to the correct band for CD32-BimA and actin.

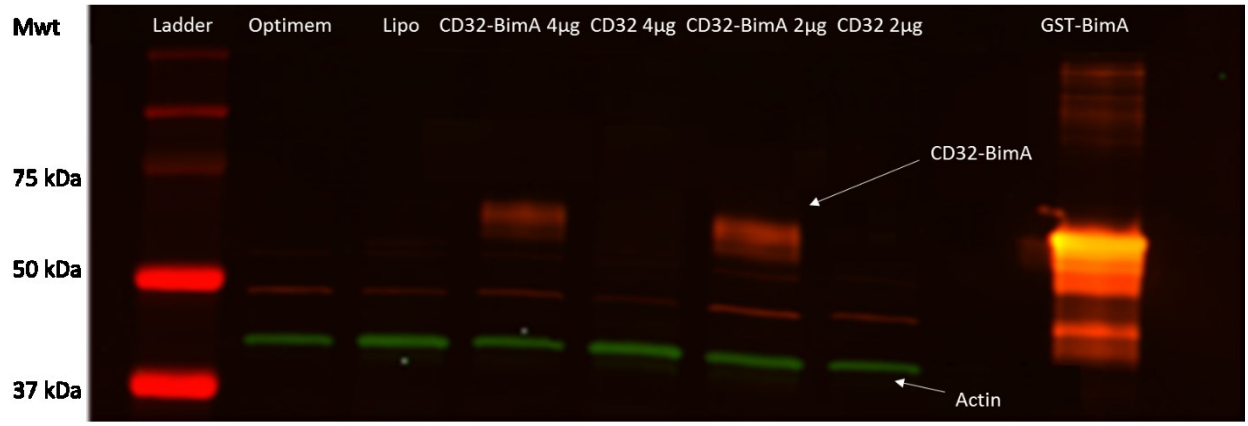

Having optimised the amount of DNA for transfection the next experiment was to optimise the time of lysis to obtain maximal CD32-BimA yield. HeLa cells were seeded onto coverslips and transfected with 2 µg pCD32-BimA before being fixed at 24 hours and 48 hours after transfection. Coverslips were then stained for CD32 actin and nuclei before being imaged on the confocal microscope. Example images can be seen in Figure 11. Transfected HeLa cells showed good expression at both timepoints however at 24 hours more CD32-BimA positive cells could be seen. This timepoint was chosen for the immunoprecipitation step because it showed more transfected cells and therefore was expected to yield more BimA protein.

Transfected cells appeared to show different morphology compared to untransfected cells shown in Figure 11. These cells appeared to have a disrupted and irregular shape which is likely to be because of the BimA protein recruiting actin and altering the structure of the cell. This cytoskeletal remodelling can be seen in Figure 11 by the presence of more stress fibres and membrane ruffles. Lamellipodia can also be seen as an actin projection on the leading edge of the cell. The transfection of DNA into the cell can also stress the cells and may have an effect on expression or the cell morphology. The cells may not be able to cope with too high a concentration of BimA and may be a reason why fewer cells were seen at a later timepoint of 48 hours. It is possible that at the later timepoint of 48 hours the

BimA protein has recruited more actin and disrupted the cell shape so much that the cells had detached. This could be why there are fewer cells at 48 hours after transfection or could be because of toxicity of lipofectamine.

Figure 11: HeLa cells after transfection with pCD32-BimA

Microscopy images of HeLa cells transfected with 2 µg pCD32-BimA. Cells were fixed in paraformaldehyde and then permeabilised with Triton X 100 before staining with anti-CD32 followed by anti-mouse 568, Phalloidin and DAPI. Blue channel – Nuclei, Red channel – CD32, Green channel – actin. A) Transfected HeLa cells at 24 hours and B) Transfected HeLa cells at 48 hours. Scale bar = 10 µm

A) HeLa cells at 24 hours after transfection with pCD32-BimA

Blue Channel - Nuclei

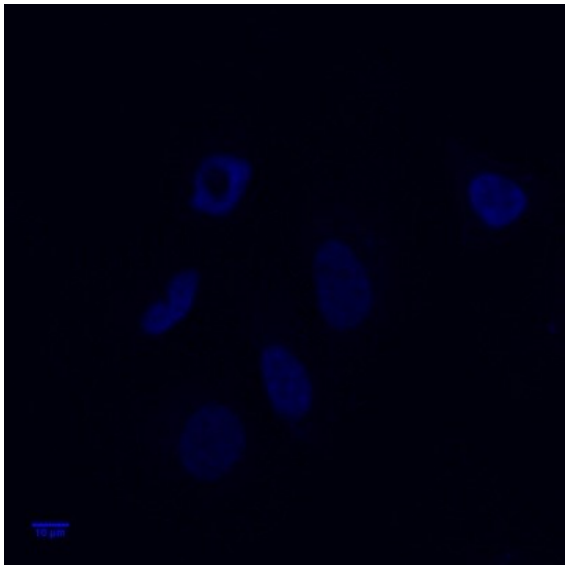

Red Channel – CD32-BimA

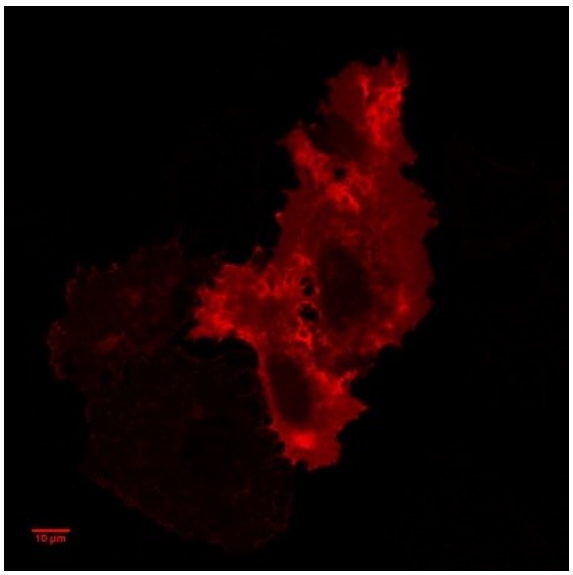

Green Channel - Actin

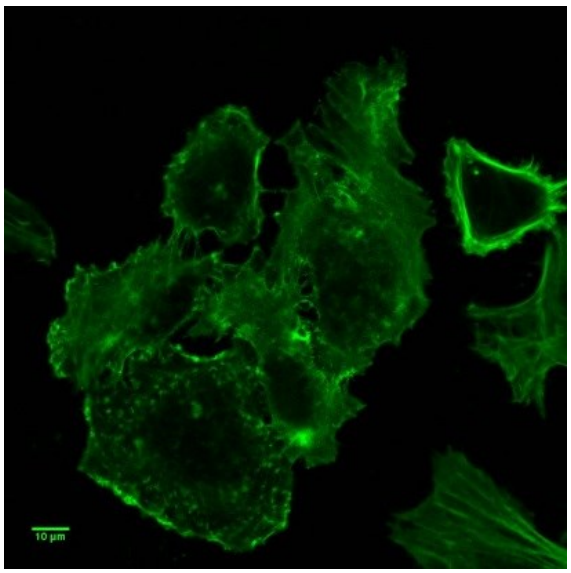

Merge

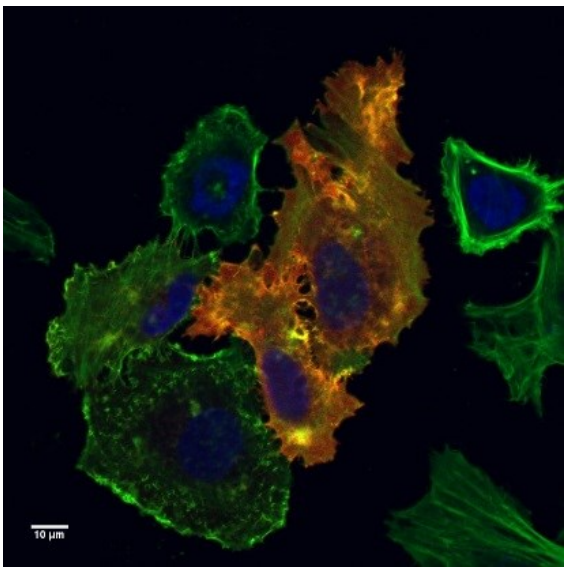

B): HeLa cells 48 hours after transfection with pCD32-BimA

Blue Channel - Nuclei

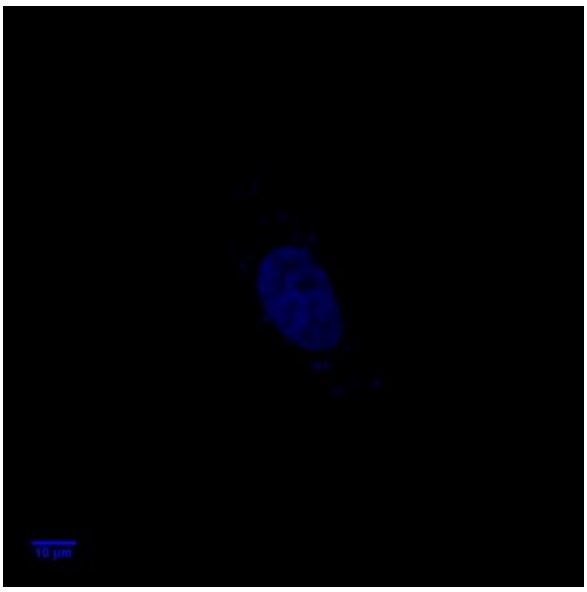

Red Channel – CD32-BimA

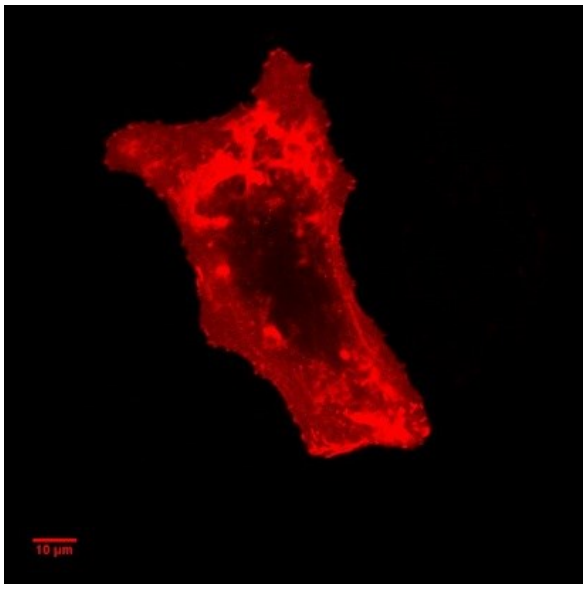

Green Channel - Actin

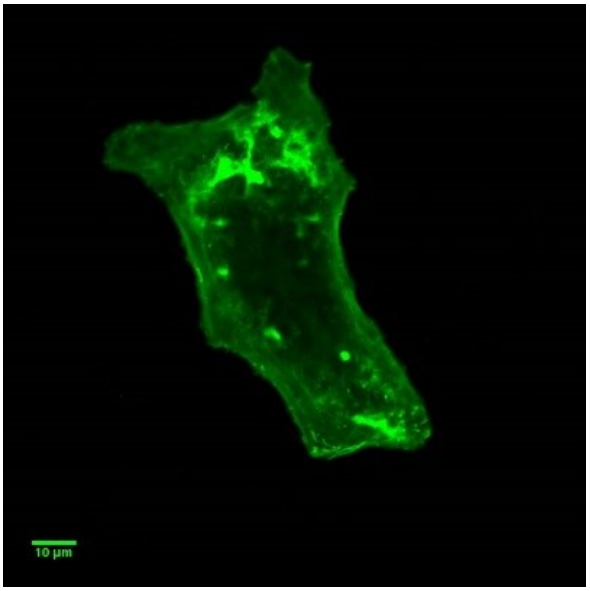

Merge

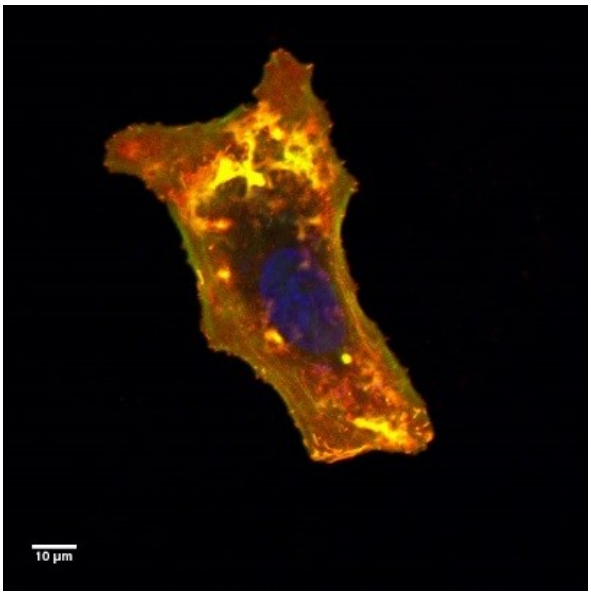

Immunoprecipitation of CD32-BimA from transfected HeLa cell lysates

The optimal expression conditions for transfection, 2 µg DNA and lysis of cells at 24 hours, were used and then CD32-BimA was immunoprecipitated. A lysis buffer containing inhibitor phosphatases was used to ensure that any phosphorylation of CD32-BimA was retained. Anti-CD32 was used to pull down CD32-BimA before adding agarose beads coated with protein A/G to bind to the antibody. This was then washed to remove any unspecific binding.

Initially the BimA protein could not be seen on a Simplyblue or silver stain gel or detected by western blot using anti-BimA (data not shown) so a series of experiments were performed to optimise the immunoprecipitation (IP). A western blot was carried out on samples from different stages of the protocol to find out where the protein was being lost. Lysates were centrifuged before IP to remove cell debris so samples were taken for the pellet (insoluble debris), supernatant (lysate that was Immunoprecipitated) and then after IP when protein is bound to the beads. A western blot was able to detect BimA in both the pellet and supernatant before IP but not after IP shown in Figure 12. There was only a faint band seen for BimA in the pellet compared to the supernatant which meant not much protein was being lost in that step. This meant therefore that the IP needed to be optimised. Actin was also detected and used as a loading control.

Figure 12: Western blot of optimisation of IP

Western blot showing levels of CD32-BimA in the different stages of IP; Pellet, Cell lysate Before IP and Cell lysate After IP. Negative controls of transfected, Lipofectamine-treated and cells transfected with pCD32 were used. Proteins detected by incubation with anti-BimA and anti-actin followed by anti-mouse 680 and anti-goat 800 and imaged by Li-COR. Arrows point to the correct band for CD32-BimA and actin.

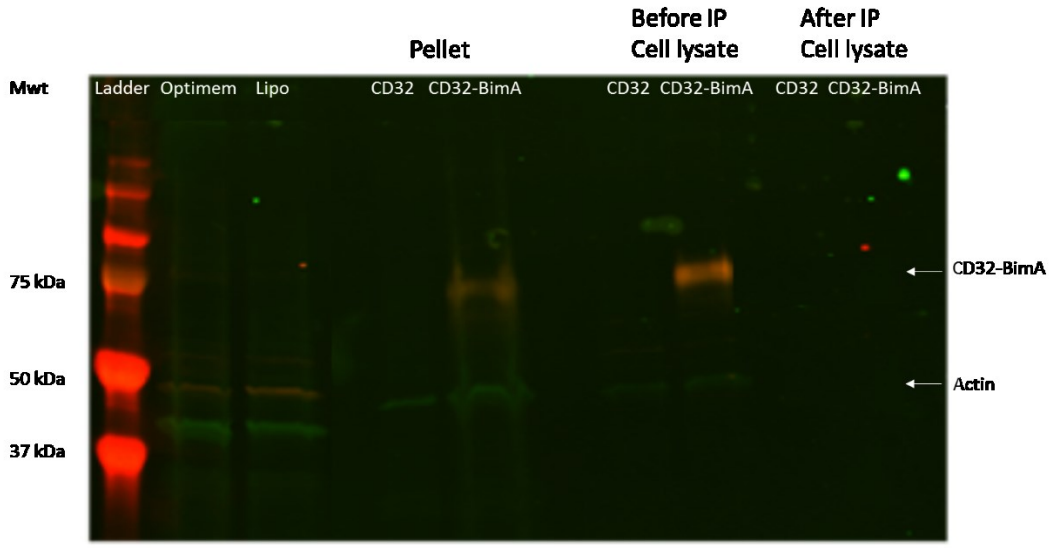

Safeblue stained gels were used to investigate whether the wash buffer had an effect on antibody binding to the beads. Results showed that a diluted wash buffer with a pH 8 increased the binding of antibody to beads (Data not shown). A western blot was carried out on lysates that had been immunoprecipitated with the diluted buffer and higher pH and was able to detect a faint band for BimA as shown in Figure 13.

Figure 13: Western blot before and after IP with optimised conditions

Western blot showing expression of CD32-BimA before and after IP with using a diluted buffer containing Tris at pH8. Negative controls of transfected, Lipofectamine-treated and cells transfected with pCD32 were used. Proteins detected by incubation with anti-BimA followed by anti-mouse 680 and imaged by Li-COR. Arrow points to the correct band for CD32-BimA.

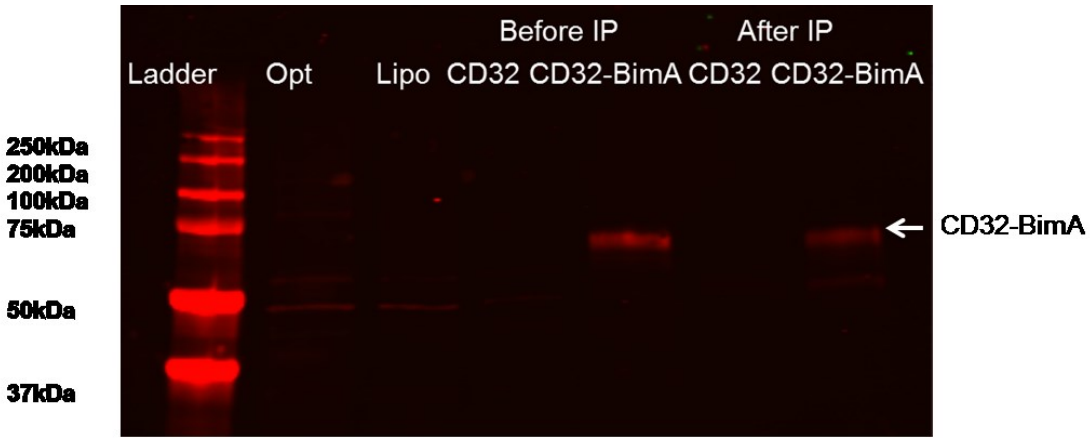

This level of protein would not be enough for a mass spectrometry analysis so more cells were transfected, 1.7 X 10^7 cells/ ml compared to 1 X 10^6 cells/ml. Figure 14 shows a western blot of lysates after transfecting a higher number of cells and optimising the IP conditions. A higher level of BimA was detected in the IP sample compared to before IP. The samples were from equivalent volumes and this indicates that the IP had been successful. A higher level of actin was detected after IP. This supports the observations by microscopy and in the literature of BimA interacting specifically with actin (Stevens *et al*. 2005) (Sitthidet *et al*. 2011). However there is also a lot of actin present in the negative controls which is probably due to non-specific binding of actin as it is the most abundant cellular protein.

Figure 14: Western blot of Immunoprecipitated lysates from transfected HeLa cells

Western blot showing expression of CD32-BimA before and after Immunoprecipitation of pCD32-BimA transfected HeLa cell lysates. Negative controls were used of untransfected HeLa cell lysates. Positive control of GST-BimA was used for the BimA antibodies. Proteins detected by incubation with anti-BimA and anti-actin followed by anti-mouse 680 and anti-goat 800 and imaged by Li-COR. Arrows point to the correct band for CD32-BimA and actin. This western blot shows expression of BimA from 1/12 of the immunoprecipitated sample and an equal proportion of the Before IP sample.

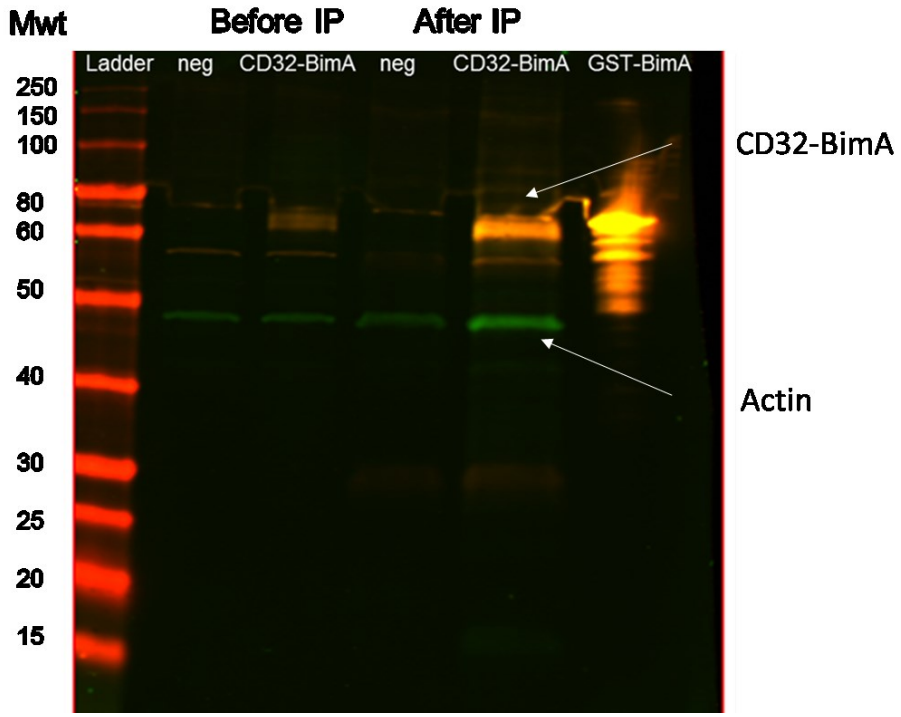

After immunoprecipitation the proteins in the sample were separated by SDS-PAGE and the gel was silver stained. Results showed many proteins present on the beads suggesting the IP was non-specific as shown in Figure 15. This may be because there is likely to be a higher concentration of host cell proteins in the lysates compared to the expressed BimA protein which would block the binding of anti-CD32 antibody to the protein A-agarose. These host proteins would bind to the protein A–agarose and are likely to represent insoluble membranes or vesicles that pellet with the beads. In order to improve this and make the binding more specific a different antibody could be used for the immunoprecipitation. Antibodies specific for BimA could be used which may decrease the non-specific binding of other host cell proteins. Coupling of antibody to beads may also improve the specificity and pull down. Further optimisation of the IP wash buffer could remove some of the non-specific proteins.

It is also possible that some of the host cell proteins identified in the sample could interact directly with BimA and be involved in the mechanism of actin-based motility of *B. pseudomallei*. After optimising the Immunoprecipitation further to decrease the number of non-specific protein bands on the gel, additional bands to BimA could be cut out of the gel and analysed by mass spectrometry to identify the host cell proteins. Any proteins identified could then be investigated further to analyse their role in actin-based motility and interaction with BimA.

Figure 15: Silver stained gel of Immunoprecipitated CD32-BimA

Figure shows a silver stained gel of Immunoprecipitated CD32-BimA. HeLa cells transfected with CD32 and CD32-BimA were immunoprecipitated with anti-CD32 before being run by SDS-PAGE and then the gel was silver stained. The Agarose beads were also loaded as a negative control.

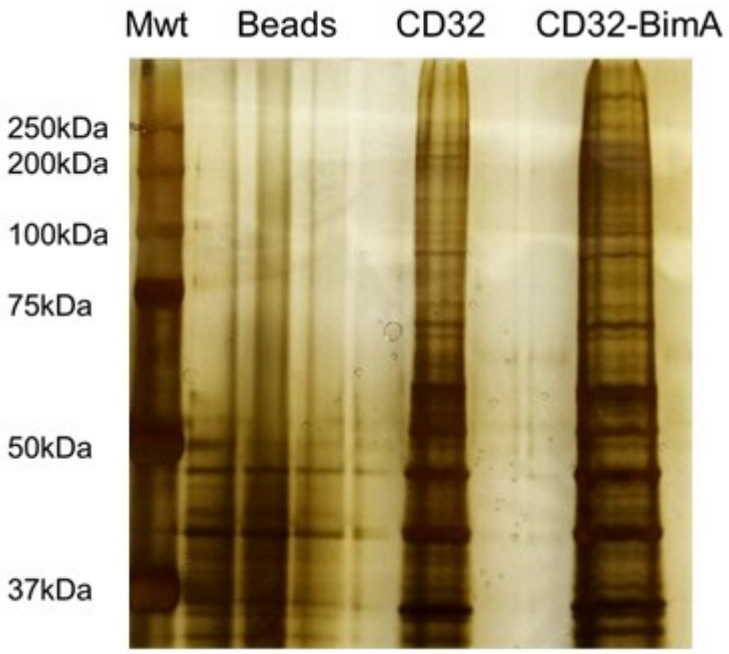

Mass Spectrometry of Immunoprecipitated CD32-BimA

In a previous experiment, multiple bands were cut out and mass spectrometry performed at Roslin was able to identify BimA however there was not enough protein for a phosphorylation analysis shown in Figure 16. Only 3 out of 40 peptides for a trypsin digest of the immunoprecipitated CD32-BimA (Figure 16) sample were detected by mass spectrometry with a 7.5 % coverage of the protein. Therefore because of the difficulty in identifying CD32-BimA and to obtain maximum protein an eluate

of the sample from the beads was analysed by mass spectrometry by Dundee Cell Proteomics who also have a more sensitive mass spectrometer shown in Figure 17.

Figure 16: Mass Spectrometry of Immunoprecipitated CD32-BimA Gel slice

Figure shows the expected peptides generated by trypsin digest of CD32-BimA *in silico* generated using ExPASY peptide cutter. In red are the actual peptides detected by mass spectrometry at the Roslin Institute.

MAMETQMSQNVPR_NLWLLQPLTVLLLLASADSQAAAPPK_AVLK_LEPPWINVLQEDSVTLTCQGAR_SPESDS
IQWFHNGNLIPTHTQPSYR_FK_ANNNDSGEYTCQTGQTSLSDPVHLTVLSEWLVLQTPHLEFQEGETIMLR_
CHSWK_ DK_PLVK_ VTFFQNGK_SQK_FSR_ DPTFSIPQANHSHSGDYHCGNIGYTLFSSKPVTITVQVPSMGSS
SPMGIIVAVVIAT_AVAAIVAAVVALIYMDAEANPPEPPGGTNIPV_PPPMPGGGANIPVPPPMPGGGANIPPPPP
PPGGIGGATPSPPPLTPVNGNPGASTPTK_TGLLK_TLNR_LSAELQNNPR_VTEDVVDNVDAVIR_NAVNLAPDA
NGDFSGR_SAMPIEMAANAALR_SLK_K_NPGDAGHAAPAYLPAER_IGQLR_EK_VR_R_TIEALESNRPPKPQP
R_STPPQSTPPKPTQHPTAPNPNVPDASTPDASTPDASTPDASTPDASTPSRPAPAPR_AGTGAPAASAATR_APA
FANR_VR_K_PNPAMPAASSHAIASDFASSNAFAIGDDSTAVGAQAIAFSEQSIAIGSR_AIAAGAR_SIAVGTDAT
AAAPDS

Figure 17: Mass Spectrometry of Immunoprecipitated CD32-BimA Eluate

Figure shows the expected peptides generated by trypsin digest of CD32-BimA *in silico*. In red are the actual peptides detected by mass spectrometry by Dundee Cell Products and in blue is the identified phosphorylated site.

MAMETQMSQNVPR_NLWLLQPLTVLLLLASADSQAAAPPK_AVLK_LEPPWINVLQEDSVTLTCQGAR_SPESDS
IQWFHNGNLIPTHTQPSYR_FK_ANNNDSGEYTCQTGQTSLSDPVHLTVLSEWLVLQTPHLEFQEGETIMLR_
CHSWK_ DK_PLVK_ VTFFQNGK_SQK_FSR_LDPTFSIPQANHSHSGDYHCGNIGYTLFSSKPVTITVQVPSMGSS
SPMGIIVAVVIAT_ AVAAIVAAVVALIYMDAEANPPEPPGGTNIPV_ PPPMPGGGANIPVPPPMPGGGANIPPPP
PPPGGIGGATPSPPPLTPVNGNPGASTPTK_TGLLK_TLNR_LSAELQNNPR_VTEDVVDNVDAVIR_NAVNLAPD
ANGDFSGR_SAMPIEMAANAALR_SLK_K_NPGDAGHAAPAYLPAER_IGQLR_EK_VR_R_TIEALESNR_PPK_
PQPR_STPPQSTPPK_PTQHPTAPNPNVPDASTPDASTPDASTPDASTPDASTPSR_PAPAPR_AGTGAPAASAAT
R_APAFANR_VR_K_PNPAMPAASSHAIASDFASSNAFAIGDDSTAVGAQAIAFSEQSIAIGSR_AIAAGAR_SIAV
GTDATAAAPDS

The analysis shows that 7 out of 40 possible tryptic peptides of the immunoprecipitated CD32-BimA sample were detected by mass spectrometry at Dundee Cell Products representing 17.5% coverage of the protein. There is a low coverage of the protein and many peptides are not detected. The experiment needs to be repeated to determine if the regions such as the PDAST repeat region that are not detected are phosphorylated by host cell kinases. This is a common issue with characterisation projects and complimentary mapping could be done to provide better coverage of the CD32-BimA protein. This would involve multiple digestions of the protein with different enzymes e.g. trypsin/chymotrypsin/AspN/V8 to generate the correct sized peptides for mass spectrometry analysis. To achieve a better coverage of peptides a higher number of cells could be transfected and then immunoprecipitated. This would increase the concentration and proportion of CD32-BimA compared to other nonspecific proteins in the sample. There are 34 predicted phosphorylation sites on the peptides that were not detected by mass spectrometry in this experiment. Previous studies have shown that BimA is phosphorylated in infected cells using ^{32}P-ATP pulse chase experiments and immunoprecipitation methods (unpublished data from the Stevens laboratory). Therefore an increase in number of peptides detected is likely to increase the number of phosphorylation sites identified.

All of the detected peptides were screened against the BimA protein and the bioinformatics analysis predicted 4 sites from these peptides to be phosphorylated; S_{135}, T_{145} and S_{171}. 1 out of 3 predicted phosphorylated sites in these peptides was identified in the CD32-BimA sample. The peptide LSAELQNNPR contained a phosphorylated Serine at position 135 in the BimA amino acid sequence. This phosphorylation site is located in one of the three WH2 domains and could be involved in the recruitment of actin and actin-binding proteins. These WH2 domains have been shown to be important for actin binding (Sitthidet *et al*. 2011) and shown to be able to mimic Ena/Vasp proteins by nucleating and elongating actin filaments (Benanti *et al*. 2015). The identified phosphorylation site could be phosphorylated by a host cell kinase to regulate the binding of actin and affect actin-based motility of *B. pseudomallei*. Phosphorylation mutants could be generated from this particular site to create a phospho-null and phospho-mimic mutant and investigate the affect on actin-based motility.

The bioinformatics analysis predicted 4 potential host cell kinases that could phosphorylate S_{135}; PKC-γ, PKA, ROCK1 and PAK4. PKC-γ is a member of the Protein kinase C family which plays a role in signal transduction by regulating neuronal receptors and its main tissue distribution is in the brain (Wetsel *et al.* 1992). *B. pseudomallei* is known to cause infection in the brain (Padiglione *et al.* 1996) and a host cell kinase specific to that tissue could be important in regulating the actin-based motility in such cell types. Cyclic-AMP (cAMP)-dependent protein kinase (PKA) is the main effector of cAMP signalling in all tissues and therefore has a ubiquitous tissue distribution (reviewed in Berthon *et al.* 2015). This

signalling pathway plays an essential role in the regulation of cortisol secretion (reviewed in Berthon *et al.* 2015). PKA has also been shown to regulate the bacterial factor IcsA in *Shigella* to effect the cell-to-cell spread (D'Hauteville and Sansonetti 1992).

ROCK-1 is involved in many types of cell motility such as: smooth-muscle contraction, cell migration and neurite outgrowth (reviewed in Riento and Ridley 2003). It is key regulator of the actin cytoskeleton and ubiquitously expressed (reviewed in Riento and Ridley 2003). ROCK-1 has been shown to phosphorylate and activate formins leading to the formation of stress fibres (Takeya *et al.* 2008). BimA is thought to mimic Ena/Vasp proteins which polymerise actin in a similar way to formins. ROCK-1 is a kinase that could phosphorylate BimA in a similar way as it does to formins. PAK 4 is also ubiquitously expressed and has a wide role in signalling pathways such as: cytoskeleton regulation, cell migration, growth, proliferation and cell survival (Ha *et al.* 2015).

Cells infected with *B. pseudomallei* could also be treated with inhibitors for these kinases and may show reduced actin-based motility if phosphorylation by the kinase is important. Inhibitors have been developed and studied for ROCK1 and PAK 4 (Liao *et al*. 2009) (Abdel-Magid 2015). The experiment would need to be optimised as these host kinases have important roles for the cell and treatment with too high a concentration of inhibitor could be toxic to the cell. An alternative experiment for analysing the effect of host cell kinases on *B. pseudomallei* actin-based motility would be to use siRNA to knockdown expression of the kinase. This method has been used to show the importance of CK2 phosphorylation on the actin-based motility in *Listeria* (Chong *et al*. 2009).

This experiment has shown that CD32-BimA can be expressed by HeLa cells and phosphorylated by a host kinase. CD32-BimA is a single monomer of 60kDa whereas native BimA forms a trimer at 180kDa. This difference in structure could have an effect on phosphorylation of BimA and this may affect the binding of a host cell kinase or which sites are exposed for phosphorylation. CD32-BimA is a fusion protein and only BimA would be normally expressed in a *B. pseudomallei* infection. This difference in structure could also affect which sites are phosphorylated. The identified phosphorylation site has been identified from BimA protein that was phosphorylated in an uninfected cell. During infection it is possible that the host cell processes may well be different and this could affect the phosphorylation of proteins.

To determine if phosphorylation of the identified site is important to *B. pseudomallei* actin-based motility, phosphorylation mutants could be generated. A phospho-null and phospho-mimic mutant could be generated and then expressed *in trans* in a *bimA* mutant as a trimer in *B. pseudomallei*. Cells could be infected and analysed for actin-based motility. Any difference seen in actin tail formation, length or structure would indicate that this phosphorylation site is important to actin-based motility.

Further studies could then be done to look at virulence of the phosphorylation mutants. A *Galleria mellonella* model could be used as an initial infection model before using a mouse model. For both models the effect of phosphorylation mutants on survival would be investigated. Infection models for *B. pseudomallei* have been well established and many studies have used them (Laws *et al.* 2011) (Wand *et al.* 2011).

In addition to phosphorylation there are other protein modifications that occur in the cell to affect protein function. Glycosylation, farnesylation and acetylation are examples of protein modifications that could affect the function of BimA. Mass spectrometry of the same immunoprecipitated sample of CD32-BimA could look for these other modifications which could then be analysed further by generating mutants in a similar way as with the phosphorylation site.

In vitro kinase reaction GST-BimA

Phosphorylation sites of a protein can also be identified by *in vitro* kinase reactions where specific host cell kinases can be studied. CK2 was used because it has previously been shown to phosphorylate *Listerial* bacterial factor ActA and regulates its actin-based motility (Chong *et al.* 2009). It is predicted to phosphorylate BimA and been shown by Jo Stevens to phosphorylate a GST-BimA fusion protein (unpublished data). GSK3, another prominent kinase that was predicted to phosphorylate BimA was also studied. GST-BimA was used as a template for *in vitro* kinase assays because a high concentration could be obtained from the *E. coli* engineered to express the protein. GSH-agarose was used to purify GST-BimA and GST from bacterial cell lysates. The purified protein was then analysed by SDS-PAGE and SimplyBlue staining (shown in Figure 18). The correct size band of GST-BimA was seen at 68 kDa and GST at 28 kDa. The results show a high concentration of GST-BimA and GST purified with only 1/100 of the sample loaded onto the gel.

Figure 18: Simplyblue stained gel of purified GST and GST-BimA

Gel shows a Simplyblue stain on purified GST-BimA and GST that was bound to the beads. Arrows point to correct size bands of GST and GST-BimA.

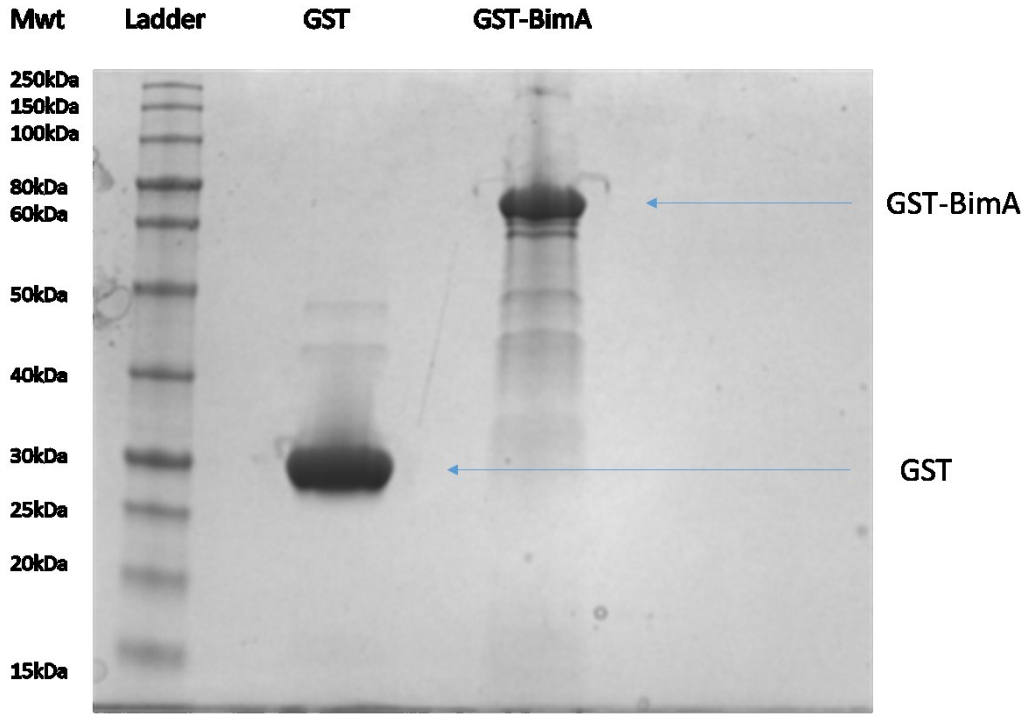

Mass spectrometry of *in vitro* kinase reaction of GST-BimA

The GST-BimA protein was eluted and concentrated to 3 mg/ml. 60 µg of the sample was incubated with commercially available CK2 and GSK3 before being analysed on a phostag gel. Phostag is a novel selective phosphate-binding tag used for detection of phosphorylated proteins in SDS-PAGE. During electrophoresis, phosphorylated proteins migrate through the gel and are labelled with the phostag. Migration speed decreases as they are separated from the non-phosphorylated proteins resulting in a mobility shift. This gel was Simplyblue stained and showed a mobility shift in the phosphorylated GST-BimA by both CK2 and GSK3 (data not shown). No mobility shift was seen for GST when incubated with CK2 or GSK3. The bands were excised and sent for mass spectrometry analysis at Dundee Cell Products shown in Figure 19.

Figure 19: Mass spectrometry of in vitro kinase reaction of GST-BimA

Figure shows the expected peptides of a trypsin digest of GST-BimA as predicted by ExPASY peptide cutter. In red are the actual peptides detected by mass spectrometry. A) Shows GST-BimA peptides phosphorylated by CK2 B) shows GST-BimA peptides phosphorylated by GSK3.

a) CK2

MSPILGYWK_IK_GLVQPTR_LLLEYLEEK_YEEHLYER_DEGDK_WR_NK_K_FELGLEFPNLPYYIDGDVK_LTQS
MAIIR_YIADK_HNMLGGCPK_ER_AEISMLEGAVLDIR_YGVSR_IAYSK_DFETLK_VDFLSK_LPEMLK_MFEDR
_LCHK_TYLNGDHVTHPDFMLYDALDVVLYMDPMCLDAFPK_LVCFK_K_R_IEAIPQIDK_YLK_SSK_YIAWPLQ
GWQATFGGGDHPPK_SDLVPR_GSPEFPGR_LER_PHR_DR_GSMNPPEPPGGTNIPVPPPMPGGGANIPVPPP
MPGGGANIPPPPPPPGGIGGATPSPPP_LTPVNGNPGASTPTK_TGLLK_TLNR_LSAELQNNPR_VTEDVVDNVD
AVIR_NAVNLAPDANGDFSGR_SAMPIEMAANAALR_SLK_K_NPGDAGHAAPAYLPAER_IGQLR_EK_VR_R_
TIEALESNR_PPK_PQPR_STPPQSTPPK_PTQHPTAPNPNVPDASTPDASTPDASTPDASTPDASTPSR_PAPAPR
_AGTGAPAASAATR_APAFANR_VR_K_PNPAMPAASSHAIASDFASSNAFAIGDDSTAVGAQAIAFSEQSIAIGS
R_AIAAGAR_SIAVGTDATAAAPDSVALGSGSIAER_EGTVSVGR_DGHER_QITHVASGTEPTDAVNVTQLR_AA
MSNANAYTNQR_IGDLQQSITDTAR

b) GSK3

MSPILGYWK_IK_GLVQPTR_LLLEYLEEK_YEEHLYER_DEGDK_WR_NK_K_FELGLEFPNLPYYIDGDVK_LTQS
MAIIR_YIADK_HNMLGGCPK_ER_AEISMLEGAVLDIR_YGVSR_IAYSK_DFETLK_VDFLSK_LPEMLK_MFEDR
_LCHK_TYLNGDHVTHPDFMLYDALDVVLYMDPMCLDAFPK_LVCFK_K_R_IEAIPQIDK_YLK_SSK_YIAWPLQ
GWQATFGGGDHPPK_SDLVPR_GSPEFPGR_LER_PHR_DR_GSMNPPEPPGGTNIPVPPPMPGGGANIPVPPP
MPGGGANIPPPPPPPGGIGGATPSPPP_LTPVNGNPGASTPTK_TGLLK_TLNR_LSAELQNNPR_VTEDVVDNVD
AVIR_NAVNLAPDANGDFSGR_SAMPIEMAANAALR_SLK_K_NPGDAGHAAPAYLPAER_IGQLR_EK_VR_R_
TIEALESNR_PPK_PQPR_STPPQSTPPK_PTQHPTAPNPNVPDASTPDASTPDASTPDASTPDASTPSR_PAPAPR
_AGTGAPAASAATR_APAFANR_VR_K_PNPAMPAASSHAIASDFASSNAFAIGDDSTAVGAQAIAFSEQSIAIGS
R_AIAAGAR_SIAVGTDATAAAPDSVALGSGSIAER_EGTVSVGR_DGHER_QITHVASGTEPTDAVNVTQLR_AA
MSNANAYTNQR_IGDLQQSITDTAR

The analysis shows that 43 out of 68 tryptic peptides (60 % coverage) GST-BimA treated by CK2 and 37 peptides (50 % coverage) GST-BimA treated by GSK3 were detected by mass spectrometry. There was a higher coverage of protein detected than from the immunoprecipitated CD32-BimA sample. This is likely to be because there was a higher concentration of GST-BimA present in the sample compared to CD32-BimA. Clear Simplyblue stained bands were seen on a protein gel for GST-BimA whereas a more sensitive silver stain had to be used to show a CD32-BimA band. The immunoprecipitated CD32-BimA sample would have contained many other host cell proteins and they may have been detected instead of CD32-BimA peptides.

Peptides from both GST and BimA were identified however no phosphorylation sites were identified. The peptides that were detected from the CD32-BimA sample were also detected in the GST-BimA samples suggesting these are the peptides the mass spectrometer can detect from a trypsin digest. Both kinases are predicted to phosphorylate BimA in the PDAST repeat region which was not detected. Only one of the peptides detected was predicted to be phosphorylated by GSK3 so it is perhaps unsurprising to see that phosphorylation was not detected. A repeat of the *in vitro* kinase assay should be done and complimentary mapping should be used to provide better coverage of the GST-BimA protein. This would involve multiple digestions of the protein with different enzymes e.g. trypsin/chymotrypsin/AspN/V8 to generate the correct peptides for mass spectrometry analysis. Settings for the instrument may need to be adjusted so that the peptide could be detected and the phosphorylation reaction may also need to be optimised.

Alternative kinases from the prediction could be investigated to see if they phosphorylate BimA. Once phosphorylation of BimA has been detected by mass spectrometry, the phosphorylated protein could be investigated further in an actin-pyrene polymerisation assay (Cooper *et al.* 1983). This assay involves the fluorescence of pyrene-conjugated actin that occurs during polymerization and has been used in studies before for GST-BimA (Stevens *et al*. 2005) (Sitthidet *et al*. 2011). Differences in actin polymerisation could show that phosphorylation of BimA by a host kinase is important to actin-based motility.

Chapter 4: Investigation of the role of predicted CK2 phosphorylation sites on BimA-mediated actin-based motility

Generation of a *B. thailandensis* BimA mutant

The closely related avirulent soil saprotype *B. thailandensis* has been categorised by the Advisory Committee on Dangerous Pathogens (ACDP) as a hazard group 1 microbe compared to *B. pseudomallei* which is categorized as a hazard group 3. It has been used a model for *B. pseudomallei* in many studies (Haraga *et al.* 2008) (Sarkar-Tyson *et al.* 2009).

To generate a *bimA* mutant, PCR-Ligation-PCR mutagenesis (Based on the method described by Ali and Steinkasserer 1995) was attempted to amplify the flanking regions of the *bimA* gene, ligate them together and then amplify the ligation product (Figure 21). The plasmid and insert would be cut by restriction enzymes to create sticky ends before ligation. This product could then be cloned into the suicide vector pDM4 which contains the sacBR genes conferring sucrose sensitivity. The resulting plasmid could then be transformed into *E. coli* before being conjugated with *B. thailandensis*. Homologous recombination would then take place, thereby generating a merodiploid where the plasmid would integrate into the genome (Figure 22). Strains would next be selected by sucrose-resistance due to the loss of sacBR, indicating that the suicide vector had been excised. Colony PCR would be performed to identify whether the colonies are either wildtype or a *ΔbimA* mutant.

Figure 21: PCR-Ligation-PCR method

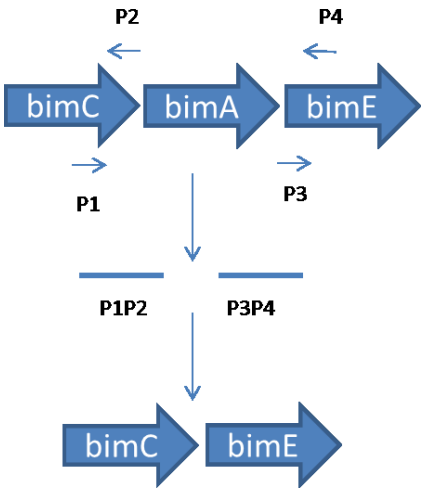

Figure shows the PCR-Ligation-PCR method. Flanking sequences of *bimA* were amplified by primers P1, P2, P3 and P4 to generate P1P2 and P3P4. These two fragments would then be phosphorylated and ligated together to generate the deletion construct.

Figure 22: Homologous recombination in *B. thailandensis*

Method for allele replacement mutagenesis. Conjugation of the deletion construct into *B. thailandensis* would allow for homologous recombination to occur. The resulting merodiploid strain would be selected for chloramphenicol resistance and would be sucrose-sensitive due to the presence of sacBR. Excision of the integrated suicide vector from the genome results in either: generation of a deletion strain; or conversion back to wild-type. Strains are selected by sucrose-resistance due to the loss of sacBR, indicating that the suicide vector has been excised. (Logue *et al.* 2009)

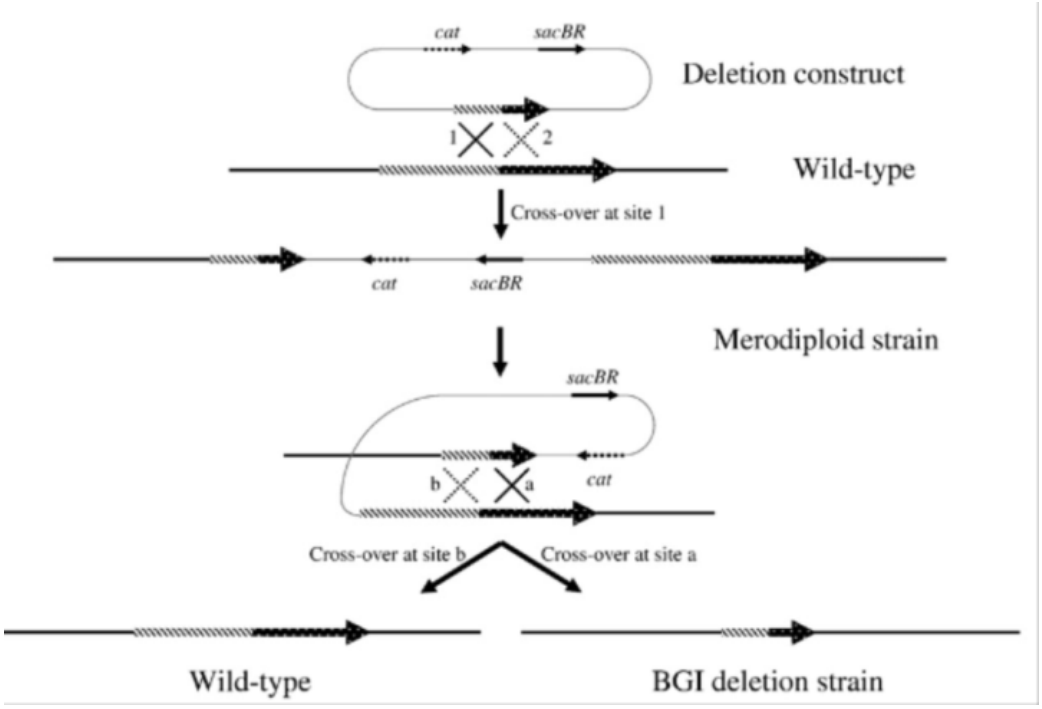

Expression of mutant phospho $BimA_{ps}$ proteins in a *B. thailandensis* BimA mutant would allow analysis of infected cells by real time microscopy. This would provide much more detailed analysis of the mechanism of BimA-mediated movement compared to still images obtained from the Hazard Group 3 *B. pseudomallei* strain.

Generation and ligation of flanking sequences

A yield of 2 µg/µl of *B. thailandensis* (E30 strain) genomic DNA was obtained by CTAB extraction. This DNA was used as a template for generating the flanking sequences and as a wildtype control when screening for the mutant. The flanking sequences of *bimA*, P1P2 and P3P4, were successfully generated by PCR at the correct size bands of 413 bp and 510 bp (Figure 23). Both were then phosphorylated and ligated however the ligation product of 929 bp could not be amplified using the

flanking primers P1 and P4. The *B. thailandensis* genome is GC rich so the reagents DMSO and high GC rich buffer were tried to generate the P1P4 product. A low concentration of around 40 ng/µl was obtained for P1P2 and P3P4 and could be why the fragments did not ligate efficiently, hence no P1P4 product following PCR. Repeat PCR of the fragments to achieve a higher concentration of P1P2 and P3P4 would increase the chances of ligation. Redesigning the primers may also improve the yield of fragments.

Figure 23: Generation of flanking sequences

Figure shows the correct band sizes of the flanking sequences of BimA. A) P1P2 =429 bp and B) P3P4 = 516 bp. *B. thailandensis* genomic DNA was amplified using primer pairs P1 + P2 (A), P3 + P4 (B). The resulting products were visualised by agarose gel electrophoresis.

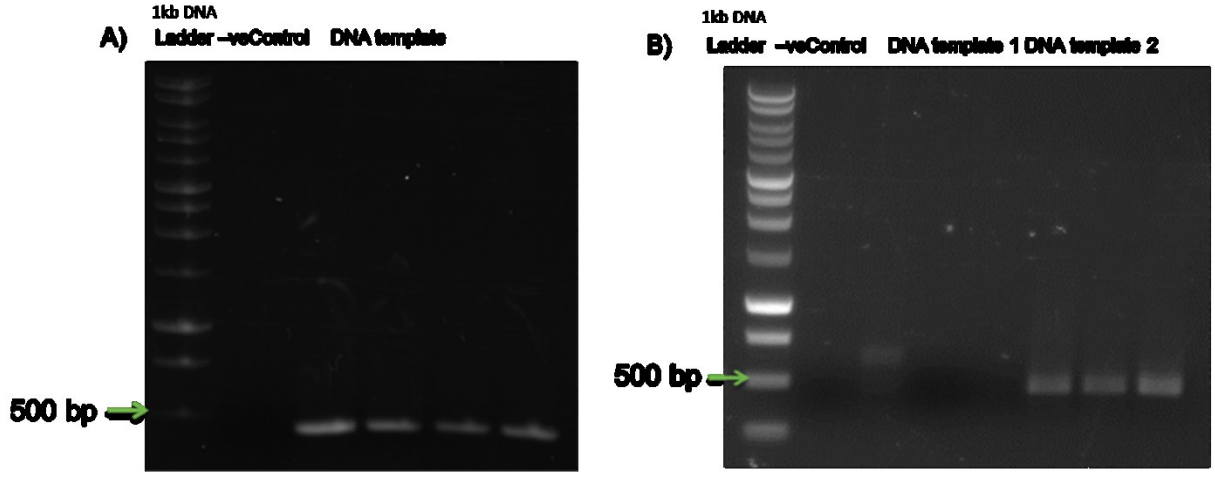

Subcloning P1P2 into pGEMT

To improve ligation of the fragments, subcloning each individually into the vector pGEMT was attempted. By cloning them into a vector it would be easier to replicate and generate more DNA than by PCR. The fragment was cloned by A-tailing and then ligating into the vector before transformation into *E. coli*. Despite recovery of colonies on selective agar, restriction digests showed that there was no insert in the plasmid (data not shown). EcoR1 was used as a restriction enzyme to cut the plasmid at the A overhangs where the insert was ligated. A high transformation efficiency was obtained of 1.5 X 10^8 cfu / µg DNA using a transformation control of pUC18. It is unlikely therefore that the problem was with the *E. coli* transformation efficiency but because of a problem cloning the insert into the plasmid. It is possible the Taq polymerase was not able to A-tail the fragments and could be why there

was no insert in the plasmid. A different polymerase could be used for A-tailing and may improve the efficiency of ligation into the vector step.

Cloning P1P2 into pDM4

Direct cloning of P1P2 into the vector pDM4 was also tried by using restriction enzymes and ligating the sticky ends. Restriction digests of possible pDM4 *bimA* plasmids showed only cut plasmid and not the expected P1P2 band at 413 bp (Figure 24). A single enzyme control was also performed for the same conditions and showed that both enzymes were able to cut pDM4 (data not shown). One possibility for a lack of insert in the plasmid could be that it is ligating back on itself. Other combinations of restriction enzymes could be tried to see if this improves the ligation of the insert into the vector. Inclusion of a phosphatase step to dephosphorylate the vector could be used to prevent re-ligation.

Figure 24: Restriction digest of pDM4-P1P2

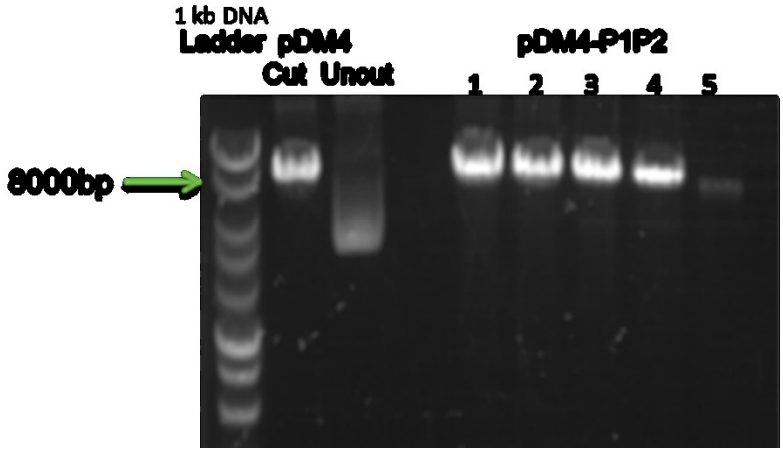

Figure shows restriction digests of pDM4-P1P2 from independent colonies 1-5. Xba1 and Xho1 were used as restriction enzymes at 37°C for 4 hrs. A cut plasmid control and an uncut plasmid control were used.

The generation of pDM4 containing a *B. thailandensis bimA* deletion construct was proving difficult to generate and in the interests of time an alternative strategy was attempted to generate a *B. thailandensis bimA* mutant.

A pDM4 *bimA* mutant plasmid (based on *B. pseudomallei* sequences) has previously been generated by Charles Vander Broek. The genomes among the *Burkholderia* species are very similar and the *bim* locus is highly conserved at the nucleotide level except for the *bimA* gene which is divergent. Any phenotype demonstrated by the *bimA* mutant could be checked by expressing BimA back *in trans*.

This would ensure the phenotype is a result of *bimA* deletion. The existing pDM4-BimA$_{ps}$ has been used to generate unmarked deletion mutants in two *B. pseudomallei* strains. It should be possible to make a *B. thailandensis ΔbimA* mutant because of the high similarity in sequence of the flanking regions and two groups have previously described a similarly-constructed mutant (Benanti *et al*. 2015) (French *et al*. 2011).

Resistance of *B. thailandensis* strains

Different *B. thailandensis* strains were cultured on selective media containing kanamycin and/or chloramphenicol to identify a strain that could be used for conjugation with *E.coli* S17-λ pir with the existing pDM4-BimA plasmid. The strain needed to be resistant to kanamycin so it could be selected specifically for *B. thailandensis* and not the donor *E.coli* strain. The strain would also need to be susceptible to chloramphenicol so colonies would only grow when *B. thailandensis* contained the pDM4-BimA plasmid as it encodes chloramphenicol resistance. Table 1 shows the results of the selection. Strains Bp9, BpG488, Bp69 and E30 showed the correct selection (Kan^r and Cm^s).

Table 1: Resistance of *B. thailandensis*

Table displays the growth of different *B. thailandensis* strains on LA plates containing either kanamycin, chloramphenicol or both. R indicates resistant, S indicates susceptible. In red are the identified strains suitable for conjugation studies.

Strain	LB	Chloramphenicol 50 µg/ml	Kanamycin 50 µg/ml	Chloramphenicol + Kanamycin 50 µg/ml
Bp4	R	S	S	S
Bp9	R	S	R	S
BpG1190	R	S	R	R
BpG488	R	S	R	S
Bp69	R	S	R	S
E30	R	S	R	S

Conjugation of *B. thailandensis* and *E.coli* S17-λ pir pDM4-*bimA*

B. thailandensis E30 and BpG488 strains were conjugated with *E. coli* S17-λ pir pDM4-*bimA* and plated out on selective plates then incubated at 37 ˚C for 2 days. An S17-λ pir control showed that the plates were selective because only 2 colonies grew compared to the conjugated strains. 120 colonies grew for *B. thailandensis* E30 conjugated with S17-λ pir and 14 colonies grew for *B. thailandensis* BpG488 conjugated with S17-λ pir.

PCR screening for *bimA* mutant

Putative merodiploids were then PCR screened to detect insertion of the plasmid. None of colonies for BpG488 showed the correct size band for a mutant. A negative control was used which contained all reagents used for the PCR reaction except for template DNA to ensure no contaminants would be amplified. A wildtype *B. thailandensis* genomic DNA template (E30) was used as another negative control which would give an expected band size of 2039 bp. This is because the primers would amplify the flanking regions and *bimA* gene. The expected band size for the pDM4-*bimA* P1P4 sequence was at 539 bp with just the flanking regions being amplified. Initially the PCR screen had to be optimised by adjusting the annealing temperature and DMSO was used for the controls to show the correct band sizes. DMSO helps separate the DNA strands by disrupting base pairing. Using the optimised PCR conditions E30 colonies were screened and one showed the correct size band of 539 bp which was taken forward for sucrose selection. Figure 25 shows the potential mutant identified and the correct band size for wildtype control. Additional bands can be seen on the gel suggesting the primers are not specific enough. Redesigning of the primers or further optimisation of the PCR conditions would increase the specificity.

Figure 25: PCR screen of selected colonies from conjugation of E30 and S17-λ pir pDM4-*bimA*

Figure shows an agarose gel of the PCR screen to detect insertion of the plasmid into *B. thailandensis*. Two negative controls were used shown in the first two lanes: negative control where no template was added, WT control is *B. thailandensis* genomic DNA. The remaining lanes are colonies from conjugation. Arrow points to the correct size band and possible P1P4 PCR fragment amplified from pDM4-$bimA_{ps}$ plasmid.

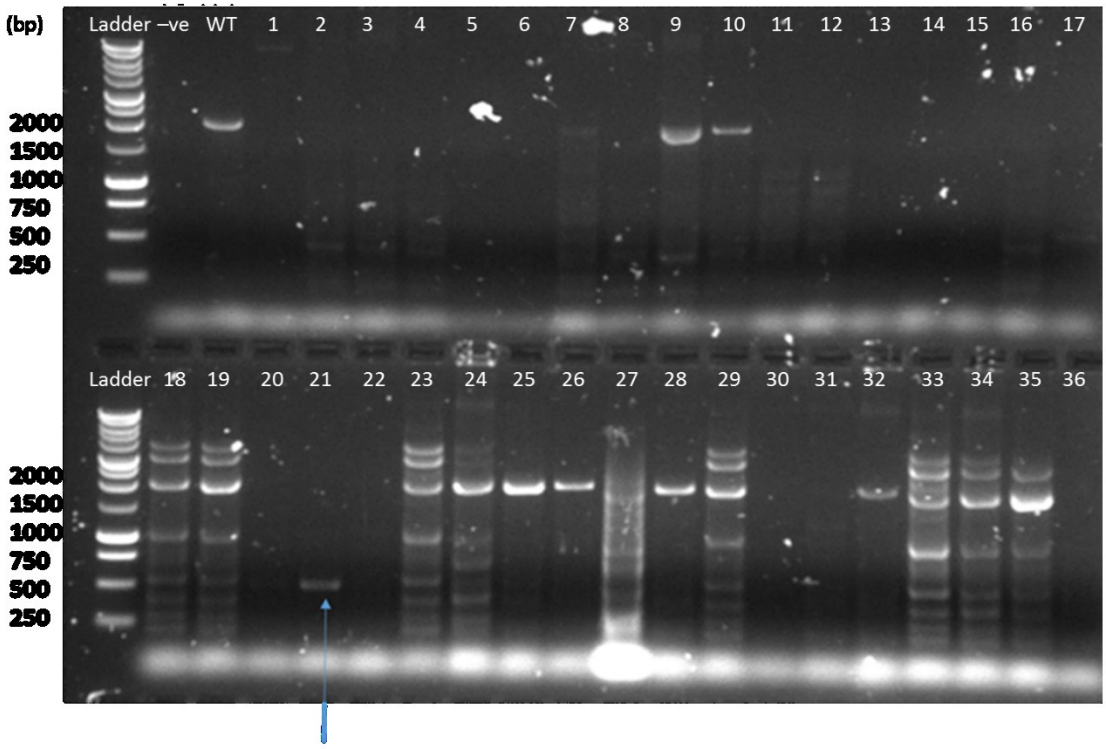

Sucrose selection of potential *bimA* mutant

The potential merodiploid colony was grown overnight in the absence of selection then plated out onto sucrose plates and incubated at 30 ˚C for 2 days. The plasmid pDM4 contains a SacBR gene which when expressed is toxic to the bacteria when grown in the presence of sucrose (Logue *et al.* 2009). This provides direct selection for loss of the plasmid and when it excises it can either delete the Wildtype gene or the mutated one.

137 colonies grew on the sucrose plates. These colonies were then PCR screened and 3 showed the correct size band of 539 bp for a *bimA* mutant. To confirm these colonies were mutants, HeLa cells were infected with the potential mutants before being analysed by immunostaining for *B. thailandensis*, actin and nuclei and imaged by confocal microscopy. The analysis showed that all three potential mutants displayed actin tails and therefore *bimA* had not been successfully deleted. A *B.*

thailandensis bimA mutant would not be able to form actin tails and the correct band sizes seen for the potential mutants were false positives. It is very common for colony PCR screening to show false positives and any contamination in the PCR reaction can lead to the appearance of an aberrant band. To increase the selection for a mutant, 2 sets of primers could be used for each colony. One could be used to amplify the total insertion and another to amplify a sequence within the insertion. A second PCR screen could then be used to remove any false positives identified in the first screen. It is also possible that *B. thailandensis* does not recombine with the plasmid because it is recognised by the bacteria as being foreign DNA.

The generation of a *B. thailandensis bimA* mutant has previously been demonstrated and its role has been investigated in actin-based motility (French *et al.* 2011) (Benanti *et al.* 2015). Although generation of the *B. thailandensis*-specific suicide plasmid by PCR-Ligation-PCR mutagenesis has been unsuccessful**,** studies by French *et al* (2011) have generated *bimA* mutants by this method. Studies by Benanti *et al* 2015 have generated a *bimA* mutant by an alternative method. This involves construction of multiple plasmids for allelic exchange and could be used as further work to generate a *B. thailandensis bimA* mutant for this project (Lopez *et al*. 2009). However for this study a different strain, E264, was used and further studies using E264 could be performed to generate a *bimA* mutant.

Effect of mutation of predicted CK2 phosphorylation sites on BimA-mediated actin-based motility

Many potential phosphorylation sites of BimA were identified by the bioinformatics analysis and one particular region predicted to be phosphorylated was the PDAST repeat region. This region varies in number between 2-7 motifs and studies have previously shown that the number of PDAST motifs affected the polymerisation of actin in an additive manner (Sitthidet *et al*. 2011). This repeat region contains many Serines and Threonines which are common targets for phosphorylation. The bioinformatics analysis predicted these amino acids to be phosphorylated by CK2 and GSK3. It is possible that actin polymerisation mediated by BimA could be affected by phosphorylation in the PDAST repeat region and previous work has shown CK2 could phosphorylate GST-BimA (unpublished data from the Stevens laboratory). BimA phosphorylation mutants were generated to investigate the effect of phosphorylation of Serines in the PDAST repeat region, Figure 26. Serines were chosen in this region because they are predicted to be phosphorylated by CK2, a kinase that is known to affect the actin-based motility of other intracellular pathogens. As the generation of a *B. thailandensis bimA* mutant had been unsuccessful, a *B. pseudomallei bimA* mutant was used to express the BimA phosphorylation mutant proteins.

Figure 26: Schematic of mutated proteins

Figure shows the PDAST repeat region sequence for Wildtype (BimA), Phospho-null mutant (BimA S/A) and Phospho-mimic mutant (S/D). In red are the mutated Serine residues at positions 260, 265, 270 and 275. For the phospho-null mutant Serine residues have been mutated to an Alanine and for the phospho-mimic mutant Serines have been mutated to an Aspartic acid residue.

Wildtype (BimA)	NVPDASTPDASTPDASTPDASTPDASTPS
Null (BimA S/A)	NVPDAATPDAATPDAATPDAATPDAATPS
Mimic (BimA S/D)	NVPDADTPDADTPDADTPDADTPDADTPS

To generate the phosphorylation mutants, Serine residues at positions 260, 265, 270 and 275 in pME-BimA were mutated to Alanines for phospho-null and to Aspartic acids for phospho-mimic. The pME-BimA plasmid has previously been generated (Stevens *et al.* 2005). The mutant plasmids were then

transformed into a *B. pseudomallei ΔbimA* mutant. This would ensure no homogenous BimA would also be expressed. A *ΔbimA* mutant was complemented with pME-BimA as a control and compared to a wildtype strain. A *ΔbimA* mutant was also complemented with pME as a negative control. Serines within the target PDAST repeat region of pME-BimA were mutated to Alanines for a phospho-null mutant. Therefore, when the plasmid is expressed in *B. pseudomallei* the BimA protein would not be phosphorylated at these sites. A phosphorylation mimic was also generated by mutating the Serines to Aspartic acids so when the plasmid is expressed the BimA protein will mimic constitutively phosphorylated sites. Expression of BimA was confirmed in the phosphorylation mutant strains before they were then observed in HeLa cells and analysed for differences in actin-based motility. Strains containing the plasmid pME were grown with tetracycline to select specifically for bacteria transformed with the plasmid. IPTG was used to induce expression of the plasmid pME.

Expression of BimA in Phosphorylation mutants

B. pseudomallei ΔbimA mutants transformed with either pME-BimA, pME-BimA S/A or pME-BimA S/D showed expression of BimA by western blot of lysates at 20 hours and confirmed transformation of the plasmids was successful (shown in Figure 27). The correct size band of 180 kDa was seen for BimA in the lysates of pME-BimA, pME-BimA S/A and pME-BimA S/D (Figure 27). BimA was absent from the Wildtype bacterial lysate because it does not express BimA in LB broth as it is tightly regulated by VirAG but will express it in a cell lysate (Chen *et al.* 2011). BimA is a trimeric protein and therefore has a molecular weight three times 60 kDa. Negative controls used were Wildtype *B. pseudomallei* (WT), *B. pseudomallei* BimA mutant (ΔBimA) and *B. pseudomallei* pME (pME).

Figure 27: Western blot of *B. pseudomallei* lysates

B. pseudomallei ΔbimA mutants carrying pME, pME-bimA, pME-bimA S/A and pME-bimA S/D were grown in LB broth containing tetracycline and IPTG. At 20 hrs bacteria were lysed with bugbuster and lysates were run by SDS-PAGE before western blot. A) Proteins detected by incubation with anti-BimA followed by anti-mouse 680 and imaged by Li-COR.

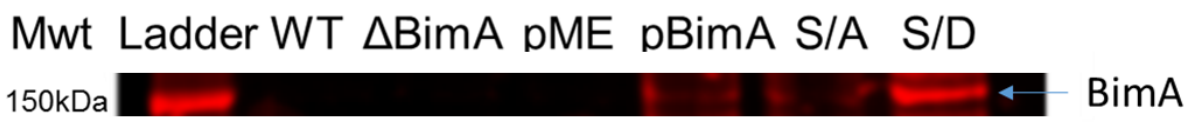

Infection of HeLa cells with BimA phosphorylation mutants

HeLa cells were seeded onto coverslips and infected with *B. pseudomallei* before being fixed at 20 hours post-infection. The coverslips were stained for *B. pseudomallei*, BimA and nuclei before being imaged by confocal microscopy to investigate the effect on BimA localisation. Results can be seen in Figure 28 with all strains except *ΔbimA* displaying polar localisation of BimA at a single pole of the bacterium. Duplicate coverslips were also stained for *B. pseudomallei*, actin and nuclei before being imaged by confocal microscopy to investigate the effect on actin tail formation. Results can be seen in Figure 29. *B. pseudomallei ΔbimA* transformed with pME-BimA, pME-BimA S/D and pME-BimA S/A all demonstrated actin tails whilst the pME *ΔbimA* alone strain did not.

Figure 28: BimA localisation of phosphorylation mutants 20 hours after infection in HeLa cells

Confocal microscopy images of HeLa cells 20 hours after infection with *B. pseudomallei ΔbimA* mutants carrying pME-bimA, pME-bimA S/A and pME-bimA S/D. Coverslips were fixed in paraformaldehyde before being permeabilised with Triton X 100. Coverslips were stained with anti-LPS followed by anti-rabbit 568, anti-BimA followed by anti-mouse 488 and DAPI. Blue channel – nucleus, red channel – *B. pseudomallei* and green channel – BimA. A) Control, infection with *B. pseudomallei* containing pME-BimA. B) Phospho-mimic, infection with *B. pseudomallei* containing pME-BimA S/D. C) Phospho-null, infection with *B. pseudomallei* containing pME-BimA S/A.

A) pME-BimA B) pME-BimA S/D C) pME-BimA S/A

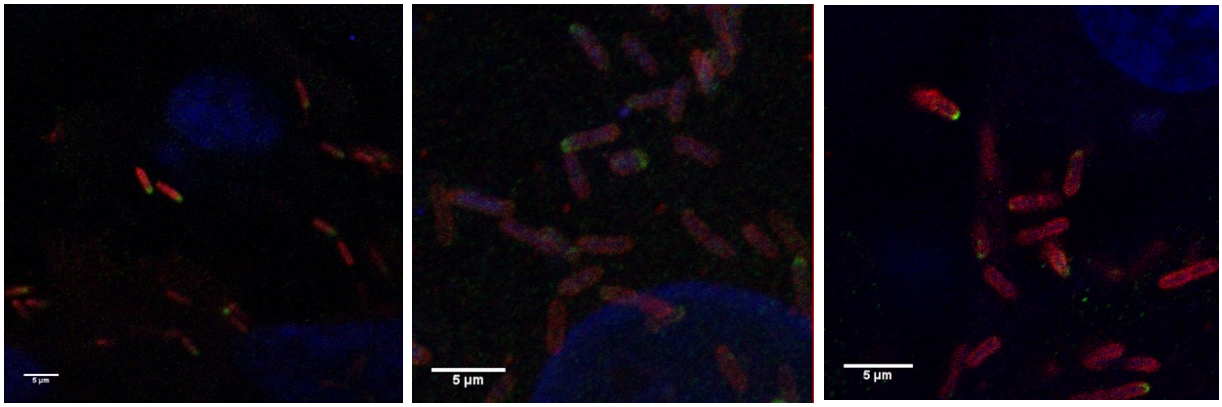

Figure 29: HeLa cells 20 hours after infection with BimA phosphorylation mutants

Confocal microscopy images of HeLa cells 20 hours after infection with *B. pseudomallei* ΔbimA mutants carrying pME, pME-bimA, pME-bimA S/A and pME-bimA S/D. Coverslips were fixed in paraformaldehyde before being permeabilised with Triton X 100. Coverslips were stained with anti-LPS followed by anti-mouse 568, Phalloidin and DAPI. Blue channel – nucleus, red channel – *B. pseudomallei* and green channel – actin. A) Control, infection with *B. pseudomallei* containing pME-BimA. B) Control, infection with *B. pseudomallei* containing pME. C) Phospho-mimic, infection with *B. pseudomallei* containing pME-BimA S/D. D) Phospho-null, infection with *B. pseudomallei* containing pME-BimA S/A.

A) pME-BimA - Control

Blue channel - Nuclei

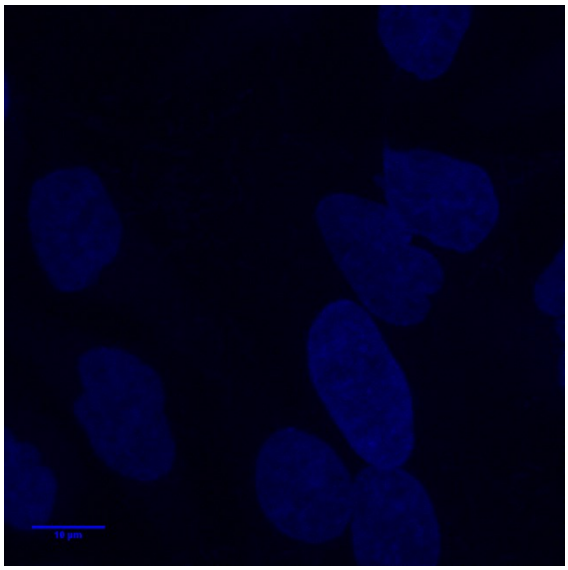

Red channel – *B. pseudomallei*

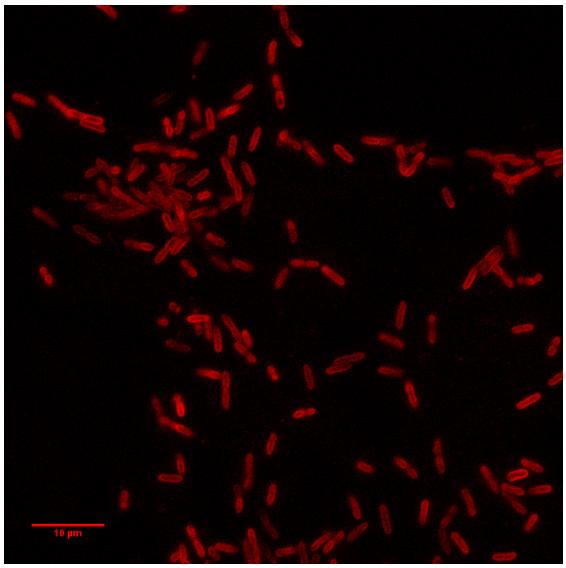

Green channel - Actin

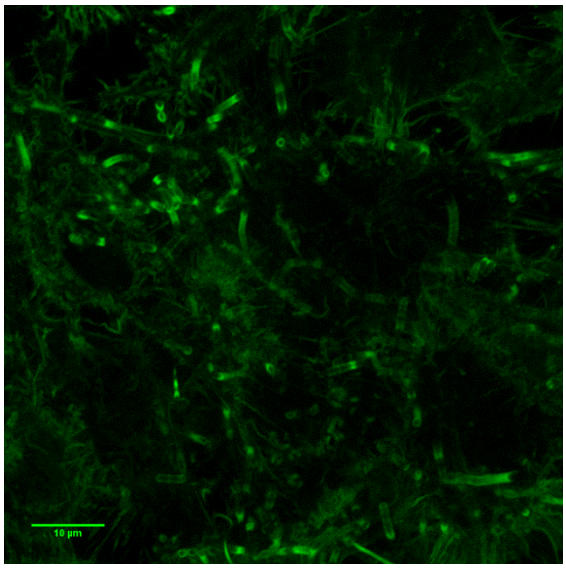

Merge

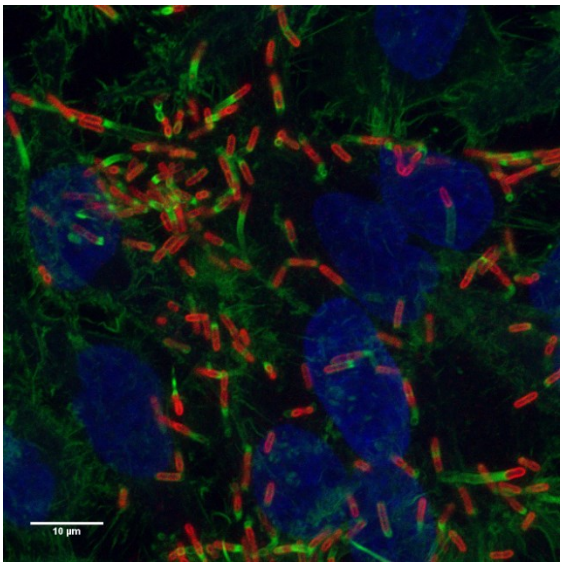

B) pME - Control

Blue channel - Nuclei

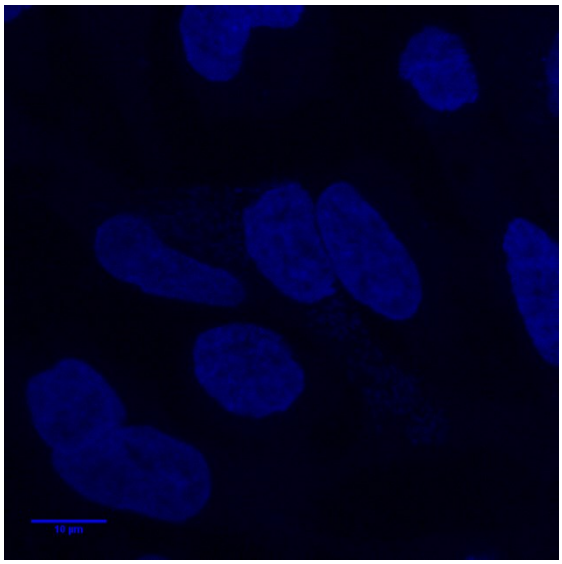

Red channel – *B. pseudomallei*

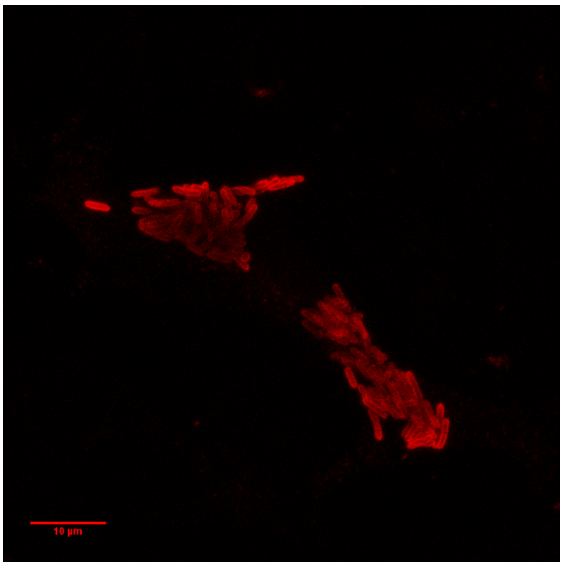

Green channel - Actin

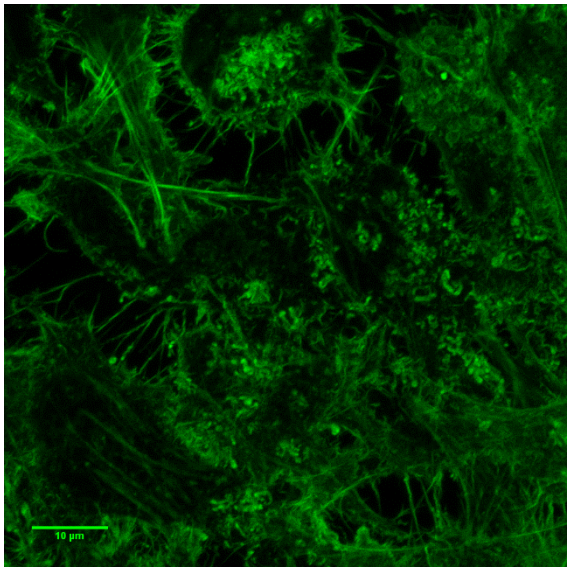

Merge

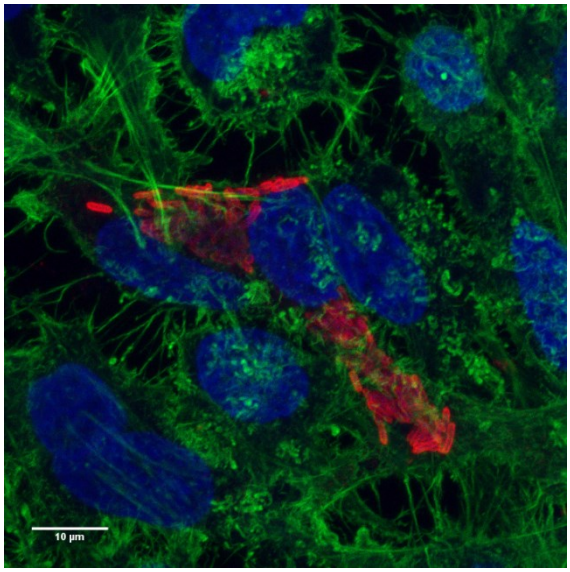

C) pME-BimA S/D – Phospho mimic mutant

Blue channel - Nuclei

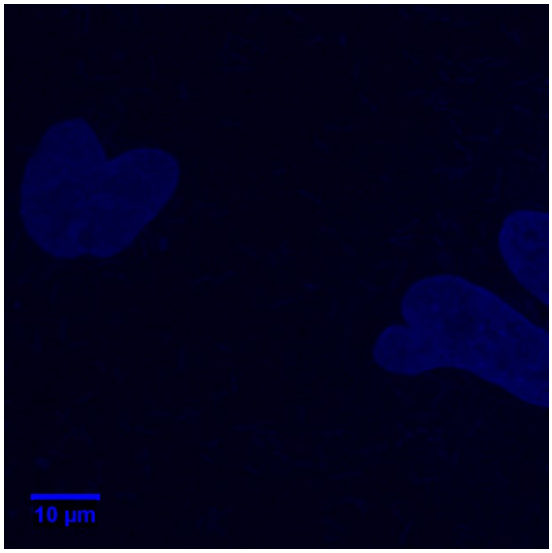

Red channel – *B. pseudomallei*

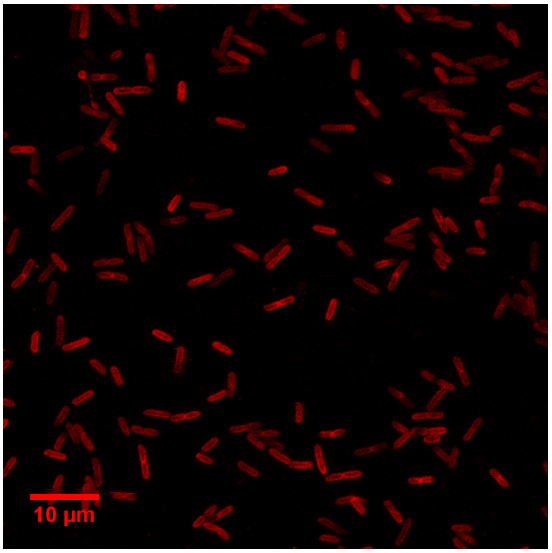

Green channel - Actin

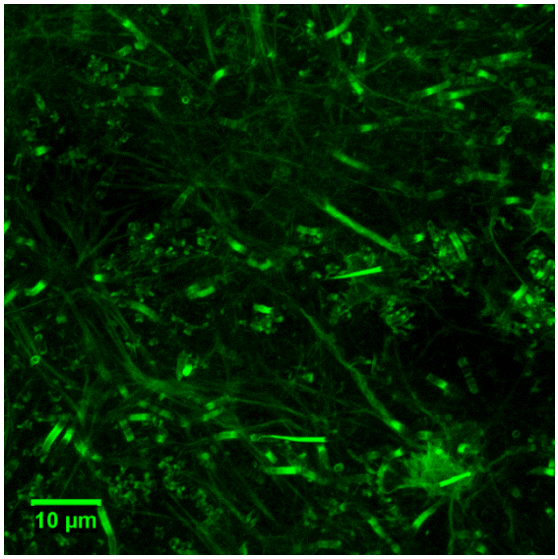

Merge

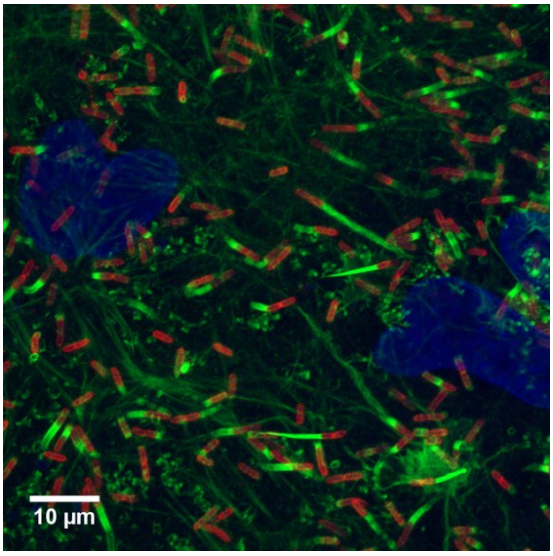

D) pME-BimA S/A – Phospho null mutant

Blue channel - Nuclei

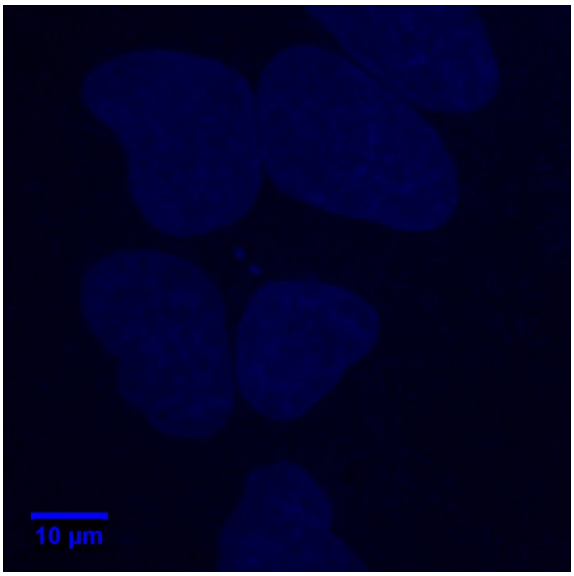

Red channel - *B. pseudomallei*

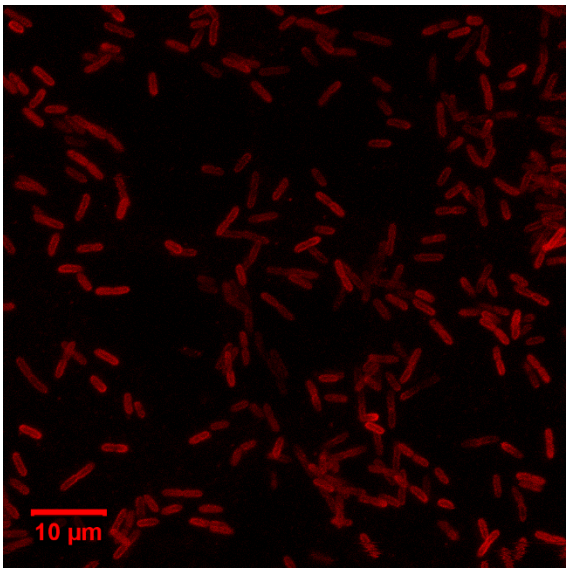

Green channel - Actin

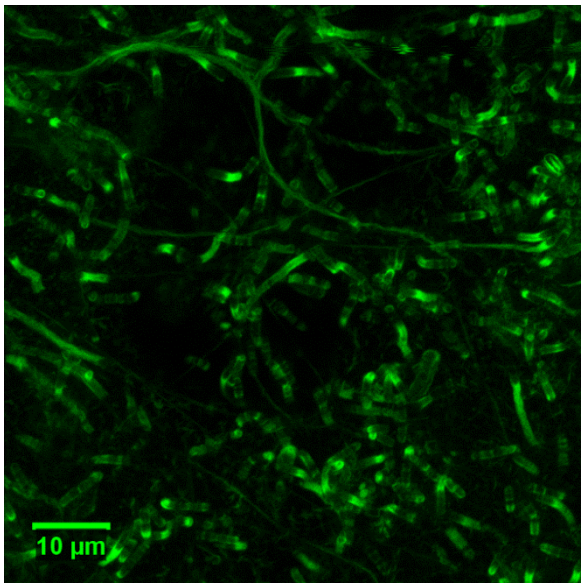

Merge

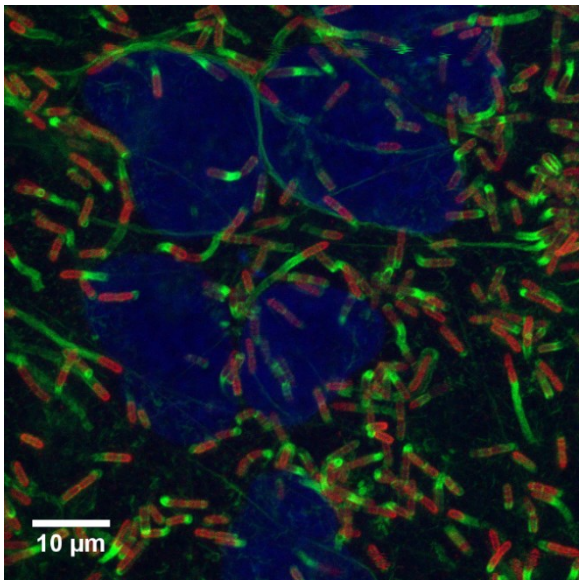

Figure 28 shows that for pME-BimA, pME-BimA S/D and pME-BimA S/A the BimA protein is localised to the pole of the cell. This is where BimA is expressed in wildtype *B. pseudomallei* and the position at which the actin tail forms. It is possible that mutations in the amino acid sequence of BimA could affect the structure of the protein. A change in structure could potentionally display a different localisation of BimA. However phosphorylation of Serines in the PDAST repeat region has been shown not to have an effect on localisation of BimA. Some bacteria are not showing BimA present and this could be because they have lost the plasmid since they are cultured in the absence of tetracycline during the infection experiment.

Analysis of the confocal microscopy images showed there to be no obvious effect on actin tail formation with both the phospho-null and phospho-mimic displaying actin tails similar to the control. Studies in *Listeria* have shown that a phospho-null mutant was unable to form actin tails (Chong *et al.* 2009). It was thought that the phospho-null mutant in *B. pseudomallei* would function similarly and not be able to form actin tails if phosphorylation of the Serines in the PDAST repeat region was important to tail formation. Further repeats are needed to confirm this result and also further studies investigating the number of *B. pseudomallei* with a tail. Some bacteria transformed with pME-BimA do not display a tail and it is likely these are bacteria not expressing BimA seen in Figure 29A, C and D. No tails were seen for *B. pseudomallei* transformed with pME as it does express a *bimA* gene. Without BimA the bacteria are unable to form an actin tail, seen in Figure 29B. The actin tail allows for bacteria to display intracellular motility and they can be seen spaced out within the cell cytosol which is as seen in Figure 29A, C and D. However as the pME mutant does not form a tail it cannot move inside the cell and therefore the bacteria are all very close together as seen in Figure 29B.

An earlier time point in infection could also be investigated. It is possible that phosphorylation may be important to the rate of tail formation and **a**ffect the rate of the *B. pseudomallei* life cycle. Phosphorylation of Serines in the PDAST repeat region may not have an effect on tail formation but could have an effect on actin-based motility by regulating actin tail length and structure. The structure of the tail for *B. pseudomallei* can be seen in Figure 29 with many bacteria displaying a helical spiral structure in agreement with Benanti *et al* 2015. Phosphorylation of sites in the BimA protein could be important to regulating this spiral structure and further studies should look at the difference between types of tail for phosphorylation mutants.

Results showed that phosphorylation of the Serines in the PDAST repeat region had no effect on actin tail formation or localisation of BimA. However, it is possible though that phosphorylation of Serines could have an effect on regulating the actin tail length. Therefore, an analysis was performed on multiple to calculate the average actin tail length. The actin tail area was selected and tail length was

measured using Image J software to calculate the Feret's Diameter. This value is the longest distance between any two points along the selection boundary and is also known as the maximum calliper. 100 actin tails in total were measured from each strain from three biological replicates. Results are shown in Figure 30 and showed only a small increase in average tail length of pME-BimA S/D and pME-BimA S/A compared to the wildtype but not statistically significant. Unpaired Student's t tests were performed and showed a two-tailed P value equal to 0.7813 (pME-BimA and pME-BimA S/D) and 0.7130 (pME-BimA and pME-BimA S/A). All mutant strains had an average tail length between 5-5.5 µm. Studies by Benanti *et al.* 2015 have shown longer tails around 15 µm for the wildtype *B. pseudomallei*. The difference in tail length could be because wildtype *B. pseudomallei* was used instead of a pME-BimA strain or because different cell types, A459 and Cos7, were used. Different phenotypes might be cell-type specific as many kinases have restricted cell and tissue expression. Additional experiments could be performed in A459 and Cos7 to analyse the effect on actin tail length of the phosphorylation mutants.

Some variation in tail length was observed from images taken in Figure 29 and analysis shown in Figure 30. This variation in tail lengths is likely to be because of bacteria being at different stages of their life cycles. To improve the reliability of results a higher number of actin tails could be measured which may allow for a difference to be observed between the mutants. 500 actin tails could be measured compared to 100. Z-stacks were taken to account for all planes of the confocal microscope and made sure the whole of the actin tail was measured and not just part of a tail on one plane.

The actin density of the tail could also be studied by measuring the intensity of the fluorescence of the tail. Phosphorylation mutants may not affect the tail length but could be important in regulating the concentration of actin recruited to the tail.

Figure 30: Tail length of phosphorylation mutants 20 hrs after infection in HeLa cells

Figure shows the average Feret's diameter of actin tails for *B. pseudomallei* Δ*bimA* mutants carrying pME-bimA, pME-bimA S/D and pME-bimA S/A. Analysis was performed on confocal microscopy images and the data represents 100 actin tails in total from 3 biological replicates for each mutant with standard error bars.

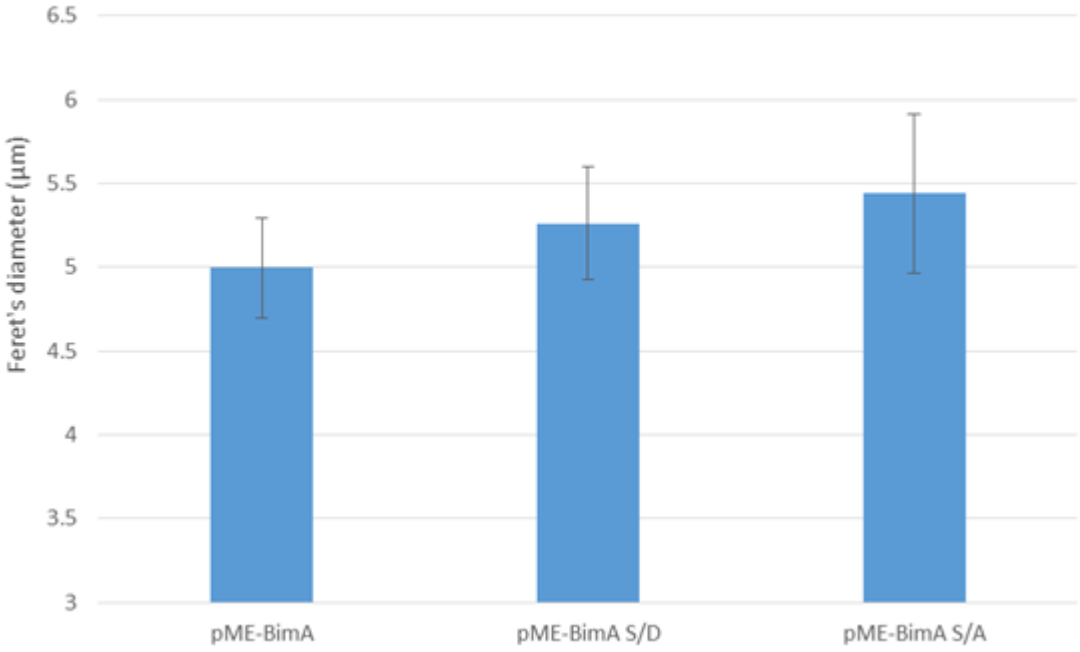

Results from this study do not show a difference in actin-based motility between the pME-BimA, pME-BimA S/D and pME-BimA S/A mutants. Confocal microscopy images have shown actin tail formation and BimA localisation to be the same as the control. Further studies into actin tail length was also not able to show a difference between the phosphorylation mutants and pME-BimA strain. These results suggest phosphorylation of Serines in the PDAST repeat region is not important for actin-based motility however further studies should investigate the number of bacteria with a tail, tail structure and tail density.

The PDAST repeat region contains many Threonines which are predicted as common targets for kinases and could be phosphorylated to affect the actin-based motility of *B. pseudomallei*. Further studies should be done to generate BimA phosphorylation mutant proteins where Threonines are substituted in the PDAST repeat region which could display differences in actin tail formation. Phosphorylation of Threonines and not Serines could be a reason for the additive effect in actin polymerisation of the PDAST repeat region seen in previous studies (Sitthidet *et al*. 2011). It is possible that the additive effect is not due to modification of the amino acids but only a difference in structure

and the number of motifs effects the actin polymerisation through altered 2˚ structure of BimA rather than phosphorylation of the protein.

Intracellular survival of HeLa cells with BimA phosphorylation mutants

An observation from the confocal microscopy was that there was a difference in number of bacteria for the phospho mimic and suggested phosphorylation could have a role in intracellular replication rate. To investigate this HeLa cells were infected at a Multiplicity Of Infection (MOI) of 200 with phosphorylation mutants and at 20 hours cells were lysed and dilutions plated and incubated at 37˚C for 2 days. Figure 31 shows the total CFU/well for each strain at 20 hours. An infection inoculum was also calculated of around 4 X 10^6 CFU/ml for each strain.

Figure 31: Bacterial load of *B. pseudomallei ΔbimA* mutants in HeLa cells 20 hours after infection.

Figure shows the CFU/well 20 hours after infection of HeLa cells with *B. pseudomallei* 10726 and *ΔbimA* mutants carrying pME, pME-bimA, pME-bimA S/A and pME-bimA S/D. The data represents 3 biological replicates with 3 technical replicates used for each replicate.

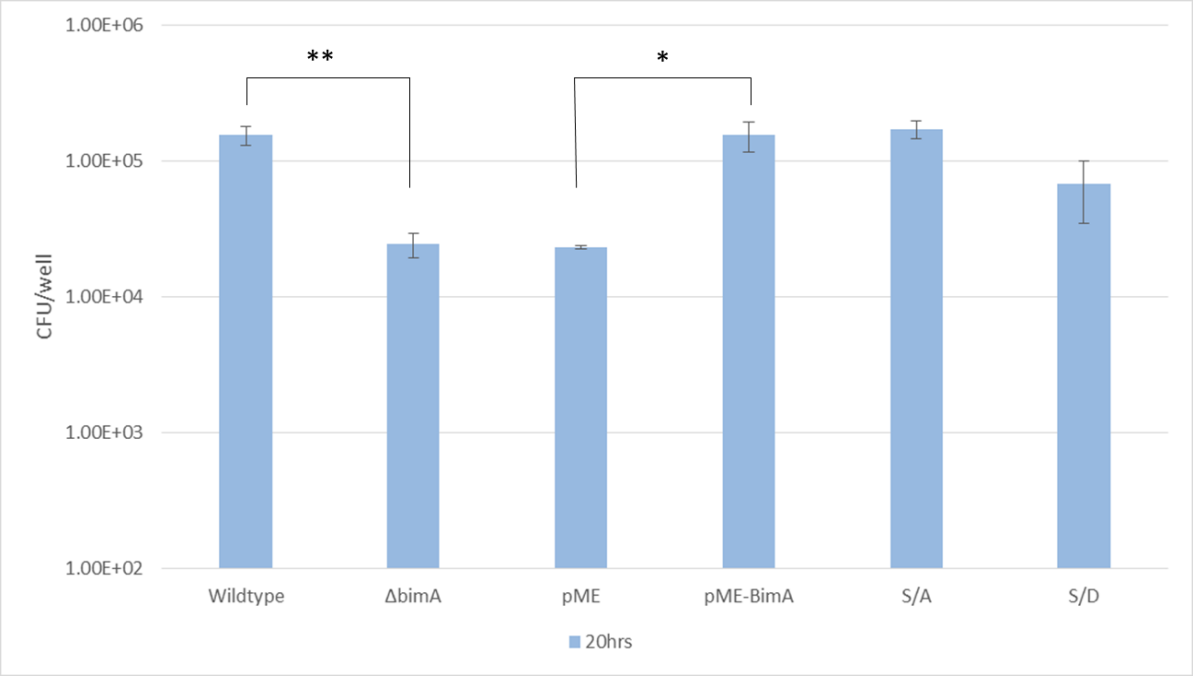

The analysis shows the bacterial load of 1 X 10^5 CFU/well of HeLa cells for wildtype, pME-BimA and pME-BimA S/A at 20 hours after infection. This is less than the infection inoculum and could be because *B. pseudomallei* has a very low invasion rate and very few bacteria are able to enter HeLa cells or because they are killed. The pME-BimA S/A mutant showed the same CFU/well as pME-BimA suggesting phosphorylation of Serines in the PDAST region is not important to intracellular survival of *B. pseudomallei*. There was a small decrease in CFU/ well for the pME-BimA S/D compared to pME-BimA however it was not statistically significant. An unpaired Students t test was performed and showed a two-tailed P value equal to 0.1614. The decrease in CFU/ well for pME-BimA S/D may have been observed as a result of a change in structure of the BimA protein because actin-based motility appears to be the same as shown in Figures 28, 29 and 30. Most proteins have specific binding motifs and the Aspartic acid residues which have replaced Serines could affect the proteins binding to BimA by changing the structure of this region. A difference in the binding of proteins to BimA could affect the survival of *B. pseudomallei* in the host cell.

It is also possible that any regulation by host cell kinases needs to be tightly regulated. A mutant that is constantly phosphorylated may hinder the bacteria. Studies in *Listeria* have shown the importance of phosphorylation of ActA to actin-based motility (Chong *et al*. 2009). However a phospho mimic mutant showed defective cell-to-cell spread and a lower survival than the wildtype in a mouse model (Chong *et al*. 2009). This could be similar in a phospho-mimic mutant of *B. pseudomallei* where the lower levels of bacteria seen in Figure 30 are because the phosphorylation site needs to be tightly regulated.

The *ΔbimA* and pME mutants showed a lower bacterial load of around 2 X 10^4 CFU/well. An unpaired Students t test showed a significant statistical difference between wildtype and *ΔbimA,* with a two-tailed P value equal to 0.0070. An unpaired Students t test showed a significant statistical difference between pME-BimA and pME, with a two-tailed P value equal to 0.0273. This result is expected because if *B. pseudomallei* is unable to express BimA, the life cycle would be affected and the replication rate reduced.

Further studies should be done at a later timepoint of 24 hours to create a time course and would be able to determine if the mutants can replicate in HeLa cells. This would allow a greater difference in CFU/well to be seen between pME-BimA and pME. The pME-BimA S/D mutant has a bacterial load in between the pME-BimA and pME strains. At 20 hours the results were not significantly different but at 24 hours a statistical difference may be seen if the time course experiment were to be performed. This experiment could also be repeated in a macrophage cell line such as J774 where bacteria are actively removed by phagosomal degradation. In a macrophage BimA function may be more important

to survival of the bacteria than in a HeLa cell and bacteria expressing mutated BimA's are likely to be rapidly cleared. A significant difference might be seen between pME-BimA S/D and pME-BimA under these conditions. An additional experiment could be to look at the effect of the phosphorylation mutants on multinucleated giant cell formation. This would measure the cell to cell spread of the mutants.

Chapter 5: Conclusions and Future Perspectives

Phosphorylation is an important post-translational modification that enhances the function of many host proteins and has been shown to be important by modifying some pathogen virulence factors and affecting the actin-based motility of some intracellular pathogens. This project investigated the effect of phosphorylation of BimA in *B. pseudomallei*. A combined bioinformatics data analysis on *B. pseudomallei* BimA amino acid sequence predicted the protein could be phosphorylated at 37 potential sites and identified a number of novel host cell kinases that could be responsible for these modifications.

The PDAST repeat region was predicted to be phosphorylated by host cell kinases and has been shown to be important for actin polymerisation (Sitthidet *et al.* 2011). CK2 and GSK3 were two host cell kinases predicted to phosphorylate this region. CK2 is a kinase that is known to regulate pathogen factors and affect actin-based motility of *Listeria*. It has also been previously shown to phosphorylate BimA (Stevens, unpublished data). GSK3 was a prominent kinase to come out of the bioinformatics analysis and a good candidate for phosphorylation of BimA.

To identify novel sites of phosphorylation sites of the PDAST repeat region for CK2 and GSK3, *in vitro* kinase assays and mass spectrometry analysis were performed. However results showed no phosphorylation of GST-BimA. Peptide coverage from the mass spectrometry was low and the PDAST repeat region was undetected so it is possible there are unidentified sites of BimA phosphorylation. Further studies should be done by repeating the *in vitro* kinase assay and using complimentary mapping to provide better coverage of the GST-BimA protein. Settings for the instrument may need to be adjusted so that the peptide could be detected and the phosphorylation reaction may also need to be optimised.

Based on the prediction and previous studies on the PDAST repeat region, it was hypothesized that phosphorylation of Serine residues in the PDAST region of BimA could affect actin-based motility. To investigate this, plasmids encoding mutated BimA proteins were generated.

As generation of *B. thailandensis* BimA mutant was unsuccessful, the phosphorylation mutant BimA proteins were expressed in a *B. pseudomallei ΔbimA* strain. *B. pseudomallei* expressing the phospho-mimic (BimA S/D) or phospho-null (BimA S/A) mutant BimA's were able to form actin tails in HeLa cells and showed no difference in actin tail length or BimA localisation. This study shows that phosphorylation of Serines in the PDAST region were not important for actin-based motility. The PDAST repeat region contains many Threonines which are predicted as common targets for kinases and could be phosphorylated to affect the actin-based motility of *B. pseudomallei*. Further studies

should be performed to generate BimA and their phosphorylation mutant proteins where Threonines are substituted in the PDAST repeat region and investigated in the same way as the Serine phosphorylation mutants. Actin tail formation, BimA localisation and actin tail length should all be analysed. Phosphorylation of Threonines and not Serines could be a reason for the additive effect in actin polymerisation of the PDAST repeat demonstrated seen in previous studies (Sitthidet *et al.* 2011).

Further studies should be performed for the survival of phosphorylation mutants and at a later timepoint to create a time course. This would allow any temporal difference between the mutant BimA's and wildtype to be detected. This experiment could also be repeated in a macrophage cell line such as J774 where bacteria are actively removed by phagosomal degradation. In a macrophage BimA function may be more important for survival of the bacteria than in a HeLa cell and bacteria expressing mutated BimA's are likely to be rapidly cleared. A significant difference might be seen between phospho-mimic and wildtype BimA's under these conditions.

The bioinformatics analysis predicted BimA to be phosphorylated by host cell kinases at many sites in different functional domains. To identify the actual sites a method for transfection of HeLa cells with pCD32-BimA and immunoprecipitating this protein has been optimised. Mass spectrometry analysis of immunoprecipitated CD32-BimA has identified a novel phosphorylation site, S_{135}. Peptide coverage was low and it is possible there are more unidentified sites of BimA phosphorylation. Further optimisation of the immunoprecipitation of CD32-BimA and then a repeat mass spectrometry analysis using complimentary mapping should be used to provide an improved protein coverage.

S_{135} was also one of the sites predicted from the bioinformatics analysis as a target for host cell kinases and is located in a WH2 domain. These WH2 domains have been shown to be important for actin binding and shown to be able to mimic Ena/Vasp proteins by nucleating and elongating actin filaments (Sitthidet *et al*. 2011) (Benanti *et al*. 2015). Phosphorylation mutants of this site should be generated to analyse the effect on actin-based motility. Cells could be infected and analysed for actin-based motility. Any difference seen in actin tail formation, length or structure would indicate that this phosphorylation site is important to actin-based motility. Further studies could then be done to look at virulence of the phosphorylation mutants. A *Galleria mellonella* model could be used as an initial infection model before using a mouse model. For both models the effect of phosphorylation mutants on survival would be investigated. Infection models for *B. pseudomallei* are well established and many studies have used them (Laws *et al.* 2011) (Wand *et al.* 2011).

The bioinformatics analysis predicted 4 potential host cell kinases that could phosphorylate S_{135}; PKC-γ, PKA, ROCK1 and PAK4. Cells infected with *B. pseudomallei* could also be treated with inhibitors for these kinases and may show reduced actin-based motility if phosphorylation by the kinase is

important. Inhibitors have been developed and studied for ROCK1 and PAK 4 (Liao *et al*. 2009) (Abdel-Magid 2015). The experiment would need to be optimised as these host kinases have important roles for the cell and treatment with too high a concentration of inhibitor could be toxic to the cell. An alternative experiment for analysing the effect of host cell kinases on *B. pseudomallei* actin-based motility would be to use siRNA to knockdown of the relevant kinase. This method has been used to show the importance of CK2 phosphorylation on the actin-based motility of *Listeria* (Chong *et al*. 2009).

Alternative kinases from the prediction could be investigated to see if they phosphorylate BimA and further *in vitro* kinases assays of GST-BimA should be performed. Once phosphorylation of BimA has been detected by mass spectrometry, the phosphorylated protein could be investigated further in an actin-pyrene polymerisation assay (Stevens *et al*. 2005) (Sitthidet *et al*. 2011). This assay involves measuring the emission of fluorescence of pyrene-conjugated actin that occurs during polymerization. Differences in actin polymerisation could indicate that phosphorylation of BimA by a host kinase is important to actin-based motility.

The aim of this project was to investigate the effect of host cell phosphorylation of BimA on actin-based motility of *B. pseudomallei*. BimA is a protein that is vital for the intracellular motility stage of this pathogen. Sites of the PDAST repeat region, predicted to be phosphorylated, have been investigated for their effect on actin-based motility. A novel phosphorylation site, S_{135}, has been identified by optimising a method for transfection of HeLa cells with pCD32-BimA and immunoprecipitating this protein. This method can now be used to immunoprecipitate CD32-BimA for further experiments on post-translational modifications. Phosphorylation of S_{135}, could affect the function of BimA and has opened up the opportunity for further research. Discovery of novel sites that are important to actin-based motility of *B. pseudomallei* will lead to a better understanding of the mechanism of this pathogen's intracellular life cycle stage. This could lead to the development of novel therapeutics and development of treatments for the severe disease melioidosis.

Acknowledgements

I would like to thank my group MMBP; Jo Stevens, Charles Vander Brook, Nina Jitprasutwit, Nurhamimah Zainal-Abidin and Kate Mathers. They have given me outstanding help and support all year during my project. In particular my supervisor Jo Stevens for her valuable advice and guidance towards the research. I have learnt so much from my year and really appreciate all the discussions and encouragement from Jo. I would like to thank Nina Jitprasutwit for her contribution to the CL3 experiments and confocal microscopy. I would also like to thank the Sydney Perry Foundation for their generous contribution towards the research costs.

References:

Lazar Adler, N. R., Govan, B., Cullinane, M., Harper, M., Adler, B., & Boyce, J. D. (2009) The molecular and cellular basis of pathogenesis in melioidosis: How does Burkholderia pseudomallei cause disease? *FEMS Microbiology Reviews*, ***33***, 1079–1099.

Lazar Adler, N. R., Stevens, J. M., Stevens, M. P., & Galyov, E. E. (2011) Autotransporters and their role in the virulence of Burkholderia pseudomallei and Burkholderia mallei. *Frontiers in Microbiology*, ***2***, 1–7.

Adler, N. R. L., Stevens, M. P., Dean, R. E., Saint, R. J., Pankhania, D., Prior, J. L., … Galyov, E. E. (2015) Systematic Mutagenesis of Genes Encoding Predicted Autotransported Proteins of Burkholderia pseudomallei Identifies Factors Mediating Virulence in Mice, Net Intracellular Replication and a Novel Protein Conferring Serum Resistance. *Plos One*, ***10,*** e0121271.

Abdel-Magid, A. F. (2015) P21-Activated Kinase 4 (PAK4) Inhibitors as Potential Cancer Therapy. *ACS Medicinal Chemistry Letters, **4***, 17–18.

Ahmed, K., Enciso, H. D. R., Masaki, H., Tao, M., Omori, A., Tharavichikul, P., & Nagatake, T. (1999) Attachment of Burkholderia pseudomallei to pharyngeal epithelial cells: A highly pathogenic bacteria with low attachment ability. *American Journal of Tropical Medicine and Hygiene*, ***60***, 90–93.

Alberts, A., & Way, M. (2011) Actin Motility: Formin a SCAry Tail. *Current Biology*, ***21***, R27–R30.

Ali and Steinkasserer (1995) PCR-Ligation-PCR Mutagenesis: A Protocol for Creating Gene Fusions and Mutations. *BioTechniques*, **18**, 746-750.

Allwood, E. M., Devenish, R. J., Prescott, M., Adler, B., & Boyce, J. D. (2011) Strategies for Intracellular Survival of Burkholderia pseudomallei. *Frontiers in Microbiology*, ***2***, 170.

Alvarez, D. E., & Agaisse, H. (2012) Casein kinase 2 regulates vaccinia virus actin tail formation. *Virology*, ***423***, 143–51.

Amann, K. J., & Pollard, T. D. (2001) Direct real-time observation of actin filament branching mediated by Arp2/3 complex using total internal reflection fluorescence microscopy. *Proceedings of the National Academy of Sciences of the United States of America*, ***98***, 15009–15013.

Auerbuch, V., Loureiro, J. J., Gertler, F. B., Theriot, J. a., & Portnoy, D. a. (2003) Ena/VASP proteins contribute to Listeria monocytogenes pathogenesis by controlling temporal and spatial persistence of bacterial actin-based motility. *Molecular Microbiology*, ***49***, 1361–1375.

Balder, R., Lipski, S., Lazarus, J. J., Grose, W., Wooten, R. M., Hogan, R. J., … Lafontaine, E. R. (2010) Identification of Burkholderia mallei and Burkholderia pseudomallei adhesins for human respiratory epithelial cells. *BMC Microbiology*, ***10***, 250.

Benanti, E. L., Nguyen, C. M., & Welch, M. D. (2015) Virulent Burkholderia Species Mimic Host Actin Polymerases to Drive Actin-Based Motility. *Cell*, ***161***, 348–360.

Berthon, A. S., Szarek, E., & Stratakis, C. a. (2015) PRKACA: the catalytic subunit of protein kinase A and adrenocortical tumors. *Frontiers in Cell and Developmental Biology*, ***3***, 1–6.

Blom, N., Gammeltoft, S., & Brunak, S. (1999) Sequence and structure-based prediction of eukaryotic protein phosphorylation sites. *Journal of Molecular Biology*, **294**, 1351-1362

Boddey, J. a., Flegg, C. P., Day, C. J., Beacham, I. R., & Peak, I. R. (2006) Temperature-regulated microcolony formation by Burkholderia pseudomallei requires pilA and enhances association with cultured human cells. *Infection and Immunity*, ***74***, 5374–5381.

Breitbach, K., Rottner, K., Klocke, S., Rohde, M., Jenzora, A., Wehland, J., Steinmetz, I. (2003) Actin-based motility of *Burkholderia pseudomallei* involves the Arp 2/3 complex, but not N-WASP and Ena/VASP proteins. *Cellular Microbiology*, **5**, 385-393

Brett, P. J., & Woods, D. E. (2000) Pathogenesis of and immunity to melioidosis. *Acta Tropica*, ***74***, 201–210.

Burton, E. a, Oliver, T. N., & Pendergast, A. M. (2005. Abl kinases regulate actin comet tail elongation via an N-WASP-dependent pathway. *Molecular and Cellular Biology*, ***25***, 8834–8843.

Campellone KG, Welch MD. (2010) A nucleator arms race: cellular control of actin assembly. Nature. Reviews. *Molecular Cell Biology,* **11**, 237-51.

Chesarone, M. a., & Goode, B. L. (2009). Actin nucleation and elongation factors: mechanisms and interplay. *Current Opinion in Cell Biology*, ***21***, 28–37.

Chen, Y., Wong, J., Sun, G. W., Liu, Y., Tan, G. Y. G., & Gan, Y. H. (2011) Regulation of type VI secretion system during Burkholderia pseudomallei infection. *Infection and Immunity*, **79**, 3064–3073.

Cheng, A. C., & Currie, B. J. (2005) Melioidosis: epidemiology, pathophysiology, and management. *Clinical Microbiology Reviews*, ***18***, 383–416.

Chong R, Swiss R, Briones G, Stone K, Gulcicek E and Agaisse H. (2009) Regulatory mimicry in *Listeria monocytogenes* actin-based motility. *Cell Host Microbe,* **17**, 268-278

Chong, R., Squires, R., Swiss, R., & Agaisse, H. (2011) RNAi screen reveals host cell kinases specifically involved in Listeria monocytogenes spread from cell to cell. *Plos One*, ***6***, e23399.

Clackson T, Güssow D, Jones PT (1991) General applications of PCR to gene cloning and manipulation. In: McPherson MJ, Quirke P, Taylor GR, editors. *PCR: A practical approach*, **1**, 187–214.

Cooper JA, Walker SB, Pollard TD. (1983) Pyrene actin: documentation of the validity of a sensitive assay for actin polymerization. Journal Muscle Research and Cell Motility, **4**, 253–262

Cory, G. O. C., Garg, R., Cramer, R., & Ridley, A. J. (2002) Phosphorylation of tyrosine 291 enhances the ability of WASp to stimulate actin polymerization and filopodium formation. *Journal of Biological Chemistry*, ***277***, 45115–45121.

Cory, G. O. C., Cramer, R., Blanchoin, L., & Ridley, A. J. (2003) Phosphorylation of the WASP-VCA domain increases its affinity for the Arp2/3 complex and enhances actin polymerization by WASP. *Molecular Cell*, ***11***, 1229–1239.

Cotter, S. E., Surana, N. K., & St. Geme, J. W. (2005) Trimeric autotransporters: A distinct subfamily of autotransporter proteins. *Trends in Microbiology*, ***13***, 199–205.

Cullinane, M., Gong, L., Li, X., Lazar-Adler, N., Tra, T., Wolvetang, E., … Adler, B. (2008) Stimulation of autophagy suppresses the intracellular survival of Burkholderia pseudomallei in mammalian cell lines. *Autophagy*, **4**, 744–753.

Darji, A., Mohamed, W., Domann, E. and Chakraborty, T. (2003) Induction of immune responses by attenuated isogenic mutant strains of *Listeria monocytogenes*. *Vaccine*, **21**, 102-109

D'Hauteville, H., & Sansonetti, P. J. (1992) Phosphorylation of IcsA by cAMP-dependent protein kinase and its effect on intracellular spread of Shigella flexneri. *Molecular Microbiology*, **6**, 833–841.

Dragoi, A.-M., Talman, A. M., & Agaisse, H. (2013) Burton's tyrosine kinase regulates Shigella flexneri dissemination in HT-29 intestinal cells. *Infection and Immunity*, ***81***, 598–607.

Edwards, M., Zwolak, A., Schafer, D. a., Sept, D., Dominguez, R., & Cooper, J. a. (2014) Capping protein regulators fine-tune actin assembly dynamics. *Nature Reviews Molecular Cell Biology*, **15**, 677–689.

Eiseler, T., Hausser, A., De Kimpe, L., Van Lint, J., & Pfizenmaier, K. (2010) Protein kinase D controls actin polymerization and cell motility through phosphorylation of cortactin. *Journal of Biological Chemistry*, **285**, 18672–18683.

Essex-Lopresti, A. E., Boddey, J. a., Thomas, R., Smith, M. P., Hartley, M. G., Atkins, T., … Titball, R. W. (2005) A type IV pilin, pilA, contributes to adherence of Burkholderia pseudomallei and virulence in vivo. *Infection and Immunity*, **73**, 1260–1264.

Firat-Karalar, E. N., & Welch, M. D. (2011) New mechanisms and functions of actin nucleation. *Current Opinion in Cell Biology*, **23**, 4–13.

Frame, S., & Cohen, P. (2001) GSK3 takes centre stage more than 20 years after its discovery. *The Biochemical Journal*, **359**, 1–16.

French, C. T., Toesca, I. J., Wu, T.-H., Teslaa, T., Beaty, S. M., Wong, W., … Miller, J. F. (2011) Dissection of the Burkholderia intracellular life cycle using a photothermal nanoblade. *Proceedings of the National Academy of Sciences of the United States of America*, **108**, 12095–12100.

Frischknecht, F., Moreau, V., Ro, S., Gonfloni, S., Reckmann, I., Superti-furga, G., & Way, M. (1999) Actin-based motility of vaccinia virus mimics receptor tyrosine kinase signalling. *Letters to nature*, **401**, 926-929

Galyov, E. E., Brett, P. J., & DeShazer, D. (2010) Molecular insights into Burkholderia pseudomallei and Burkholderia mallei pathogenesis. *Annual Review of Microbiology*, **64**, 495–517.

Garmendia, J., Carlier, M. F., Egile, C., Didry, D., & Frankel, G. (2006) Characterization of TccP-mediated N-WASP activation during enterohaemorrhagic Escherichia coli infection. *Cellular Microbiology*, **8**, 1444–1455.

Gasteiger E., Hoogland C., Gattiker A., Duvaud S., Wilkins M.R., Appel R.D., Bairoch A. (2005)

Protein Identification and Analysis Tools on the ExPASy Server. *The Proteomics Protocols Handbook*, 571-607

Goley, E. D., & Welch, M. D. (2006) The ARP2/3 complex: an actin nucleator comes of age. *Nature Reviews. Molecular Cell Biology*, **7**, 713–726.

Gong, L., Cullinane, M., Treerat, P., Ramm, G., Prescott, M., Adler, B., … Devenish, R. J. (2011) The Burkholderia pseudomallei type III secretion system and BopA are required for evasion of LC3-associated phagocytosis. *Plos one*, **6**, e17852.

Gouin, E., Egile, C., Dehoux, P., Villiers, V., Adams, J., Gertler, F., … Cossart, P. (2004) The RickA protein of Rickettsia conorii activates the Arp2/3 complex. *Nature*, **427**, 457–461.

Grassart, A., Meas-Yedid, V., Dufour, A., Olivo-Marin, J. C., Dautry-Varsat, A., & Sauvonnet, N. (2010). Pak1 phosphorylation enhances cortactin-N-WASP interaction in clathrin-caveolin-independent endocytosis. *Traffic*, **11**, 1079–1091.

Jewett, T.J., Dooley, C.A., Mead, D.J. & Hackstadt, T. (2008) Chlamydia trachomatis tarp is phosphorylated by Src family tyrosine kinases. *Biochemical and Biophysical Research Communications,* **371**, 339-344

Ha, B. H., Morse, E. M., Turk, B. E., & Boggon, T. J. (2015) Signalling, regulation and specificity of the type II p21-activated kinases. *Journal of Biological Chemistry*, **290**, 12975-12983

Haglund, C. M., Choe, J. E., Skau, C. T., Kovar, D. R., & Welch, M. D. (2010) Rickettsia Sca2 is a bacterial formin-like mediator of actin-based motility. *Nature Cell Biology*, **12**, 1057–63.

Haraga, A., West, T. E., Brittnacher, M. J., Skerrett, S. J., & Miller, S. I. (2008) Burkholderia thailandensis as a model system for the study of the virulence-associated type III secretion system of Burkholderia pseudomallei. *Infection and Immunity*, **76**, 5402–11.

Kenny, B., DeVinney, R., Stein, M., Reinscheid, D. J., Frey, E., & Finlay, B. B. (1997) (a) Enteropathogenic E. coli (EPEC) transfers its receptor for intimate adherence into mammalian cells. *Cell*, **91**, 511–520.

Kenny, B., Finlay, B. B., Kenny, B., & Finlay, B. B. (1997) (b) Intimin-dependent binding of enteropathogenic Escherichia coli to host cells triggers novel signalling events , including tyrosine phosphorylation of phospholipase C-gamma1 . Intimin-Dependent Binding of Enteropathogenic Escherichia coli to Host Cells Trig, **65**, 2528–2536.

Kenny, B. (1999) Phosphorylation of tyrosine 474 of the enteropathogenic Escherichia coli (EPEC) Tir receptor molecule is essential for actin nucleating activity and is preceded by additional host modifications. *Molecular Microbiology*, **31**, 1229–1241.

Kespichayawattana W, Rattanachetkul S, Wanun T, Utaisincharoen P, Sirisinha S. (2000) *Burkholderia pseudomallei* induces cell fusion and actin-associated membrane protrusion: a possible mechanism for cell-to-cell spreading. *Infection Immunity*, **68,** 5377-84.

Kim, H. S., Schell, M. a, Yu, Y., Ulrich, R. L., Sarria, S. H., Nierman, W. C., & DeShazer, D. (2005) Bacterial genome adaptation to niches: divergence of the potential virulence genes in three Burkholderia species of different survival strategies. *BMC Genomics*, **6**, 174.

Laemmli UK (1970) Cleavage of structural proteins during assembly of the head of bacteriophage T4. *Nature* **227**, 680-685.

Laws, T. R., Smither, S. J., Lukaszewski, R. a., & Atkins, H. S. (2011) Neutrophils are the predominant cell-type to associate with Burkholderia pseudomallei in a BALB/c mouse model of respiratory melioidosis. *Microbial Pathogenesis*, **51**, 471–475.

Liao, J. K., Seto, M., & Noma, K. (2009). NIH Public Access, **50**, 17–24.

Lipsitz, R., Garges, S., Aurigemma, R., Baccam, P., Blaney, D. D., Cheng, A. C., … Smith, T. L. (2012) Workshop on Treatment of and Postexposure Prophylaxis for Burkholderia pseudomallei and B. mallei Infection, 2010. *Emerging Infectious Disease Journal*, **18***,* e2.

Logue, C. A., Peak, I. R. a, & Beacham, I. R. (2009) Facile construction of unmarked deletion mutants in Burkholderia pseudomallei using sacB counter-selection in sucrose-resistant and sucrose-sensitive isolates. *Journal of Microbiological Methods*, **76**, 320–323

López, C. M., Rholl, D. a., Trunck, L. a., & Schweizer, H. P. (2009) Versatile dual-technology system for markerless allele replacement in Burkholderia pseudomallei. *Applied and Environmental Microbiology*, **75**, 6496–6503.

Lu, Q., Xu, Y., Yao, Q., Niu, M., & Shao, F. (2015) A polar-localized iron-binding protein determines the polar targeting of Burkholderia BimA autotransporter and actin tail formation. *Cellular Microbiology*, **17**, 408–424.

May, K. L., Grabowicz, M., Polyak, S. W., & Morona, R. (2012) Self-association of the Shigella flexneri IcsA autotransporter protein. *Microbiology (Reading, England)*, **158**, 1874–83.

Mehlitz, A., Banhart, S., Hess, S., Selbach, M., & Meyer, T. F. (2008) Complex kinase requirements for Chlamydia trachomatis Tarp phosphorylation. *FEMS Microbiology Letters*, **289**, 233–240.

Monach, D.M. and Theriot. J. A. (2001) Actin-based motility is sufficient for bacterial membrane protrusion formation and host cell uptake. *Cell Microbiology*, **3**, 633-647.

Padiglione, a, Ferris, N., Fuller, a, & Spelman, D. (1996) Burkholderia pseudomallei, **1**, 1–3.

Paunola, E., Mattila, P. K., & Lappalainen, P. (2002) WH2 domain: A small, versatile adapter for actin monomers. *FEBS Letters*, **513**, 92–97.

Pinna, L. A. (2002) Protein kinase CK2: a challenge to canons. *Journal of Cell Science*, **115**, 3873-3878

Pollitt, A. Y., & Insall, R. H. (2009) WASP and SCAR/WAVE proteins: the drivers of actin assembly. *Journal of Cell Science*, **122**, 2575–2578.

Pollard, T. D., & Borisy, G. G. (2003) Cellular motility driven by assembly and disassembly of actin filaments. *Cell*, **112**, 453–465.

Puntervoll, P., Linding, R., Gemünd, C., Chabanis-Davidson, S., Mattingsdal, M., Cameron, S., … Gibson, T. J. (2003) ELM server: A new resource for investigating short functional sites in modular eukaryotic proteins. *Nucleic Acids Research*, **31**, 3625-3630

Riento, K., & Ridley, A. J. (2003) Rocks: multifunctional kinases in cell behaviour. *Nature Reviews. Molecular Cell Biology*, **4**, 446–456.

Reed, S. C. O., Lamason, R. L., Risca, V. I., Abernathy, E., & Welch, M. D. (2014) Rickettsia actin-based motility occurs in distinct phases mediated by different actin nucleators. *Current Biology : CB*, **24***,* 98–103.

Sansonetti, P. J., Arondel, J., Fontaine, a, d'Hauteville, H., & Bernardini, M. L. (1991) OmpB (osmo-regulation) and icsA (cell-to-cell spread) mutants of Shigella flexneri: vaccine candidates and probes to study the pathogenesis of shigellosis. *Vaccine*, **9**, 416–422.

Sarkar-Tyson, M., Smither, S. J., Harding, S. V., Atkins, T. P., & Titball, R. W. (2009) Protective efficacy of heat-inactivated B. thailandensis, B. mallei or B. pseudomallei against experimental melioidosis and glanders. *Vaccine*, **27**, 4447–4451.

Sarno, S., Moro, S., Meggio, F., Zagotto, G., Dal Ben, D., Ghisellini, P., … Pinna, L. A. (2002) Toward the rational design of protein kinase casein kinase-2 inhibitors. In *Pharmacology and Therapeutics*, **93**, 159-168

Schwarz, S., Singh, P., Robertson, J. D., LeRoux, M., Skerrett, S. J., Goodlett, D. R., … Mougous, J. D. (2014) VgrG-5 is a Burkholderia type VI secretion system-exported protein required for multinucleated giant cell formation and virulence. *Infection and Immunity*, **82**, 1445–1452.

Moore, R.A., DeShazer, D., Reckseidler, S., Weissman, A. and Woods, D.E. (1999) Aminoglycoside and macrolide resistance in Burkholderia pseudomallei. *Antimicrobial Agents and Chemotherapy*, **43**, 2332.

Sitthidet C, Stevens JM, Chantratita N, Currie BJ, Peacock SJ, Korbsrisate S, Stevens MP. (2008) Prevalence and sequence diversity of a factor required for actin-based motility in natural populations of *Burkholderia* species. *Journal Clinical Microbiology*, **46,** 2418-22.

Sitthidet, C., Stevens, J.M., Field, T.R., Layton, A.N., Korbsrisate, S. and Stevens, M.P. (2010). Actin-based motility of *Burkholderia thailandensis* requires a central acidic domain of BimA that recruits and activates the cellular Arp2/3 complex. *Journal of bacteriology*. **192**: 5249-5252

Sitthidet, C., Korbsrisate, S., Layton A.N., Field, T.R., Stevens, M.P. and Stevens J.M. (2011) Identification of motifs of *Burkholderia pseudomallei* BimA required for intracellular motility, actin binding, and actin polymerisation. *Journal of Bacteriology,* **193,** 1901-1910

Smith, G. a., Theriot, J. a., & Portnoy, D. a. (1996) The tandem repeat domain in the Listeria monocytogenes ActA protein controls the rate of actin-based motility, the percentage of moving

bacteria, and the localization of vasodilator-stimulated phosphoprotein and profilin. *Journal of Cell Biology*, **135**, 647–660.

Stamm, L. M., Morisaki, J. H., Gao, L.-Y., Jeng, R. L., McDonald, K. L., Roth, R., … Brown, E. J. (2003) Mycobacterium marinum escapes from phagosomes and is propelled by actin-based motility. *The Journal of Experimental Medicine*, ***198***, 1361–1368.

Stamm, L. M., Pak, M. a, Morisaki, J. H., Snapper, S. B., Rottner, K., Lommel, S., & Brown, E. J. (2005) Role of the WASP family proteins for Mycobacterium marinum actin tail formation. *Proceedings of the National Academy of Sciences of the United States of America*, **102**, 14837–42.

Srinon, V., Korbsrisate, S., Stevens, M. P., & Stevens, J. M. (2011) Role of BimC in Actin-based Motility of Burkholderia pseudomallei, *Journal of Infectious Diseases Antimicrobial Agents*, 250.

Stevens, M.P., Wood, M.W., Taylor, L.A., Monaghan, P., Hawes, P., Jones, P.W., et al. (2002) An Inv/Mxi-Spa-like Type III protein secretion system in *Burkholderia pseudomallei* modulates intracellular behaviour of the pathogen. *Molecular Microbiology,* **46**, 649-659.

Stevens, M. P., Friebel, A., Taylor, L.A., Wood, Wood, M.W., Brown, B.J., Hardt, W.D., and Galyov, E.E. (2003) A *Burkholderia pseudomallei* type III secrete protein, BopE, facilitates bacterial invasion of epithelial cells and exhibits guanine nucleotide exchange factor activity. *Journal Bacteriology,* **185,** 4992-4996.

Stevens, M. P., Haque, A., Atkins, T., Hill, J., Wood, M. W., Easton, A., … Galyov, E. E. (2004) Attenuated virulence and protective efficacy of a Burkholderia pseudomallei bsa type III secretion mutant in murine models of melioidosis. *Microbiology*, **150**, 2669–2676.

Stevens MP, Stevens JM, Jeng RL, Taylor LA, Wood MW, Hawes P, Monaghan P, Welch MD, Galyov EE. (2005) Identification of a bacterial factor required for actin-based motility of *Burkholderia pseudomallei. Molecular Microbiology*, **56,** 40-53.

Stevens, J.M., Ulrich, R.L., Taylor, L.A., Wood, M.W., Deshazer, D., Stevens, M.P., and Galyov, E.E. (2005) Actin-binding proteins from *Burkholderia mallei* and *Burkholderia thailandensis* can functionally compensate for the actin-based motility defect of Burkholderia pseudomallei bimA mutant. *Journal of bacteriology*, **187,** 7857-7862.

Stevens JM, Galyov EE, Stevens MP. (2006) Actin-dependent movement of bacterial pathogens. Nature Reviews *Microbiology*, **4,** 91-101

Stevens JM, Stevens MP. (2009) *Burkholderia pseudomallei*. In Intracellular niches of microbes - a pathogens guide through the host cell, 393-413. Ed. Schiable UE, Haas A. Wiley-Blackwell.

Sun, G. W., & Gan, Y. H. (2010) Unraveling type III secretion systems in the highly versatile Burkholderia pseudomallei. *Trends in Microbiology*, **18**, 561–568.

Suzuki, T., Miki, H., Takenawa, T., & Sasakawa, C. (1998) Neural Wiskott-Aldrich syndrome protein is implicated in the actin-based motility of Shigella flexneri. *EMBO Journal*, **17**, 2767–2776.

Takeya, R., Taniguchi, K., Narumiya, S., & Sumimoto, H. (2008) The mammalian formin FHOD1 is activated through phosphorylation by ROCK and mediates thrombin-induced stress fibre formation in endothelial cells. *The EMBO Journal*, **27**, 618–628.

Toesca, I. J., French, C. T., & Miller, J. F. (2014) The type VI secretion system spike protein VgrG5 mediates membrane fusion during intercellular spread by pseudomallei group Burkholderia species. *Infection and Immunity*, **82**, 1436–1444.

Wand, M. E., Müller, C. M., Titball, R. W., & Michell, S. L. (2011) Macrophage and Galleria mellonella infection models reflect the virulence of naturally occurring isolates of B. pseudomallei, B. thailandensis and B. oklahomensis. *BMC Microbiology*, **11**, 11.

Welch, M. D., Rosenblatt, J., Skoble, J., Portnoy, D. a, & Mitchison, T. J. (1998) Interaction of human Arp2/3 complex and the Listeria monocytogenes ActA protein in actin filament nucleation. *Science (New York, N.Y.)*, **281**, 105–108.

Welch, M. D., & Way, M. (2013) Arp2/3-mediated actin-based motility: A tail of pathogen abuse. *Cell Host and Microbe*, **14**, 242–255.

Wetsel, W. C., Khan, W. a, Merchenthaler, I., Rivera, H., Halpern, a E., Phung, H. M., … Hannun, Y. a. (1992. Tissue and cellular distribution of the extended family of protein kinase C isoenzymes. *The Journal of Cell Biology*, **117**, 121–133.

Wiersinga, W. J., Currie, B. J., & Peacock, S. J. (2012) Melioidosis. *The New England Journal of Medicine*, **367**, 1035–44.

Winkelman, J. D., Bilancia, C. G., Peifer, M., & Kovar, D. R. (2014) Ena/VASP Enabled is a highly processive actin polymerase tailored to self-assemble parallel-bundled F-actin networks with

Fascin. *Proceedings of the National Academy of Sciences of the United States of America*, **111**, 4121–6.

Witke, W. (2004) The role of profilin complexes in cell motility and other cellular processes. *Trends in Cell Biology*, **14**, 461–469.

White, N. J. (2003) Melliodosis. *Lancet*, **361**, 1715-1722.

Xue, Y., Liu, Z., Cao, J., Ma, Q., Gao, X., Wang, Q., … Ren, J. (2011) GPS 2.1: Enhanced prediction of kinase-specific phosphorylation sites with an algorithm of motif length selection. *Protein Engineering, Design and Selection,* 1-6.

Yokoyama, N., Lougheed, J., & Miller, W. T. (2005) Phosphorylation of WASP by the Cdc42-associated kinase ACK1: Dual hydroxyamino acid specificity in a tyrosine kinase. *Journal of Biological Chemistry*, **280**, 42219–42226.

Zalevsky, J., Grigorova, I., & Mullins, R. D. (2001) Activation of the Arp2/3 complex by the Listeria ActA protein. ActA binds two actin monomers and three subunits of the Arp2/3 complex. *Journal of Biological Chemistry*, **276**, 3468–3475.